electron transport in molecular systems

Reviews: Annu. Rev. Phys. Chem. 52, 681– 750 (2001)
[http://atto.tau.ac.il/~nitzan/nitzanabs.html/#213]
Science, 300, 1384-1389 (2003);
MRS Bulletin, 29, 391-395 (2004);
Bulletin of the Israel Chemical Society, Issue 14, p. 3-13 (Dec 2003) (Hebrew)

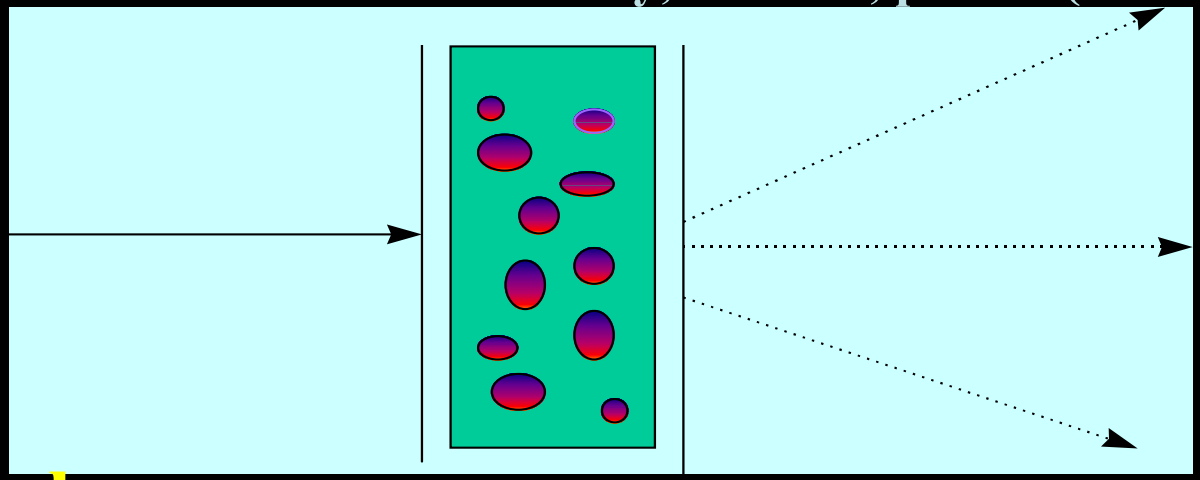

Thanks

I. Benjamin, A. Burin, G. Cuniberti, B. Davis, S. Datta, D. Evans, M. Galperin, A. Ghosh, H. Grabert, P. Hänggi, G. Ingold, J. Jortner, S. Kohler, R. Kosloff, J. Lehmann, M. Majda, A. Mosyak, V. Mujica, R. Naaman, F. v Oppen, U. Peskin, M. Ratner, D. Segal, T. Seideman, H. Tal-Ezer, A. Troisi

INELASTIC EFFECTS IN MOLECULAR CONDUCTION

Regensburg 2005

Thanks

M. Galperin, M. Ratner — Northwestern U

D. Segal — WIS

Barrier dynamics effects on electron transmission through molecular wires and layers

- Relevant timescales
- Inelastic contributions to the tunneling current
- Dephasing and activation - transition from coherent transmission to activated hopping
- Heating of current carrying molecular wires.
- HEAT CONDUCTION
- INELASTIC TUNNELING SPECTROSCOPY
- MULTISTABILITY AND HYSTERESIS
- LIGHT

Electron transfer/transmission

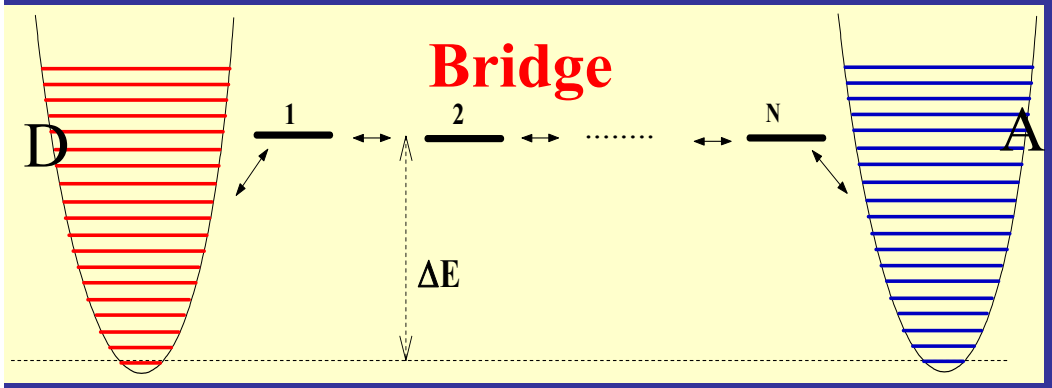

$$k_{D\to A} = \frac{2\pi}{\hbar}\left|V_{D1}V_{NA}\right|^2 \left|G_{1N}(E_D)\right|^2 \mathcal{F}$$

$$\mathcal{F}(E) = \frac{e^{-(\lambda+E)^2/4\lambda k_B T}}{\sqrt{4\pi\lambda k_B T}}$$

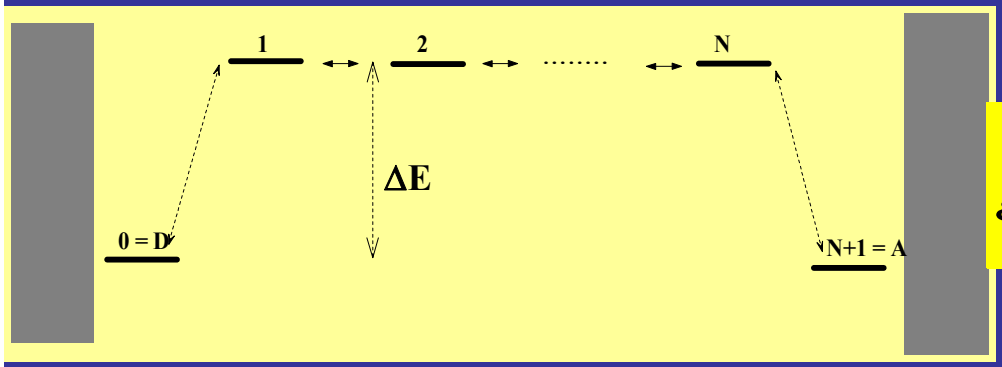

$$g(E) = \frac{e^2}{\pi\hbar}\left|G_{DA}(E)\right|^2 \Gamma_D^{(L)}(E)\Gamma_A^{(R)}(E)$$

A relation between g and k

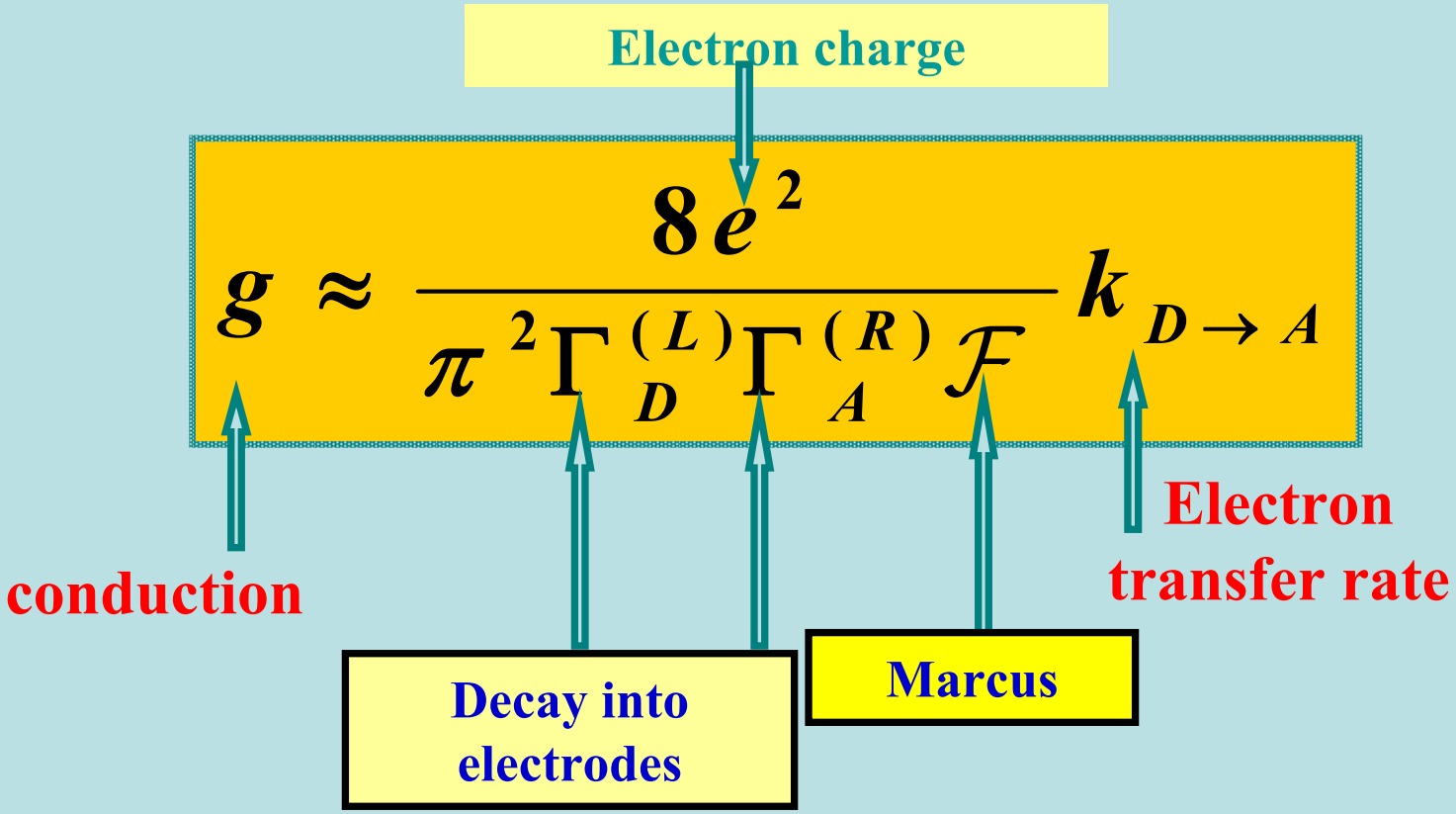

AN, J. Phys. Chem. A 105, 2677(2001)

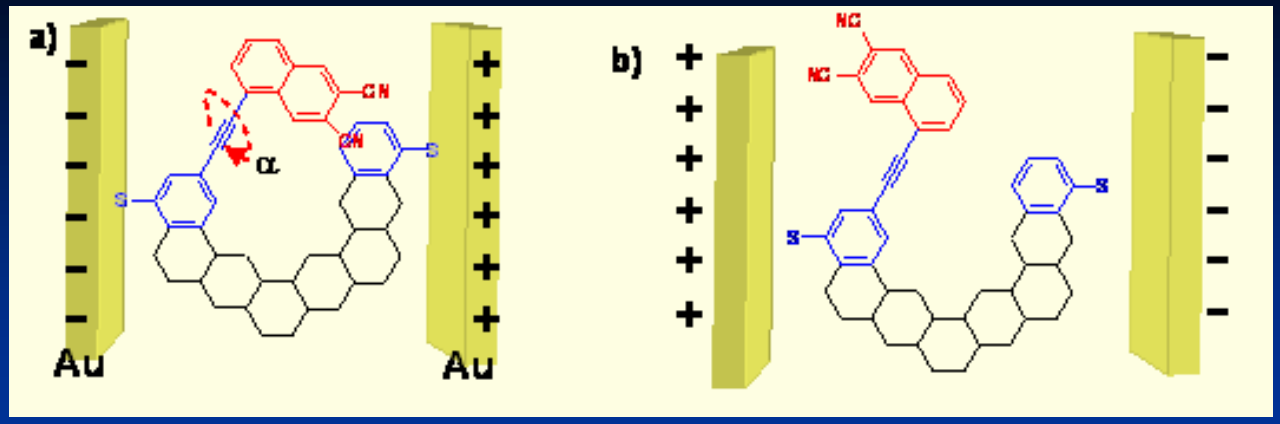

Ratner and Troisi, 2004

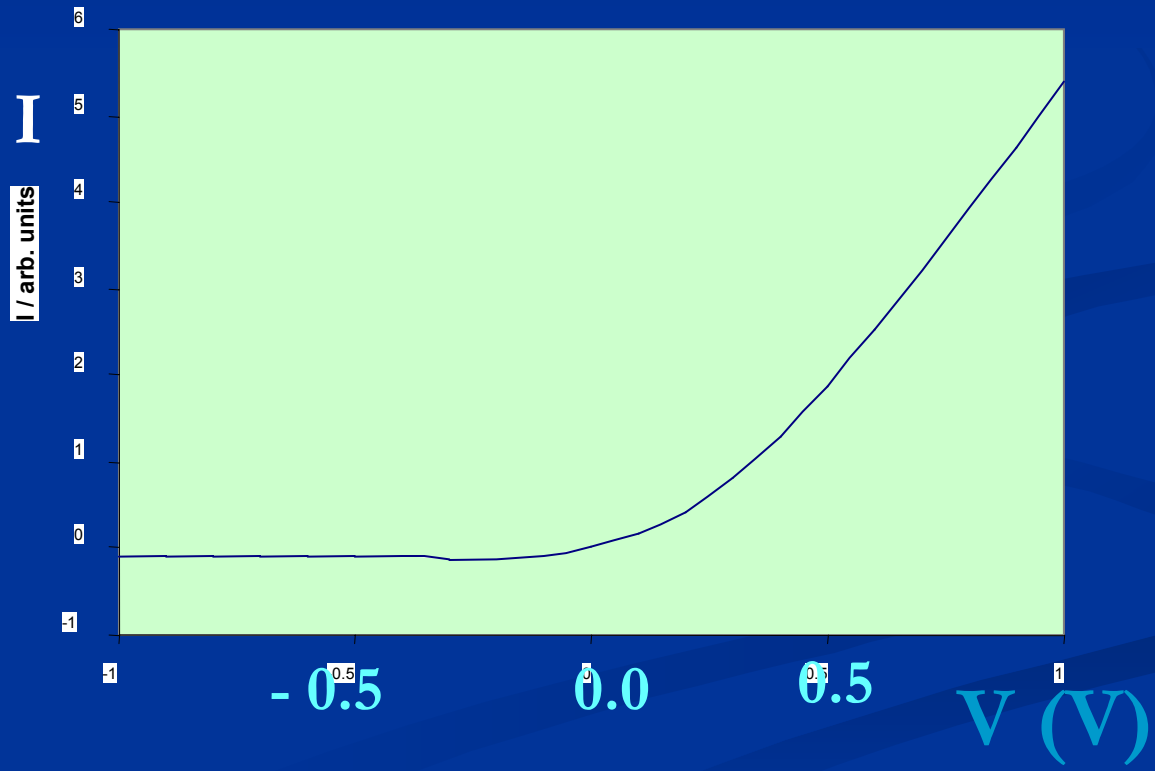

Barrier dynamics effects on electron transmission through molecular wires

- Relevant timescales
- Inelastic contributions to the tunneling current
- Dephasing and activation
- Heating of current carrying molecular wires.
- HEAT CONDUCTION and rectification
- INELASTIC TUNNELING SPECTROSCOPY
- MULTISTABILITY AND HYSTERESIS
- LIGHT

Traversal time for tunneling?

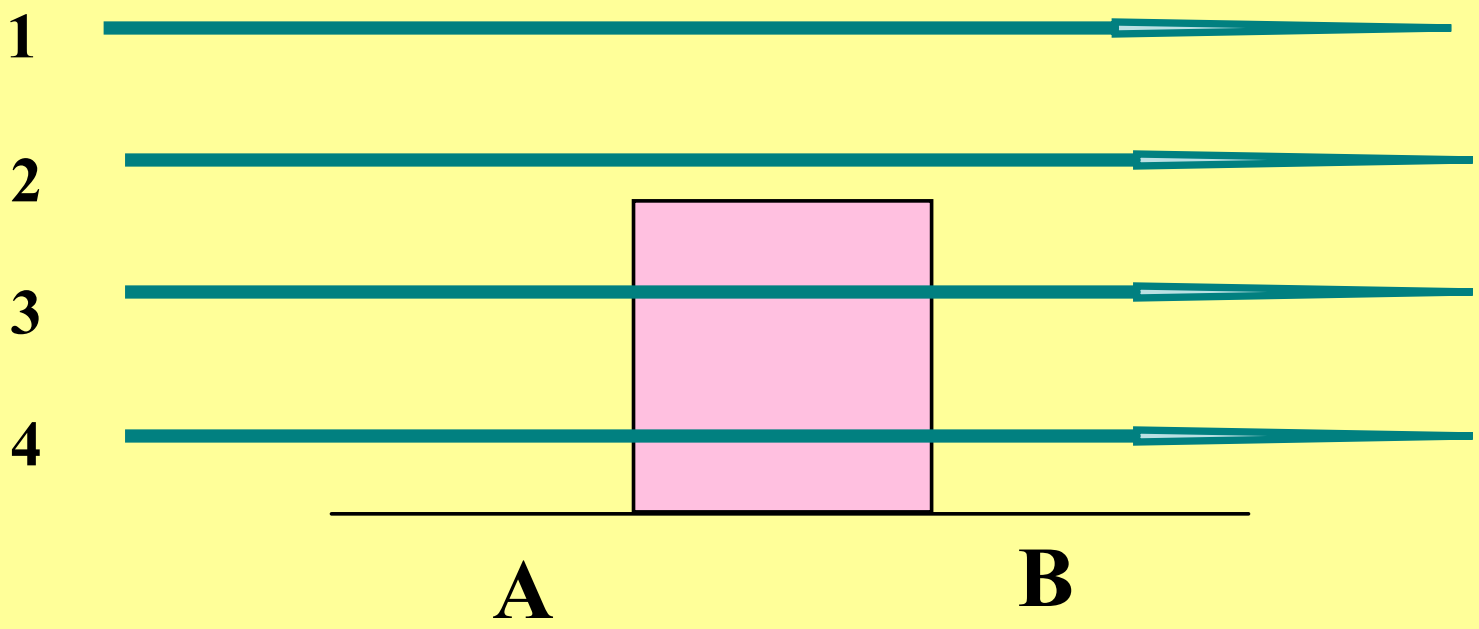

Water: Tunneling time and transmission probability

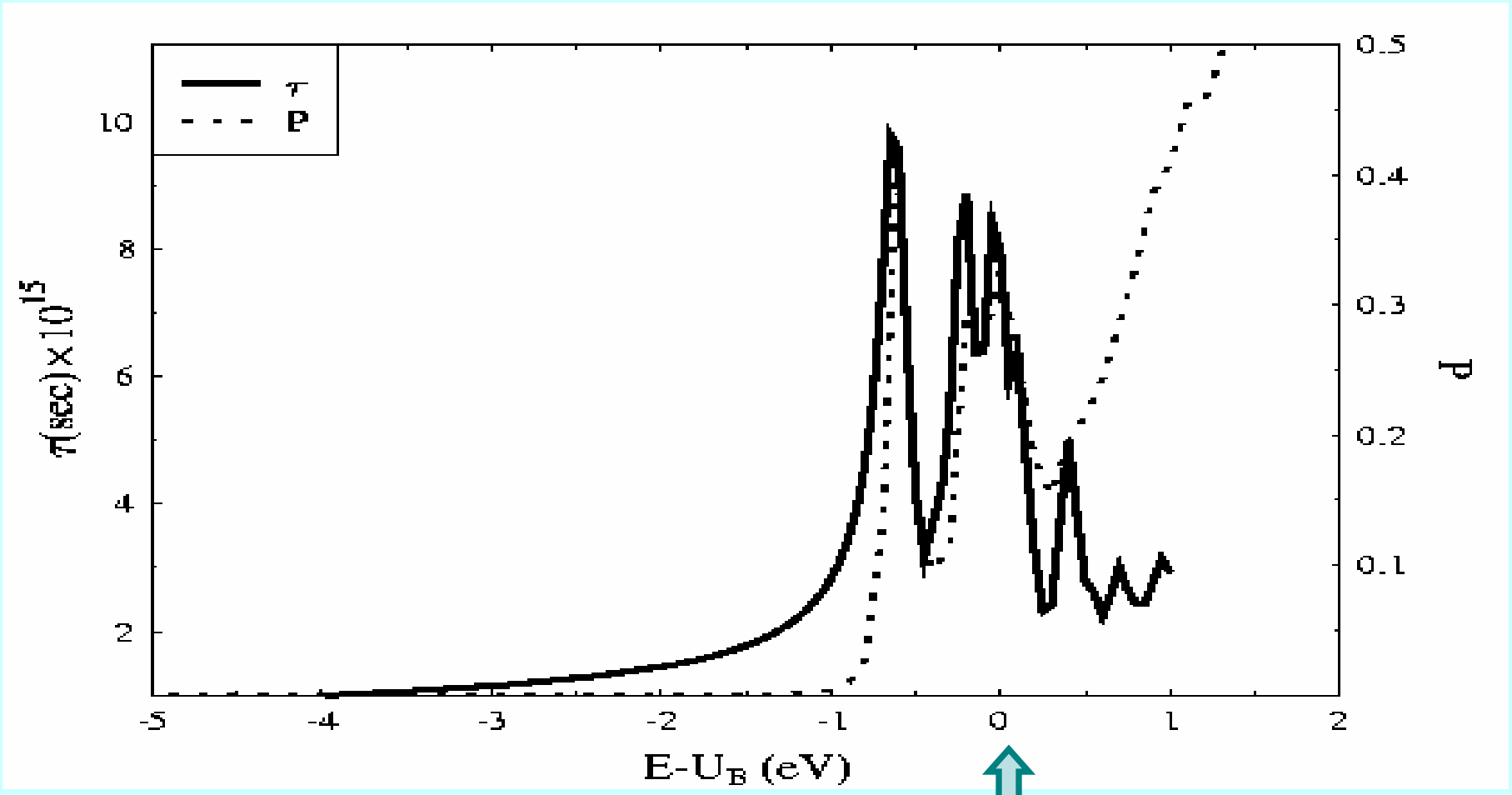

Galperin, AN, Peskin J. Chem. Phys. 114, 9205-08 (2001)

Instantaneous normal modes for water

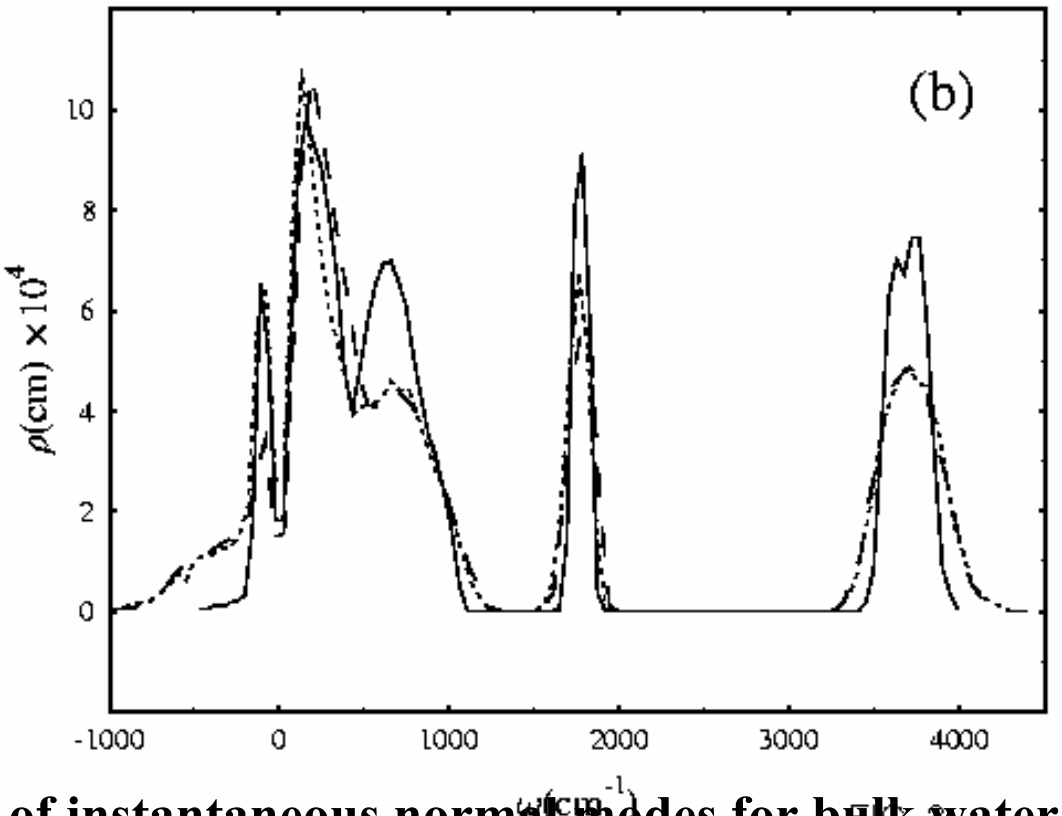

The density ρ of instantaneous normal modes for bulk water systems at 60K (full line) and 300K (dotted line) shown together with the result for a water layer comprised of three monolayers of water molecules confined between two static Pt(100) surfaces, averaged over 20 configurations sampled from an equilibrium (T=300K)(dashed line). The densities of modes shown are normalized to 1. The usual convention of displaying unstable modes on the negative frequency axis is applied here.

Solvation correlation functions for electron in water

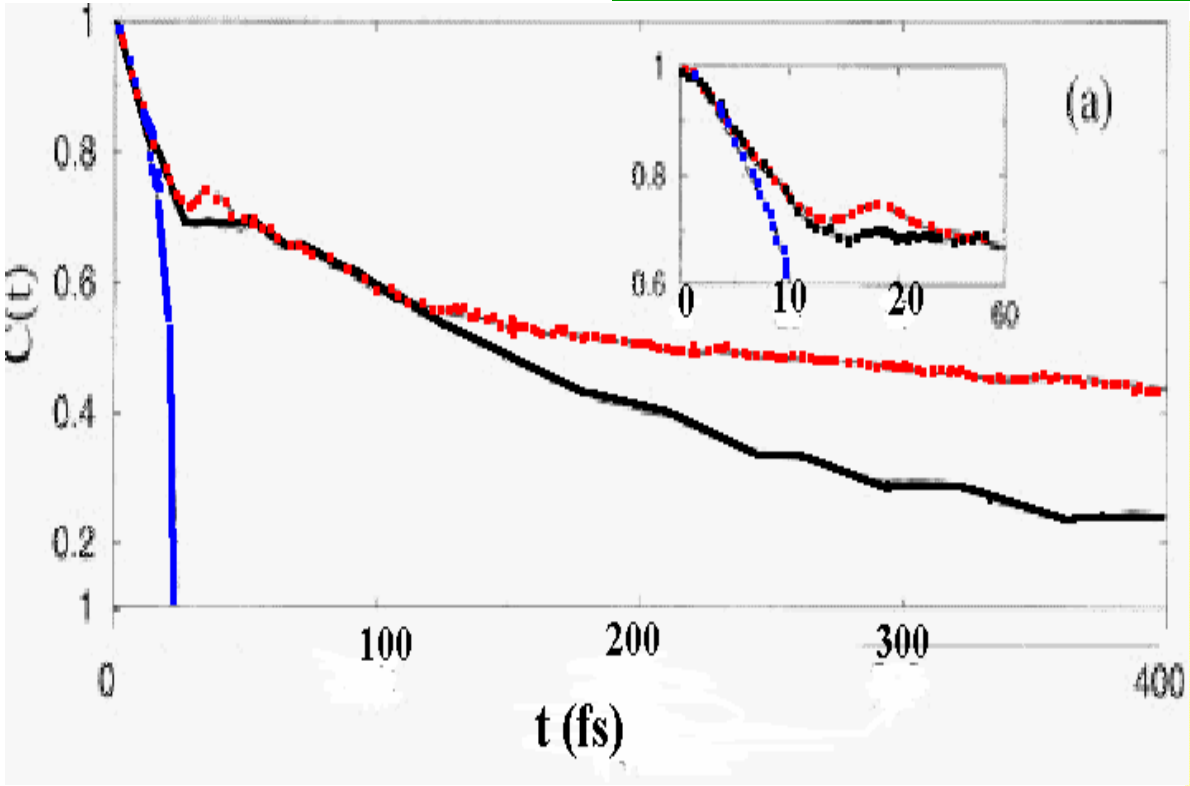

(Chao- Yie Yang, Kim F. Wong, Munir S. Skaf, and Peter J. Rossky; J. Chem. Phys. 2001)

Linearized INM and MD solvation response functions for upward (a) and downward (b) transitions. The solid lines are the MD results obtained from the fluctuations of the energy gap, the red lines are results of INM calculation using stable normal modes,and the blue lines stand for a calculation with all modes included.

$$T_{L\to R}(E',E)=\gamma_L\bar{G}^r(E)\gamma_R\bar{G}^a(E)\delta(E-E')$$

$$+MG^r(E)\gamma_L G^a(E)M^\dagger\bar{G}^a(E')\gamma_R\bar{G}^r(E')$$
$$\times\left[N_0\delta(E-E'+\omega_0)+(N_0+1)\delta(E-E'-\omega_0)\right]$$

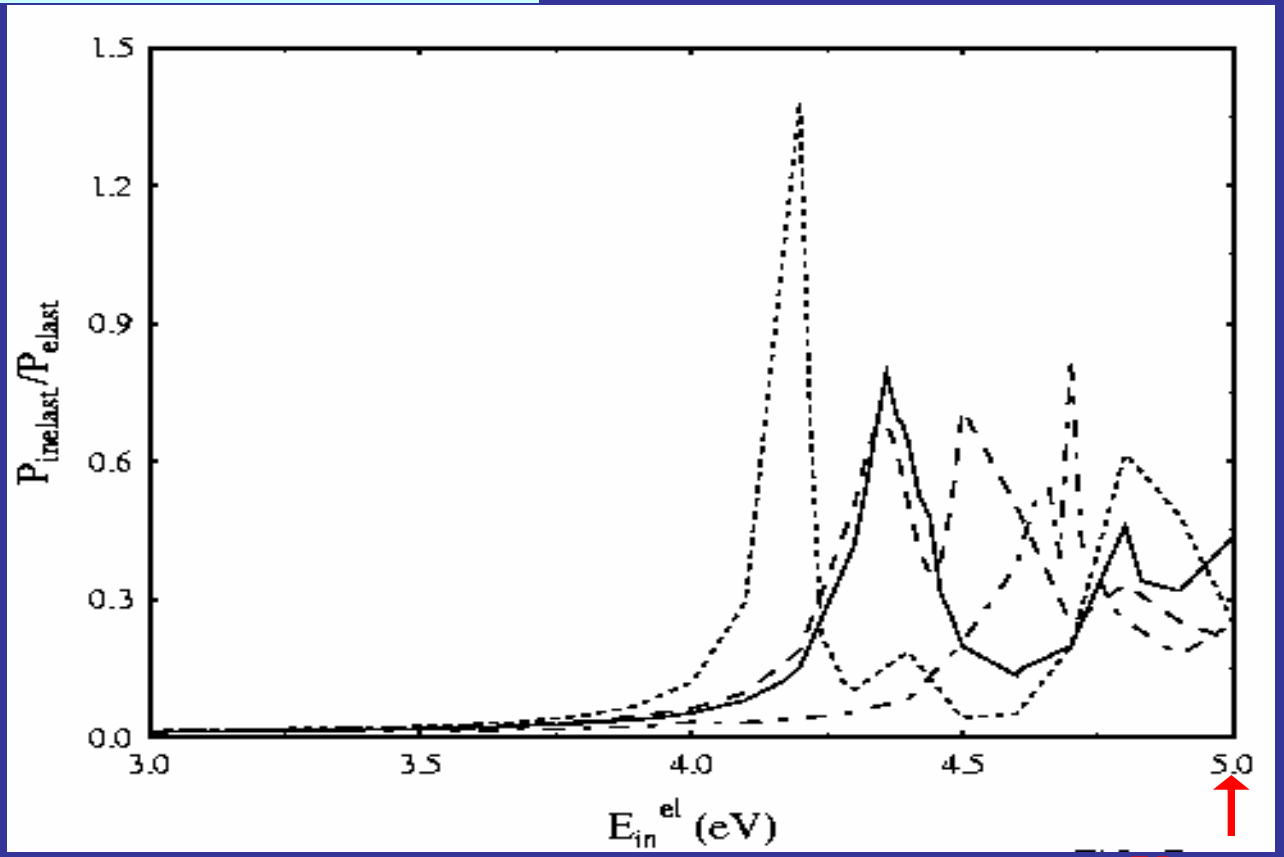

The ratio between the inelastic (integrated over all transmitted energies) and elastic components of the transmission probability calculated for different instantaneous structures of a water layer consisting of 3 monolayers of water molecules confined between two Pt(100) surfaces.

Vacuum barrier

Galperin & AN, J. Chem. Phys. **115**, 2681 (2001)

Barrier dynamics effects on electron transmission through molecular wires

- Relevant timescales
- Inelastic contributions to the tunneling current
- Dephasing and activation
- Heating of current carrying molecular wires
- HEAT CONDUCTION and rectification
- INELASTIC TUNNELING SPECTROSCOPY
- MULTISTABILITY AND HYSTERESIS
- LIGHT

Dependence on temperature

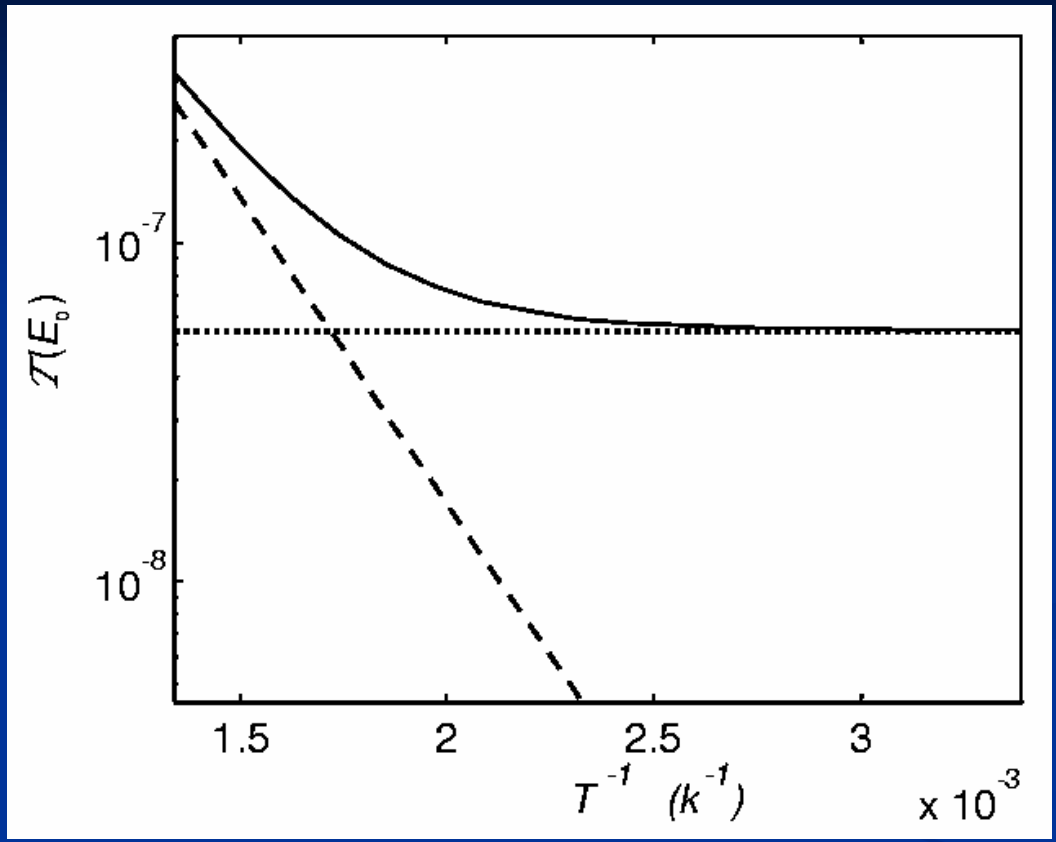

The integrated elastic (dotted line) and activated (dashed line) components of the transmission, and the total transmission probability (full line) displayed as function of inverse temperature. Parameters are as in Fig. 3.

The photosythetic reaction center

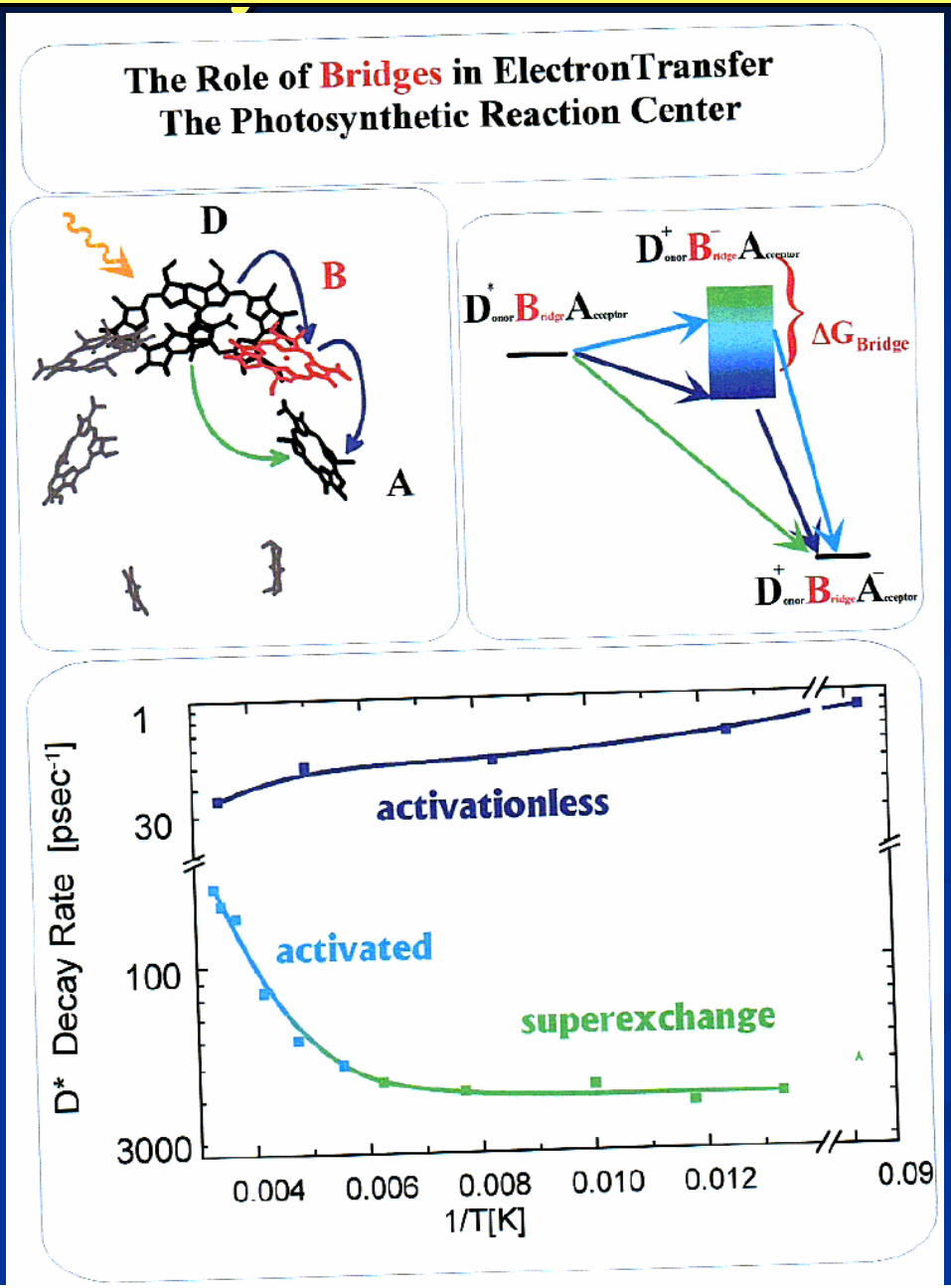

Yoram Selzer et al (2003)

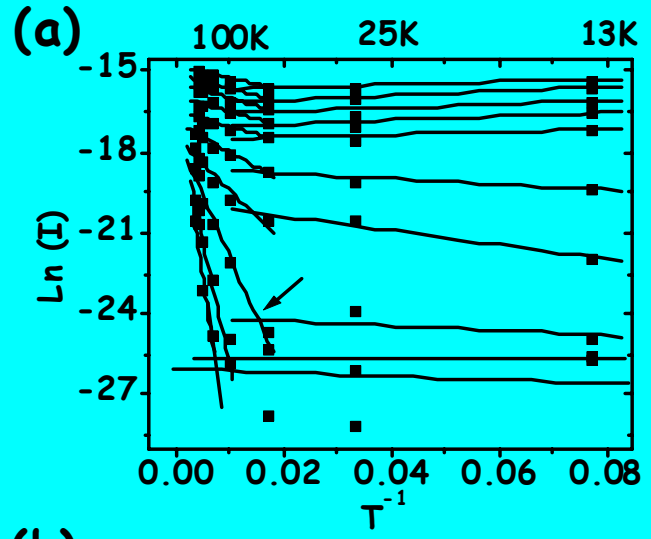

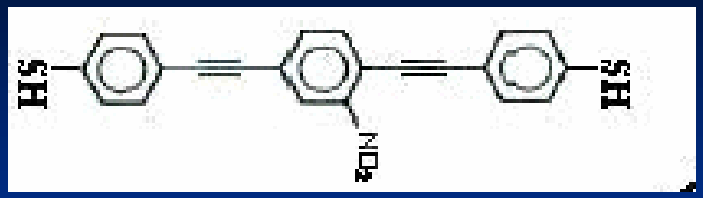

(a) Arrhenius plots of Ln current (Amperes) *vs* inverse T (K-1) at different bias voltages The transition temperatures (marked by the intersection between lines, pointed for at 0.3V by an arrow) are shifted to lower values with increasing bias. (b) Plot of the activation barrier, {ΔEBARRIER = -(1/k)[d(lnI)/d(1/T)]}, as a function of bias

Dependence on bridge length

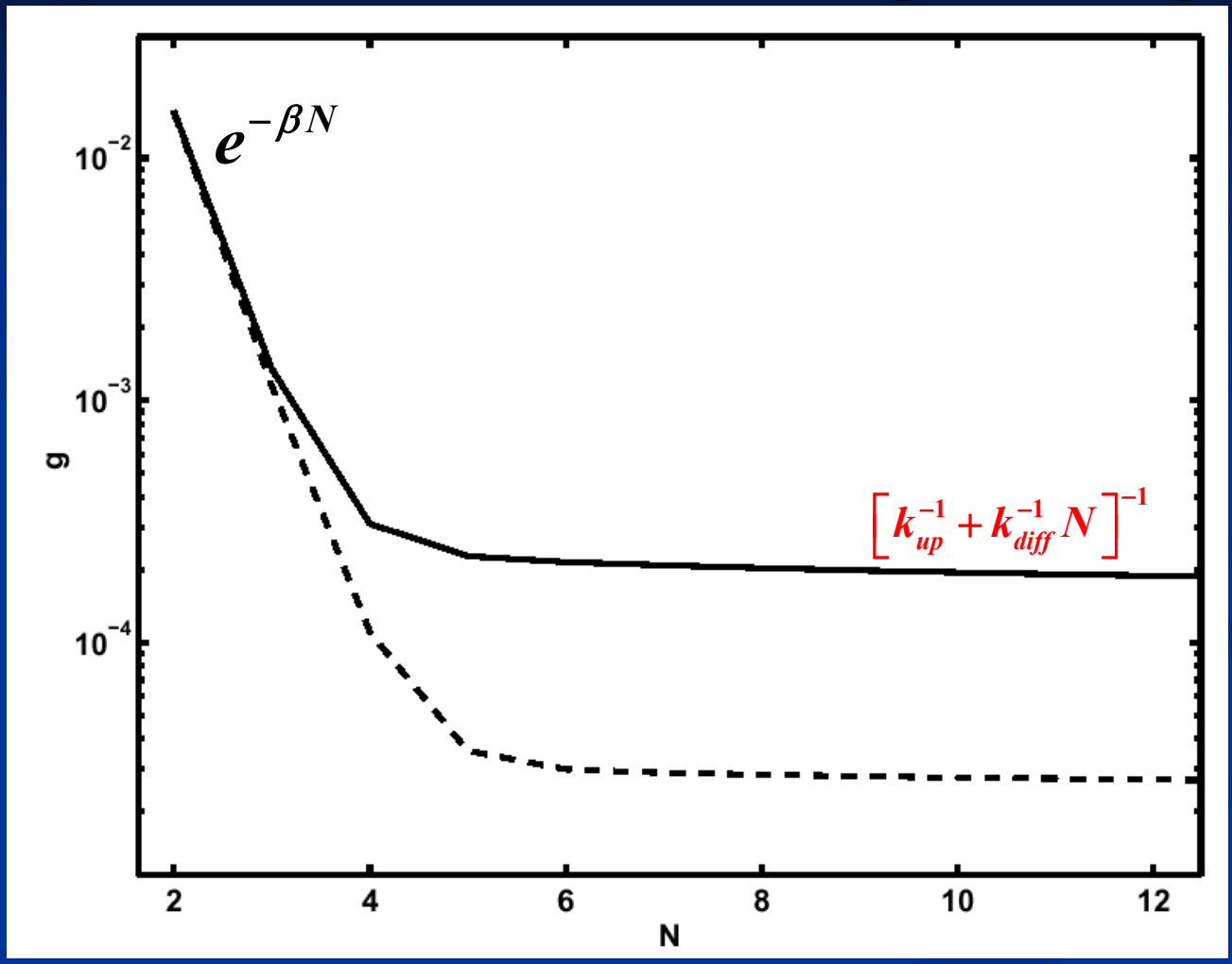

DNA (Giese et al 2001)

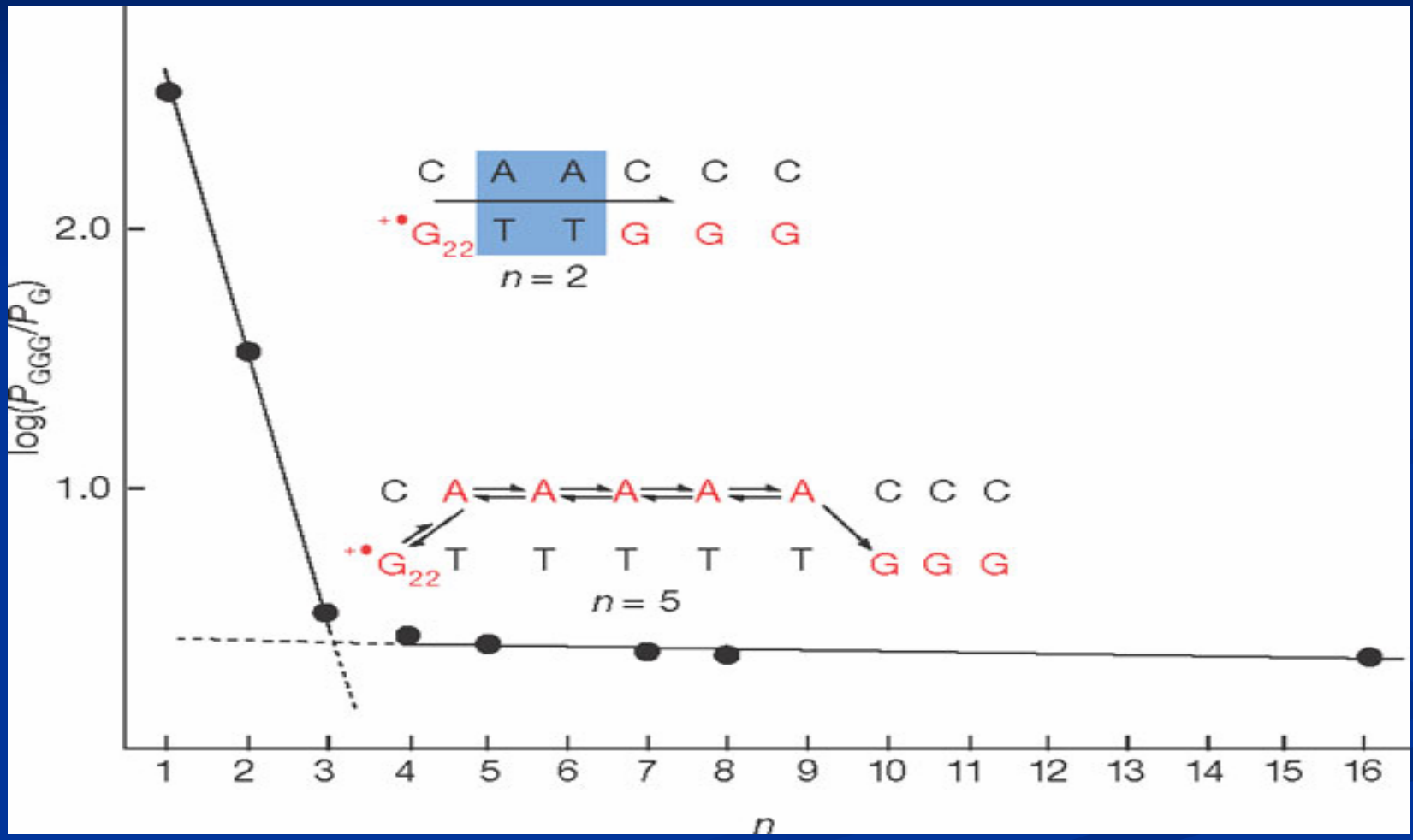

Tunneling through n-hexane

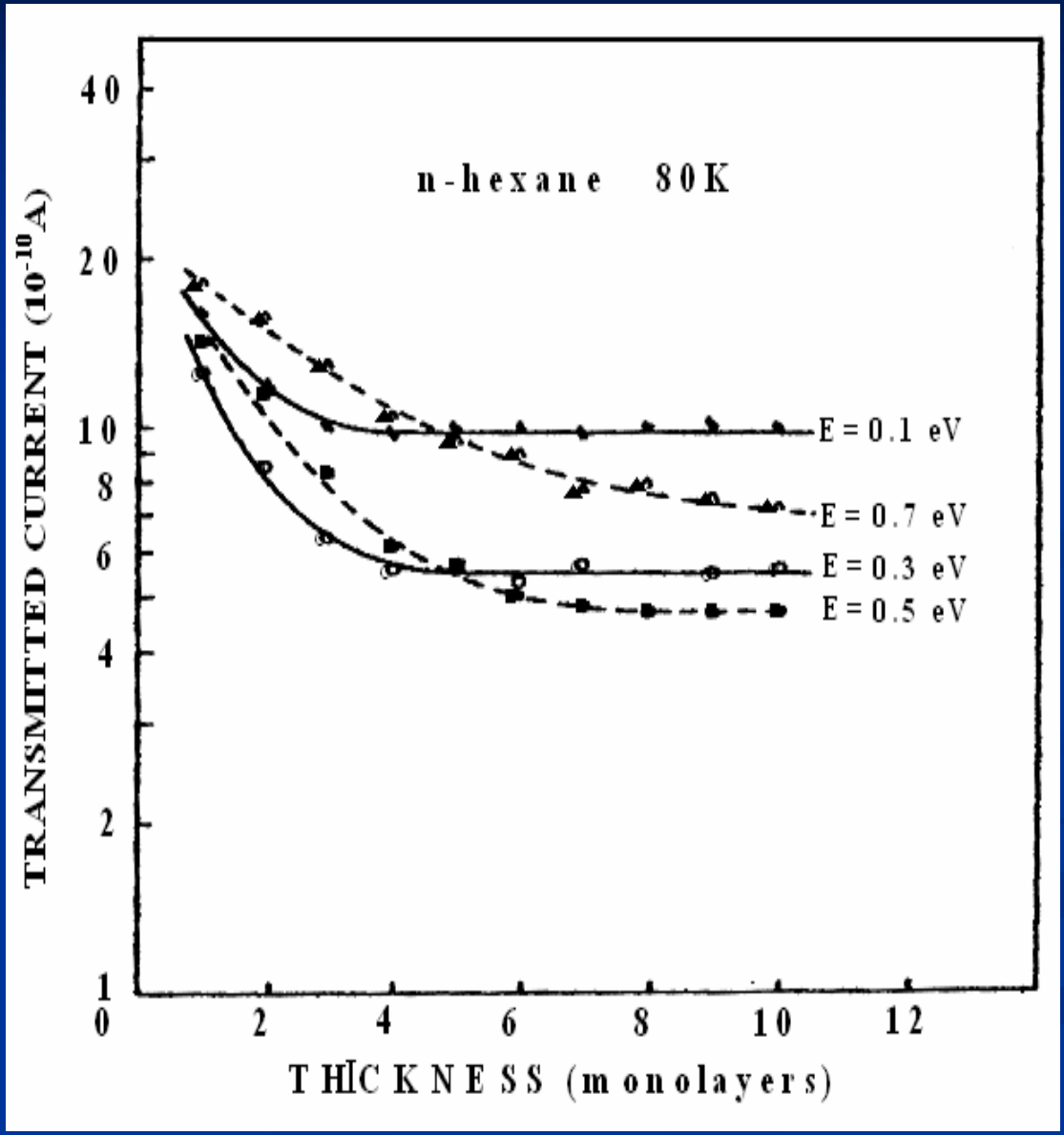

Barrier dynamics effects on electron transmission through molecular wires

- Relevant timescales
- Inelastic contributions to the tunneling current
- Dephasing and activation
- Heating of current carrying molecular wires
- HEAT CONDUCTION -- RECTIFICATION
- INELASTIC TUNNELING SPECTROSCOPY
- MULTISTABILITY AND HYSTERESIS
- LIGHT

Light Scattering

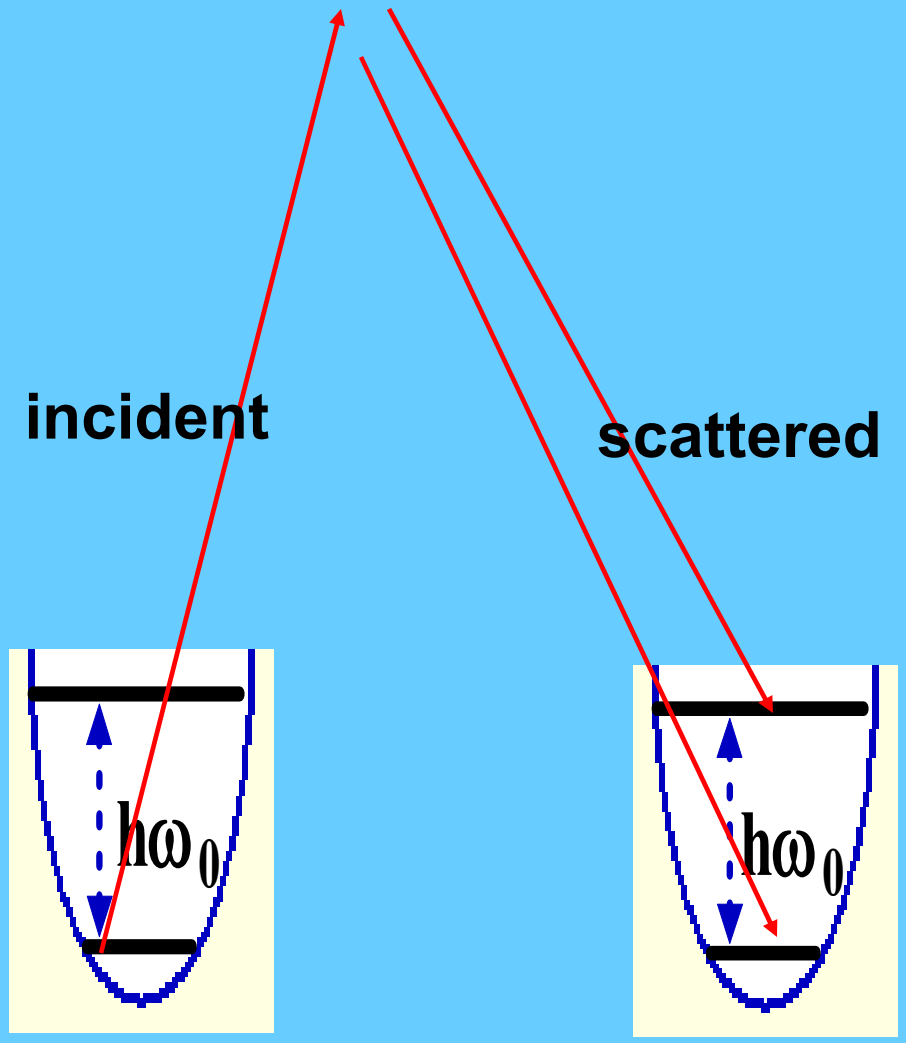

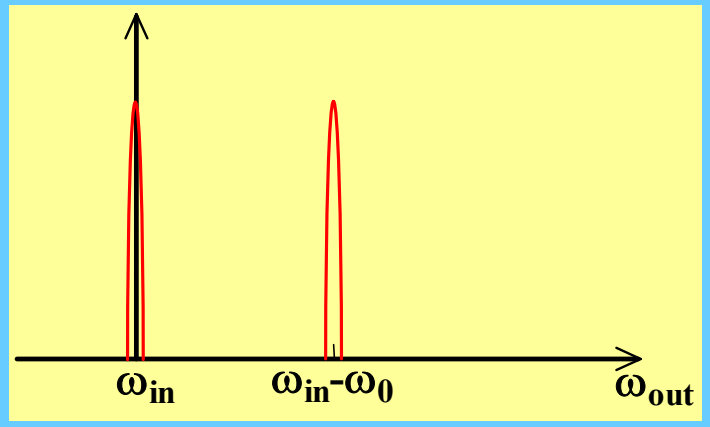

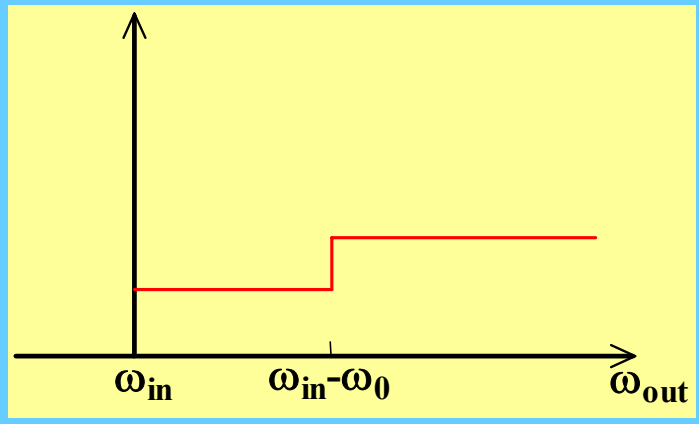

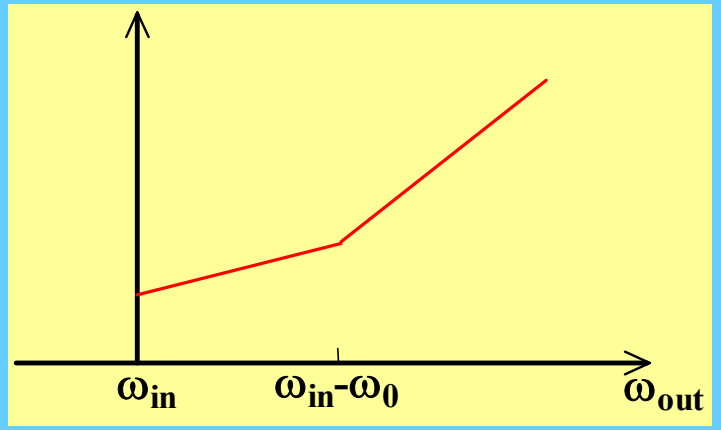

INELSTIC ELECTRON TUNNELING SPECTROSCOPY

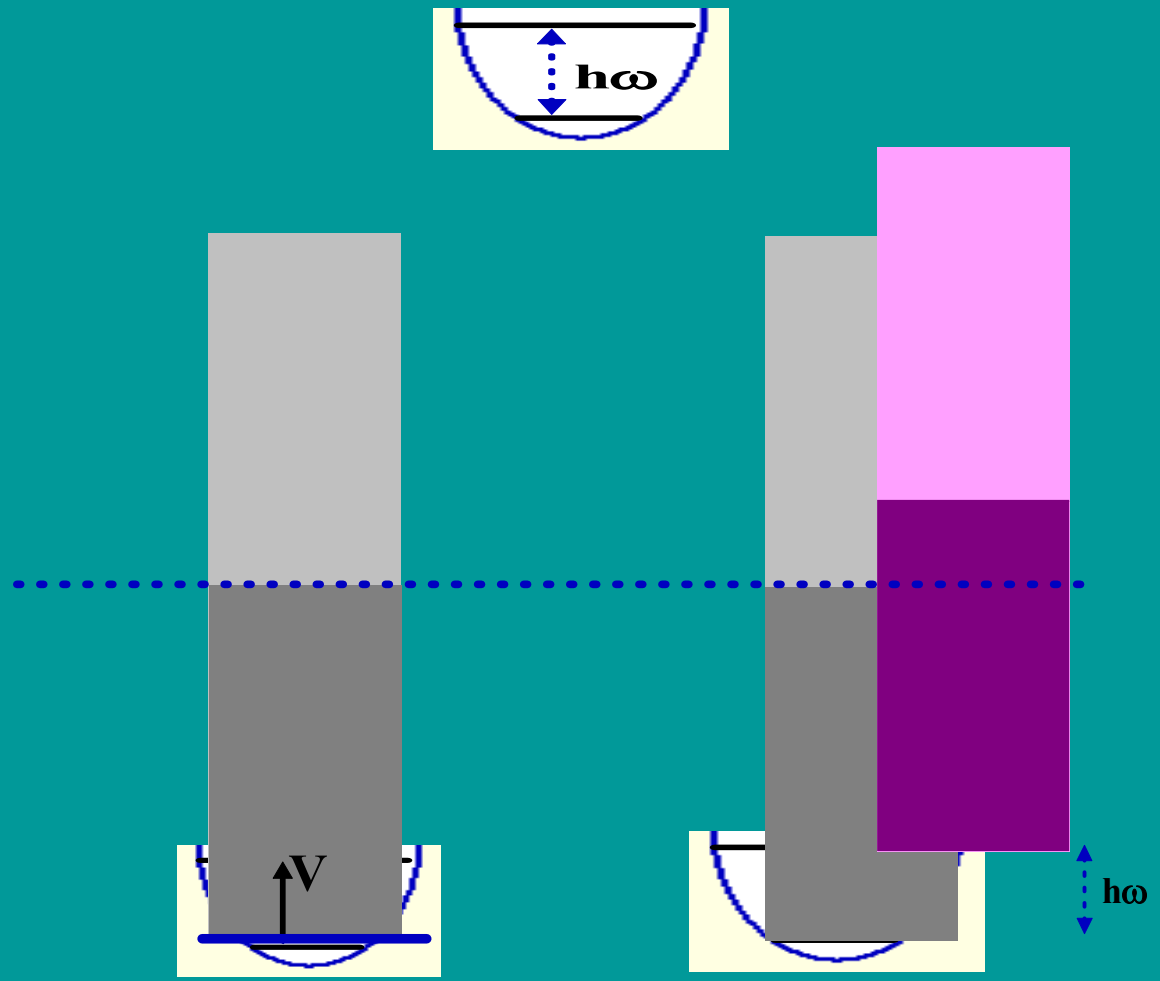

Localization of Inelastic Tunneling and the Determination of Atomic-Scale Structure with Chemical Specificity

B.C.Stipe, M.A.Rezaei and W. Ho, PRL, 82, 1724 (1999)

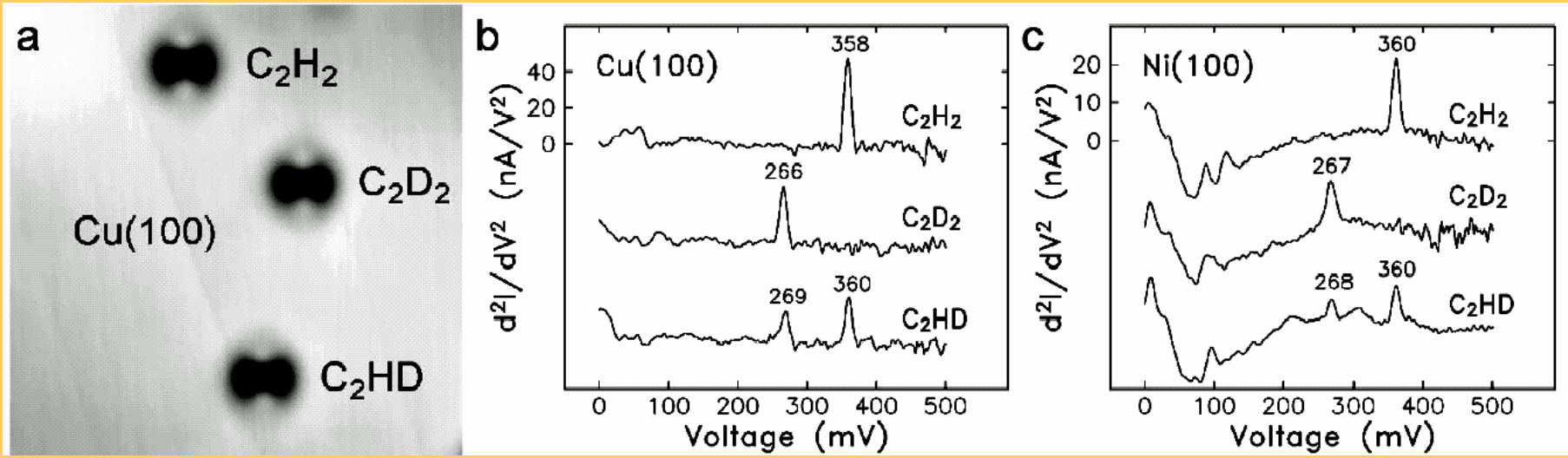

STM image (a) and single-molecule vibrational spectra (b) of three acetylene isotopes on Cu(100) at 8 K. The vibrational spectra on Ni(100)are shown in (c). The imaged area in (a), 56Å x 56Å, was scanned at 50 mV sample bias and 1nA tunneling current

Recall: van Ruitenbeek et al (Pt/H_2)- dips

Electronic Resonance and Symmetry in Single-Molecule Inelastic Electron Tunneling

J.R.Hahn,H.J.Lee,and W.Ho, PRL 85, 1914 (2000)

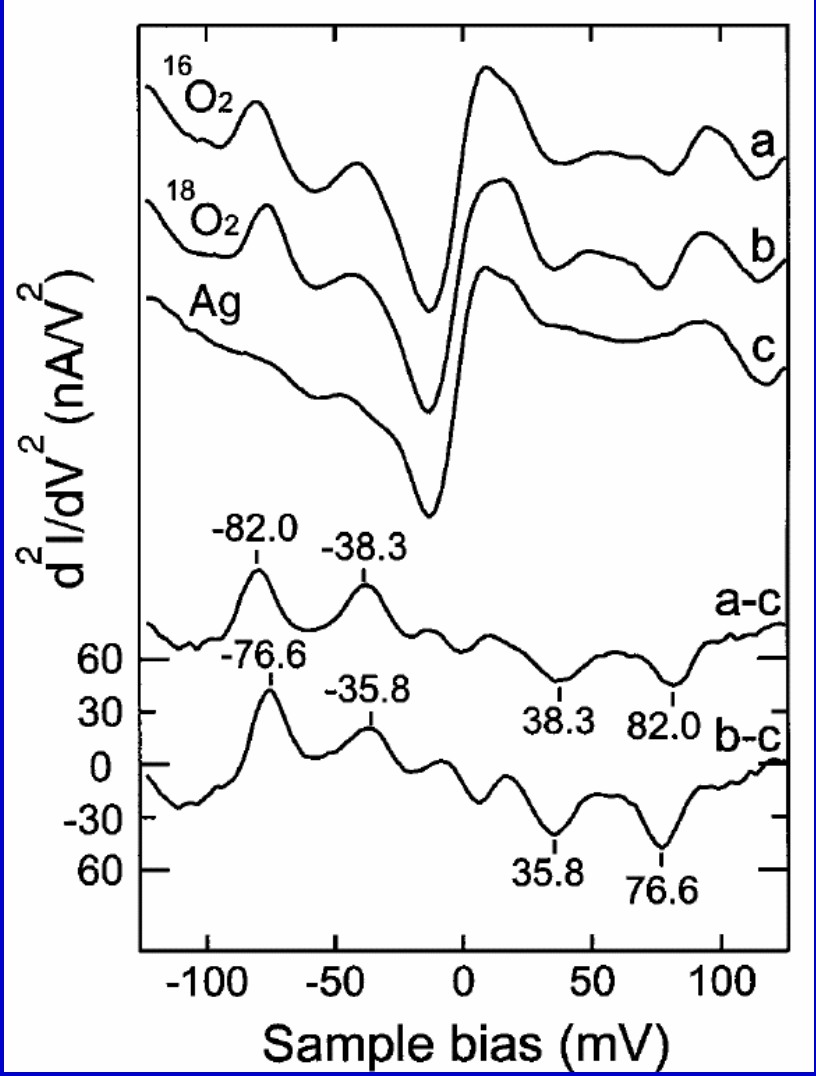

Single molecule vibrational spectra obtained by STM-IETS for $^{16}O_2$ (curve a),$^{18}O_2$ (curve b), and the clean Ag(110)surface (curve c).The O2 spectra were taken over a position 1.6 Å from the molecular center along the [001] axis.

The feature at 82.0 (76.6)meV for $^{16}O_2$ ($^{18}O_2$) is assigned to the O-O stretch vibration, in close agreement with the values of 80 meV for 16O2 obtained by EELS.
The symmetric O2 -Ag stretch (30 meV for 16O2) was not observed.The vibrational feature at 38.3 (35.8)meV for $^{16}O_2$ ($^{18}O_2$)is attributed to the antisymmetric O_2 -Ag stretch vibration.

Inelastic Electron Tunneling Spectroscopy of Alkanedithiol Self-Assembled Monolayers

W. Wang, T. Lee, I. Kretzschmar and M. A. Reed (Yale, 2004)

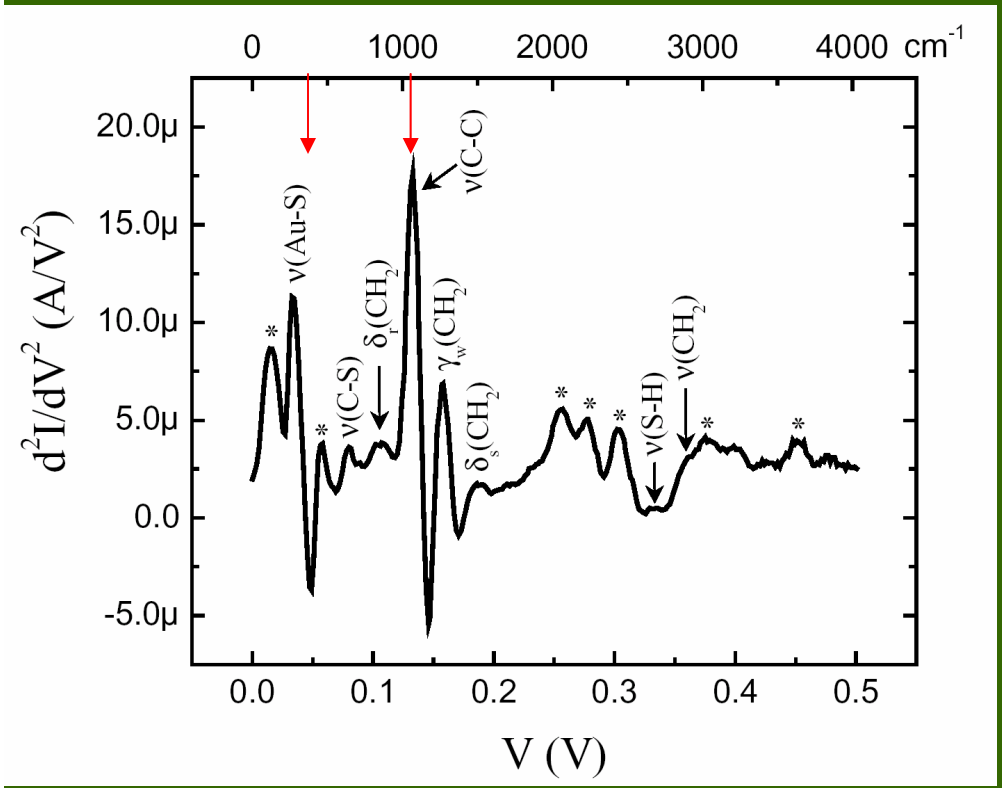

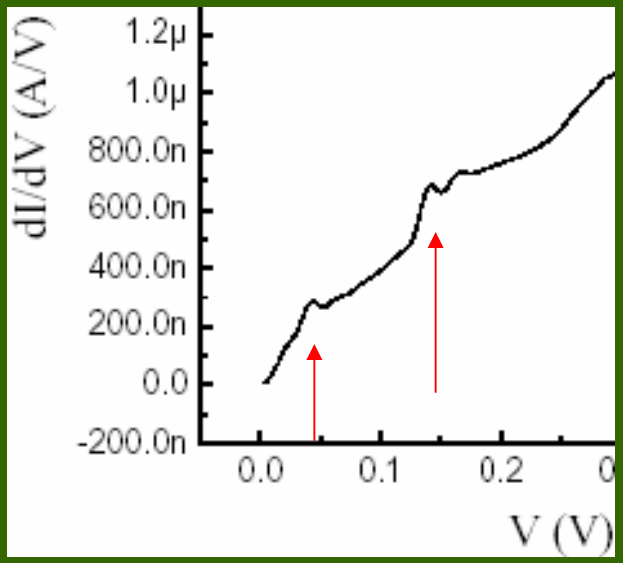

Inelastic electron tunneling spectra of C8 dithiol SAM obtained from lock-in second harmonic measurements with an AC modulation of 8.7 mV (RMS value) at a frequency of 503 Hz (T =4.2 K).Peaks labeled *are most probably background due to the encasing Si3N4

Nano letters, in press

Nanomechanical oscillations in a single C_{60} transistor

H. Park, J. Park, A.K.L. Lim, E.H. Anderson, A. P. Alivisatos and P. L. McEuen [NATURE, 407, 57 (2000)]

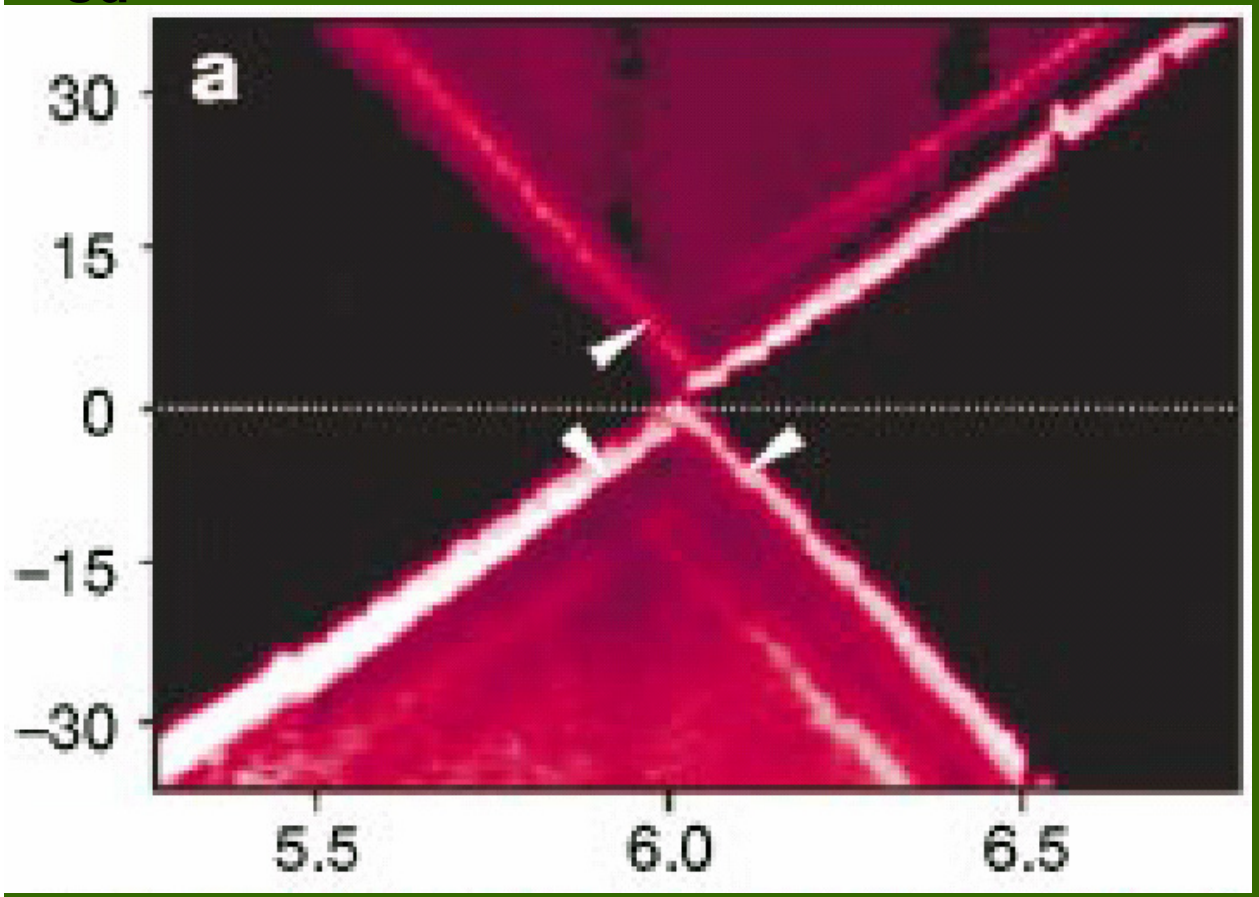

Two-dimensional differential conductance (∂I/∂V)plots as a function of the bias voltage (V) and the gate voltage (Vg). The dark triangular regions correspond to the conductance gap, and the bright lines represent peaks in the differential conductance.

Conductance of Small Molecular Junctions

N.B.Zhitenev, H.Meng and Z.Bao

PRL 88, 226801 (2002)

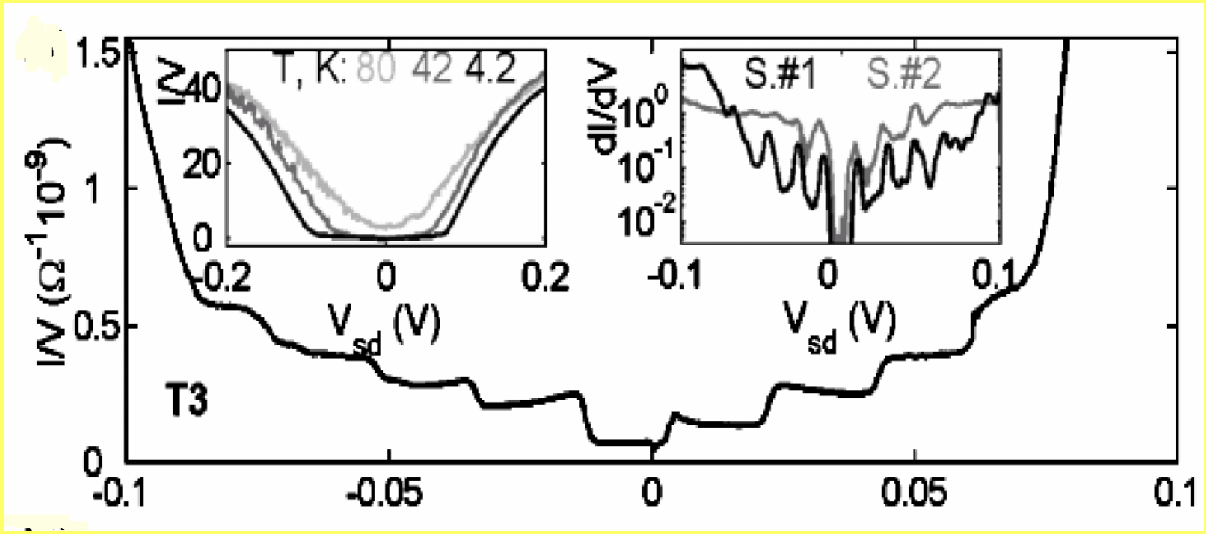

38mV

22

125

35,45,24

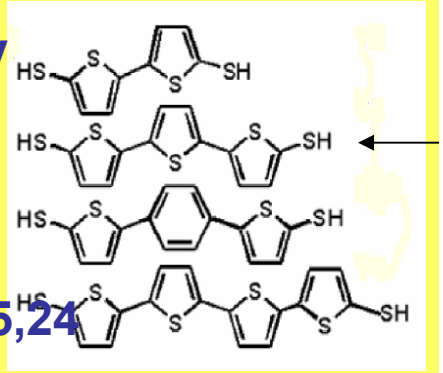

Conductance of the T3 sample as a function of source-drain bias at *T* =4.2 K. The steps in conductance are spaced by 22 mV.
Left inset: conductance vs source-drain bias curves taken at different temperatures for the T3 sample (the room temperature curve is not shown because of large switching noise).
Right inset: differential conductance vs source-drain bias measured for two different T3 samples at *T* = 4.2 K.

MODEL

$$\hat{H}_0 = \varepsilon_0 \hat{c}^\dagger \hat{c} + \sum_{k \in L,R} \varepsilon_k^{L,R} \hat{d}_k^\dagger \hat{d}_k + \omega_0 \hat{a}^\dagger \hat{a} + \sum_m \omega_m \hat{b}_m^\dagger \hat{b}_m$$

$$\hat{H}_1 = \sum_{k \in L,R} \left(V_{ki} \hat{d}_k^\dagger \hat{c} + h.c. \right) + \sum_m U_m \hat{A} \hat{B}_m + M \hat{A} \hat{c}^\dagger \hat{c}$$

$$\hat{A} = \hat{a}^\dagger + \hat{a} \; ; \quad \hat{B} = \hat{b}^\dagger + \hat{b}$$

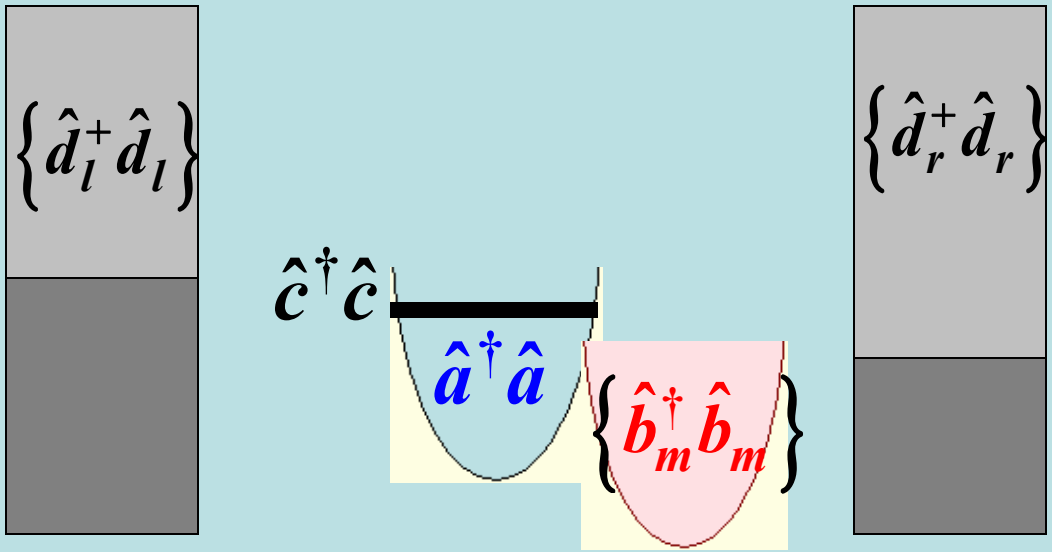

Parameters

Constant in the wide band approximation

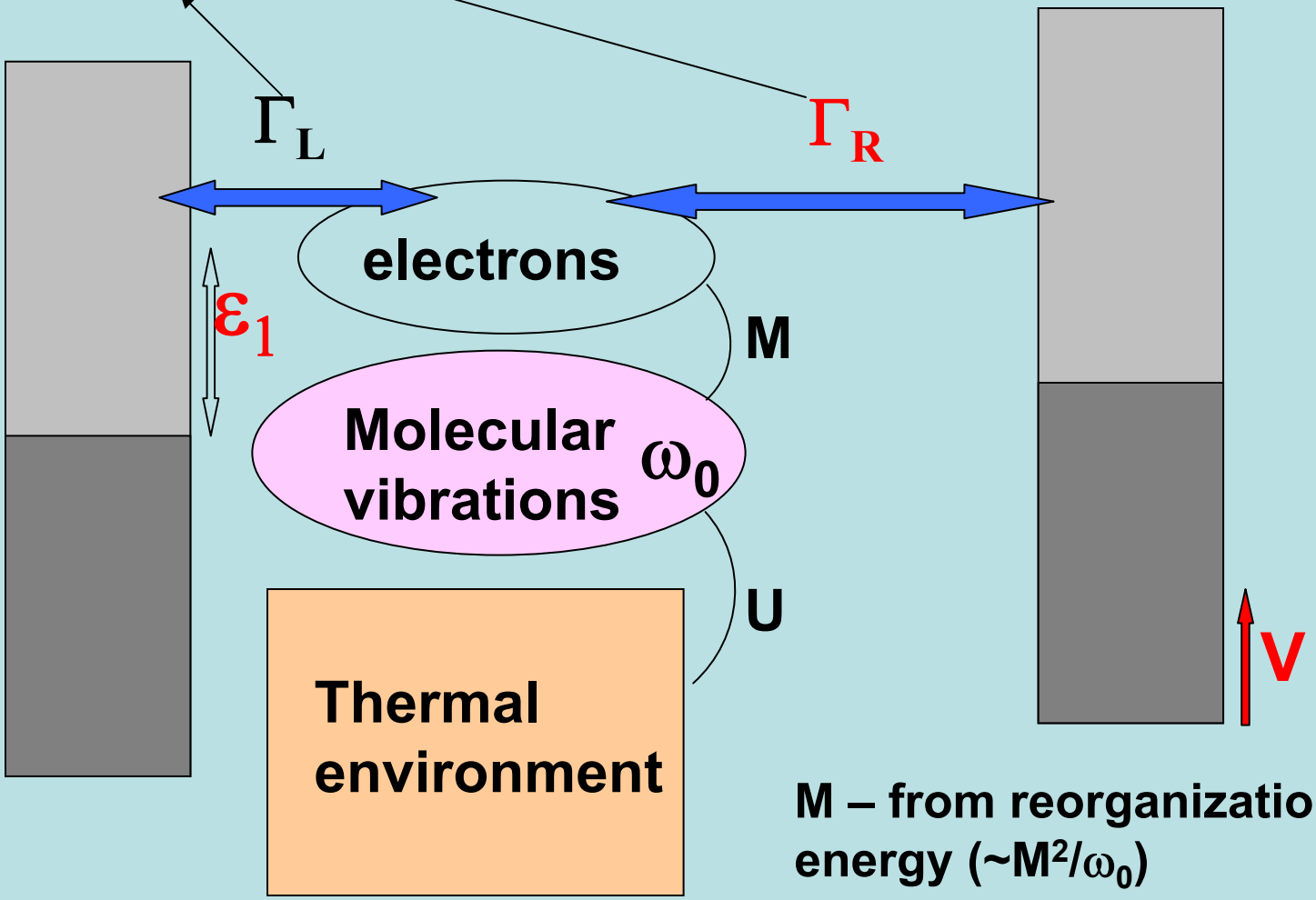

M – from reorganization energy ($\sim M^2/\omega_0$)

U – from vibrational relaxation rates

NEGF

$$G_{n,n'}^{\ r}(t,t') = -i\Theta(t-t')\left\langle \left\{ a_n(t), a_{n'}^{\ \dagger}(t') \right\} \right\rangle$$

$$G_{n,n'}^{\ a}(t,t') = i\Theta(t'-t)\left\langle \left\{ a_n(t), a_{n'}^{\ \dagger}(t') \right\} \right\rangle$$

({ }=anticommutator)

$$G_{n,n'}^{\ <}(t,t') = +i\left\langle a_{n'}^{\ \dagger}(t') a_n(t) \right\rangle$$

$$G_{n,n'}^{\ >}(t,t') = -i\left\langle a_n(t) a_{n'}^{\ \dagger}(t') \right\rangle$$

$$G^r(\omega) = G_0^r(\omega) + G^r(\omega)\Sigma^r(\omega)G_0^r(\omega)$$

$$G^a(\omega) = G_0^a(\omega) + G^a(\omega)\Sigma^a(\omega)G_0^a(\omega)$$

$$G^> = G^r\Sigma^> G^a$$

$$G^< = G^r\Sigma^< G^a$$

$$\Sigma_{ph}^r(E) = iM^2\int\frac{d\omega}{2\pi}\Big[D^<(\omega)G^r(E-\omega) + D^<(\omega)G^<(E-\omega) + D^r(\omega)G^r(E-\omega)\Big]$$

$$\Sigma_{ph}^<(E) = iM^2\int\frac{d\omega}{2\pi}D^<(\omega)G^<(E-\omega)$$

$$G_{jj'}^{0,r}(\omega) = \delta_{jj'}\frac{1}{\omega-\varepsilon_j+i\eta}$$

$$G_{jj'}^{0,a}(\omega) = \delta_{jj'}\frac{1}{\omega-\varepsilon_j-i\eta}$$

$$\rho_j(E) = -\frac{1}{\pi}\mathrm{Im}\,G_{jj}^r(E)$$

$$G_{j,j'}^{0,<}(\omega) = \delta_{j,j'}2\pi i f(\varepsilon_j)\delta(\omega-\varepsilon_j)$$

$$n_j(E) = \frac{1}{2\pi}\mathrm{Im}\,G_{jj}^<(E)$$

$$G_{j,j'}^{0,>}(\omega) = -\delta_{j,j'}2\pi i\Big[1-f(\varepsilon_j)\Big]\delta(\omega-\varepsilon_j)$$

$$I = \frac{q}{\hbar}\int\frac{dE}{2\pi}Tr\Big[\Sigma^<(E)G^>(E) - \Sigma^>(E)G^<(E)\Big]$$

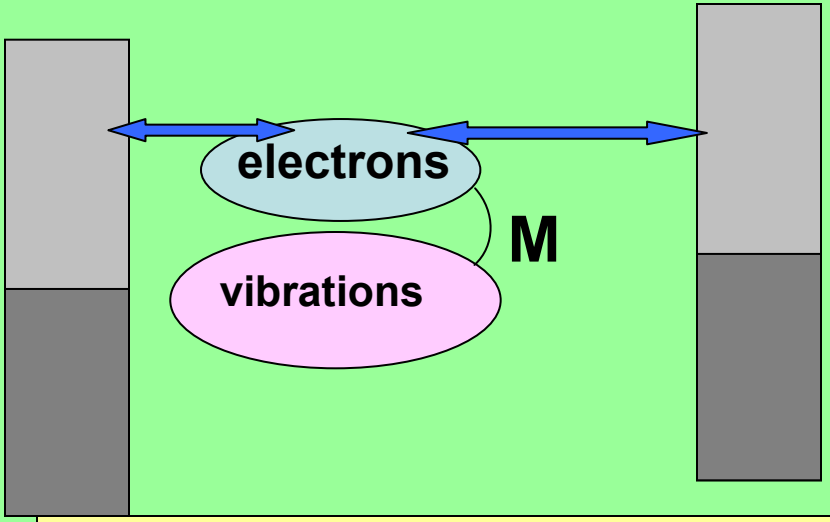

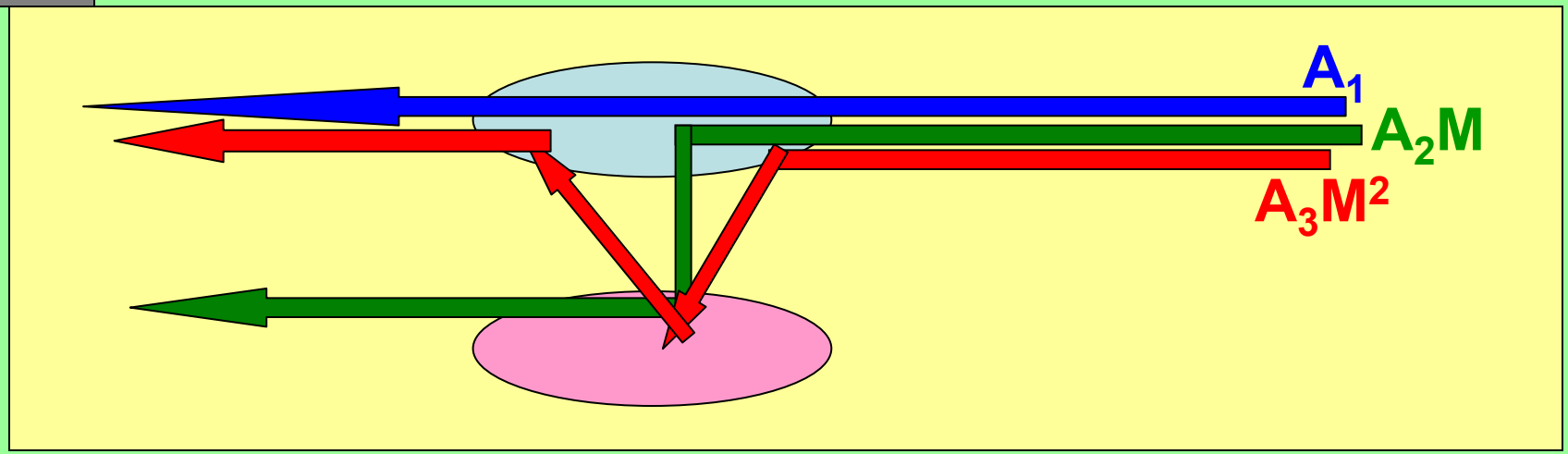

$$\left(A_1 + A_2 M + A_3 M^2\right)^2 = A_1^{\,2} + M^2\left(A_2^{\,2} + A_1 A_3\right)$$

elastic inelastic elastic

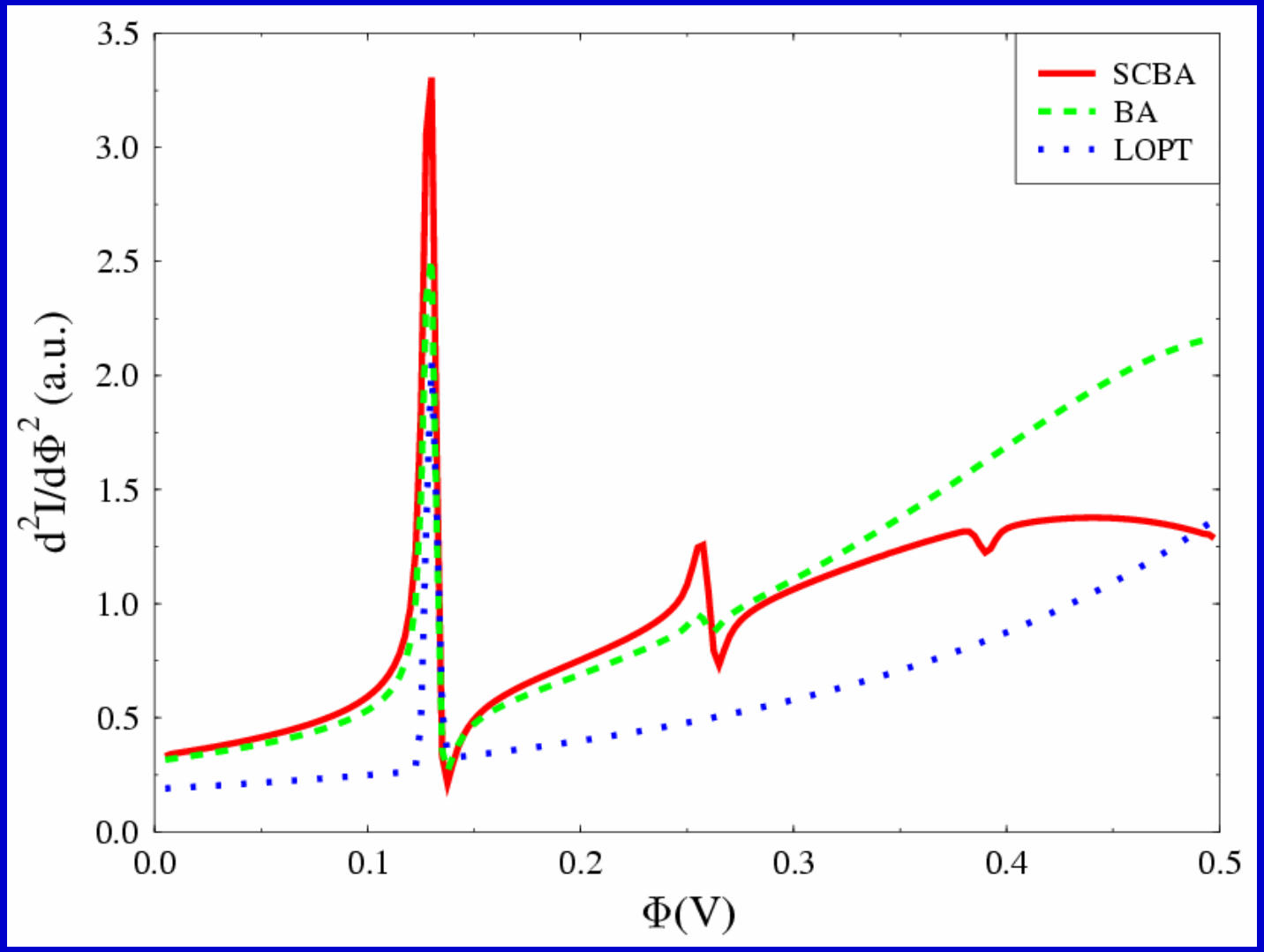
SCBA
BA
LOPT
3.5
3.0
2.5
2.0
1.5
1.0
0.5
0.0
0.0
0.1
0.2
0.3
0.4
0.5
d²I/dΦ² (a.u.)
Φ(V)

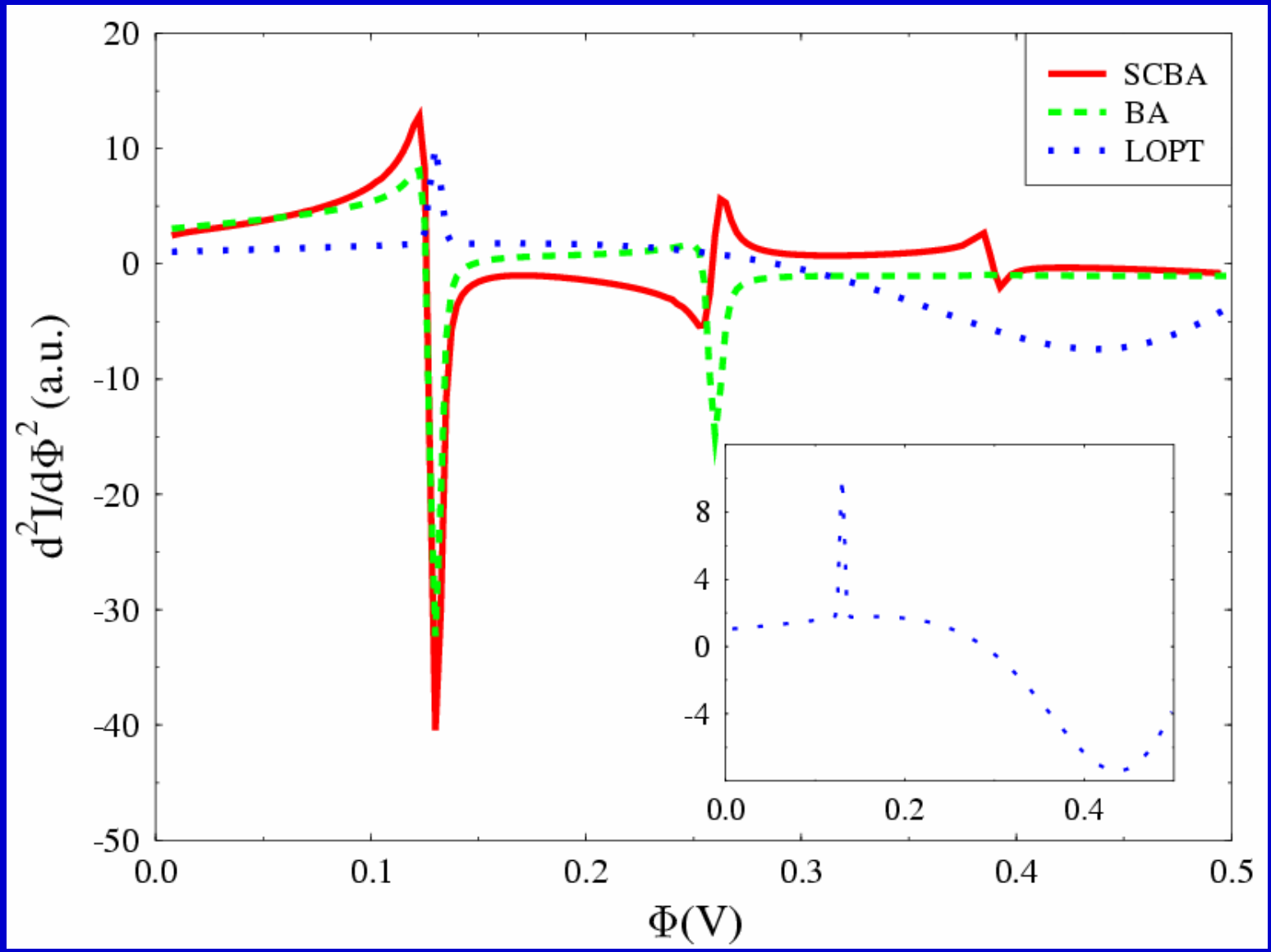
SCBA
BA
LOPT
20
10
0
-10
-20
-30
-40
-50
0.0
0.1
0.2
0.3
0.4
0.5
$d^2I/d\Phi^2$ (a.u.)
Φ(V)
8
4
0
-4
0.0
0.2
0.4

Changing position of molecular resonance:

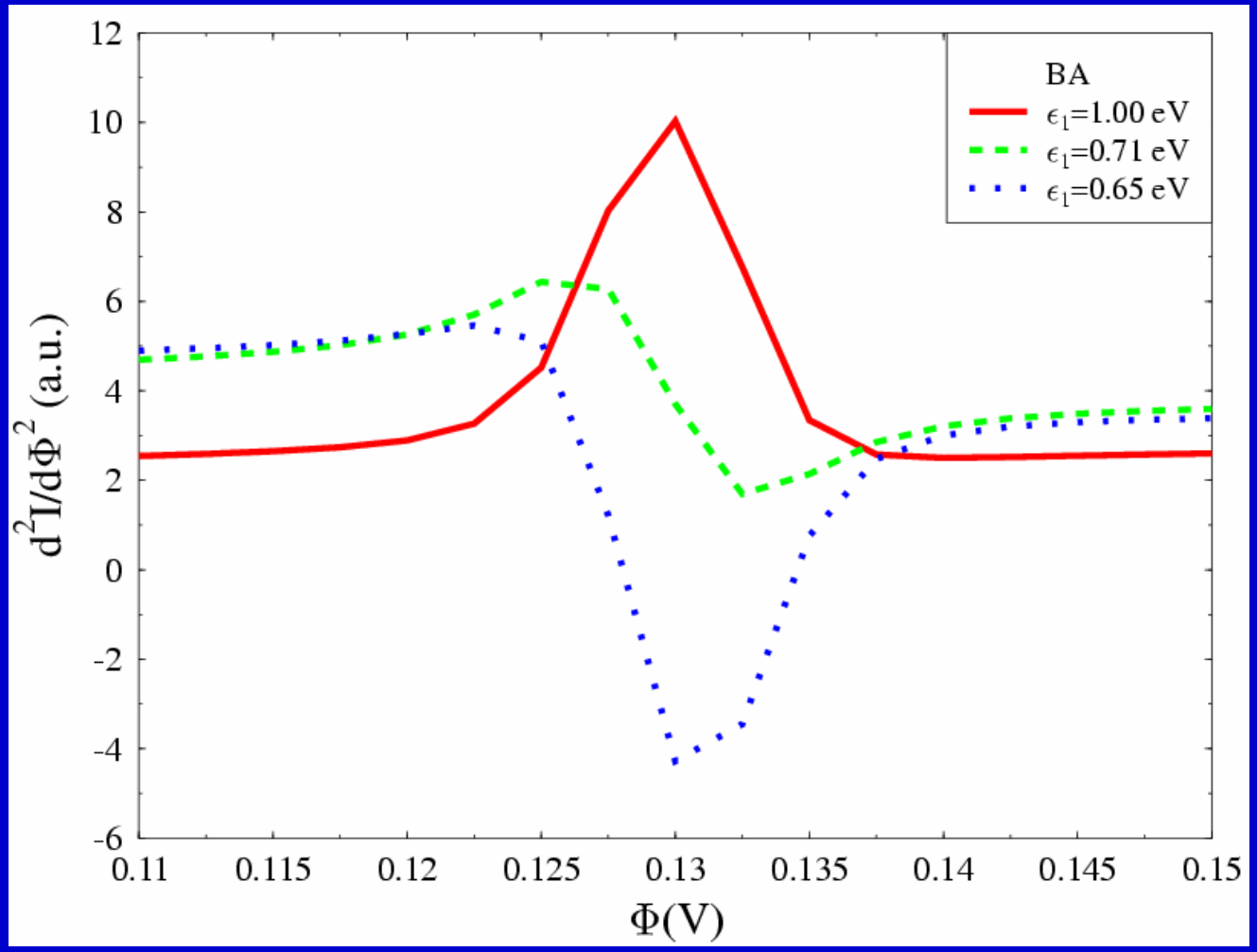

Changing tip-molecule distance

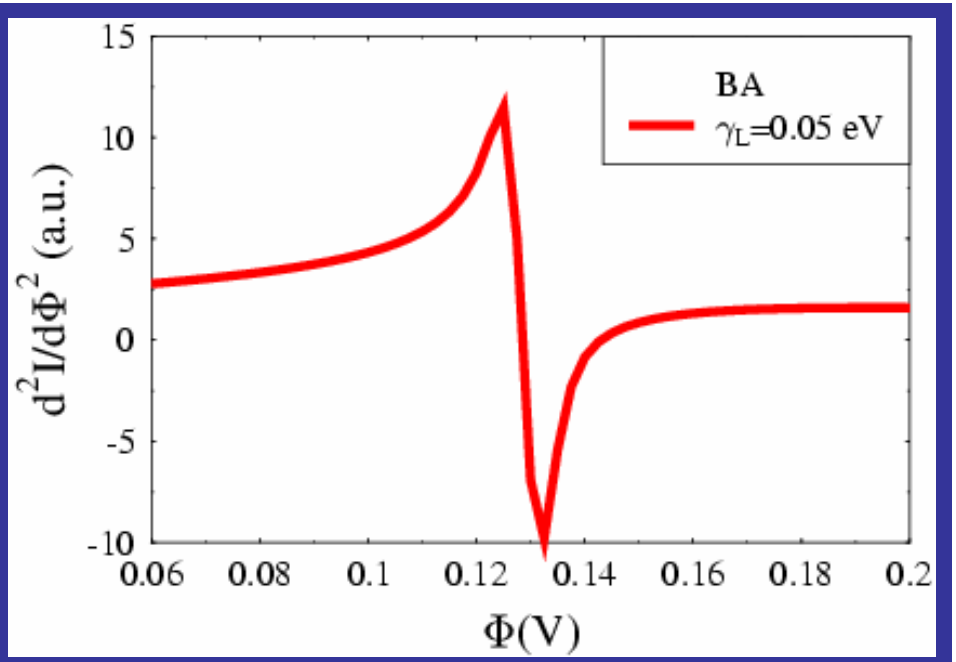

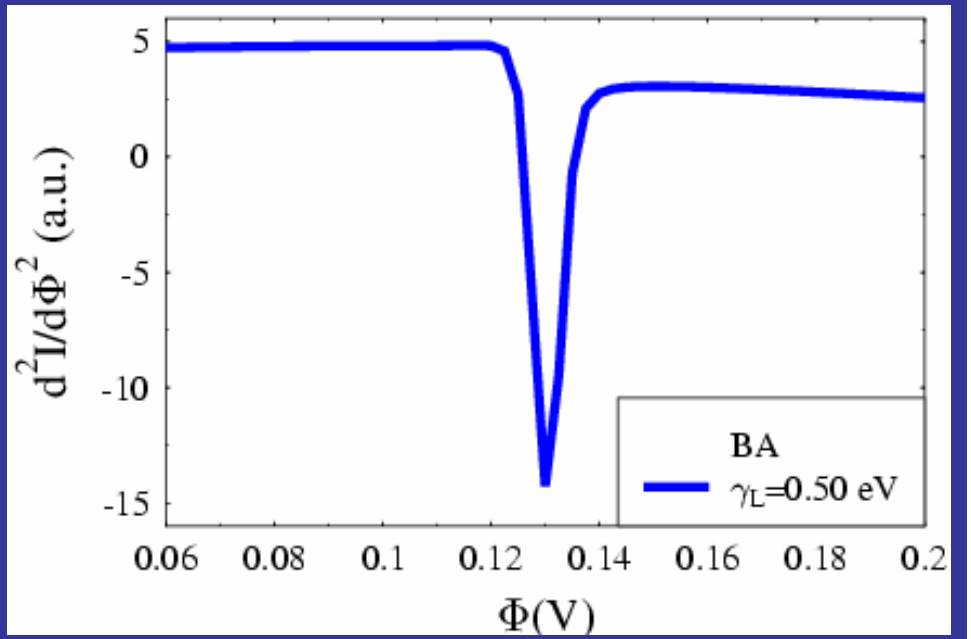

IETS (intrinsic?) linewidth

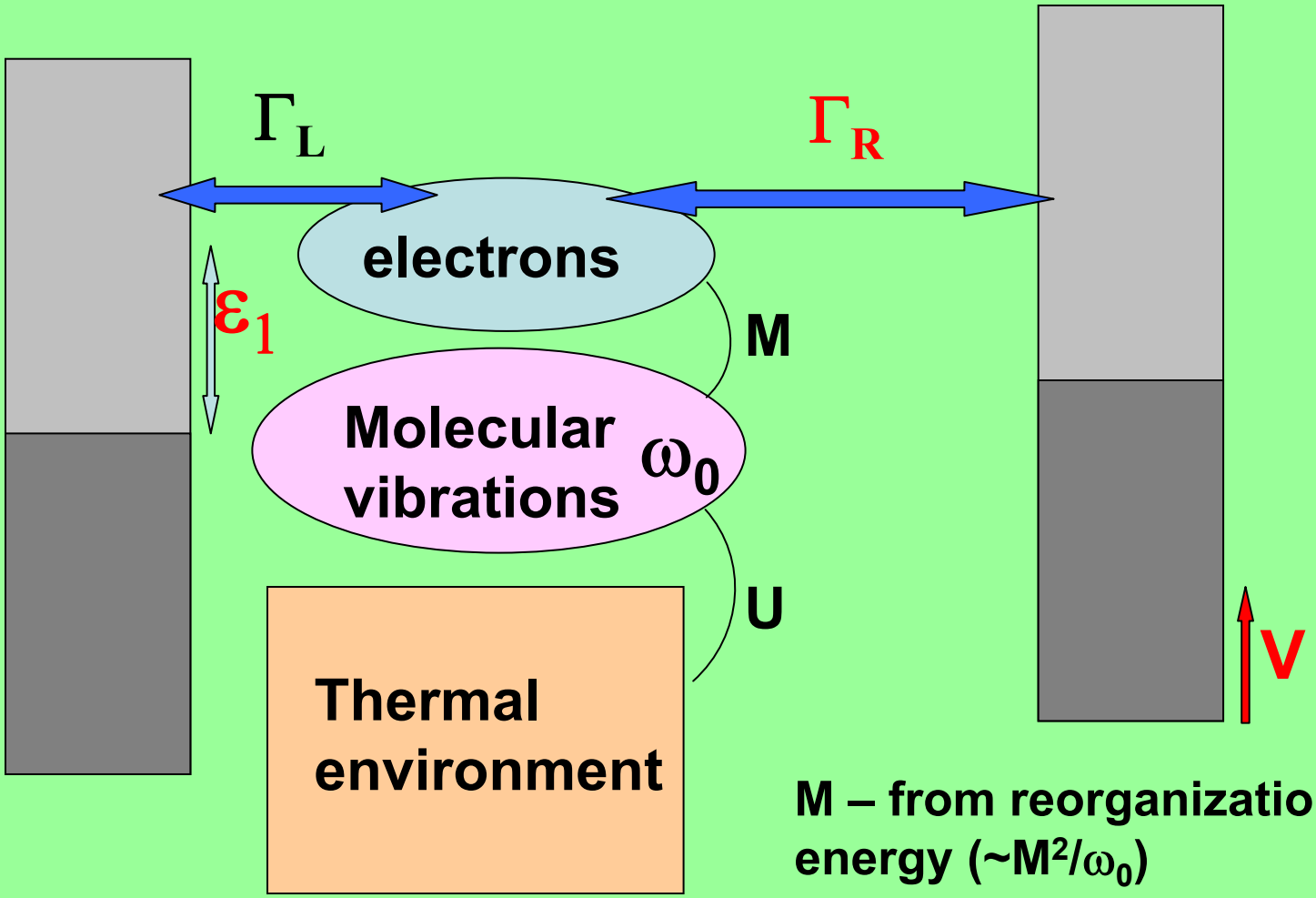

M – from reorganization energy (~M^2/ω_0)

U – from vibrational relaxation rates

IETS linewidth

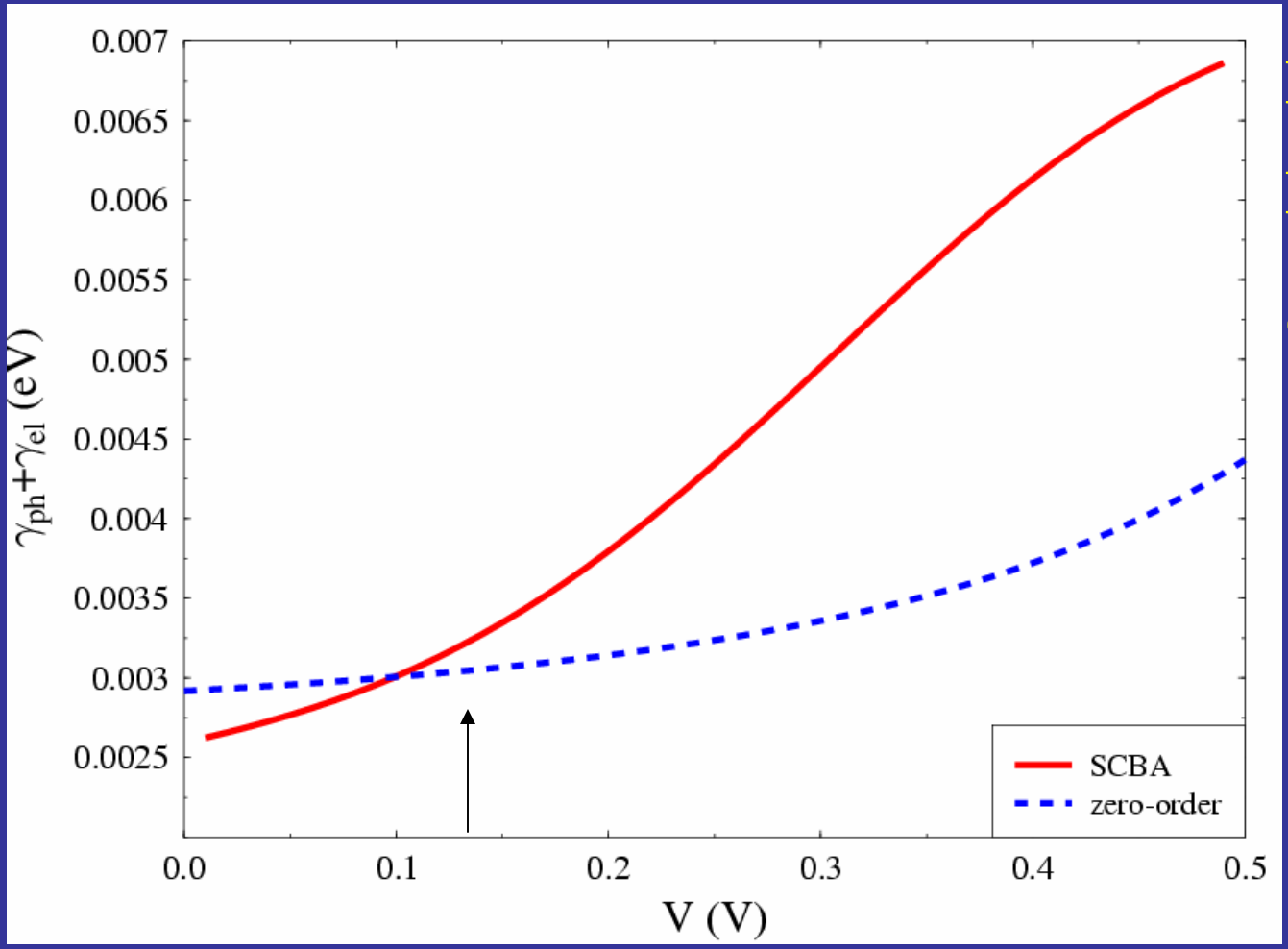

ε_1=1eV

Γ_L=0.5eV

Γ_R=0.05eV

ω_0=0.13eV

M^2/ω_0=0.7eV

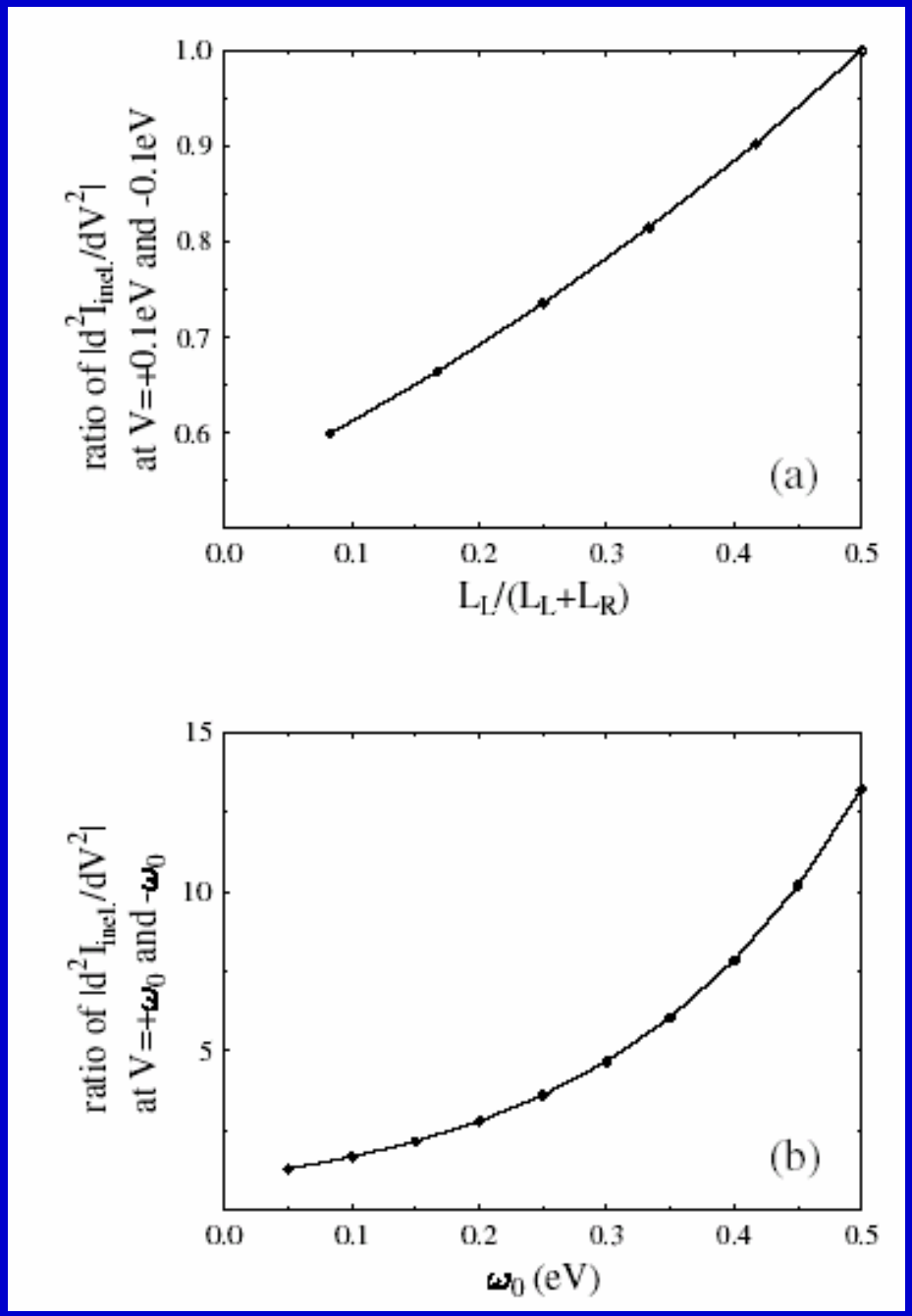
ratio of $|d^2I_{inel.}/dV^2|$ at V=+0.1eV and -0.1eV
1.0
0.9
0.8
0.7
0.6
(a)
0.0
0.1
0.2
0.3
0.4
0.5
$L_L/(L_L+L_R)$
ratio of $|d^2I_{inel.}/dV^2|$ at V=+ω_0 and -ω_0
15
10
5
(b)
0.0
0.1
0.2
0.3
0.4
0.5
ω_0 (eV)

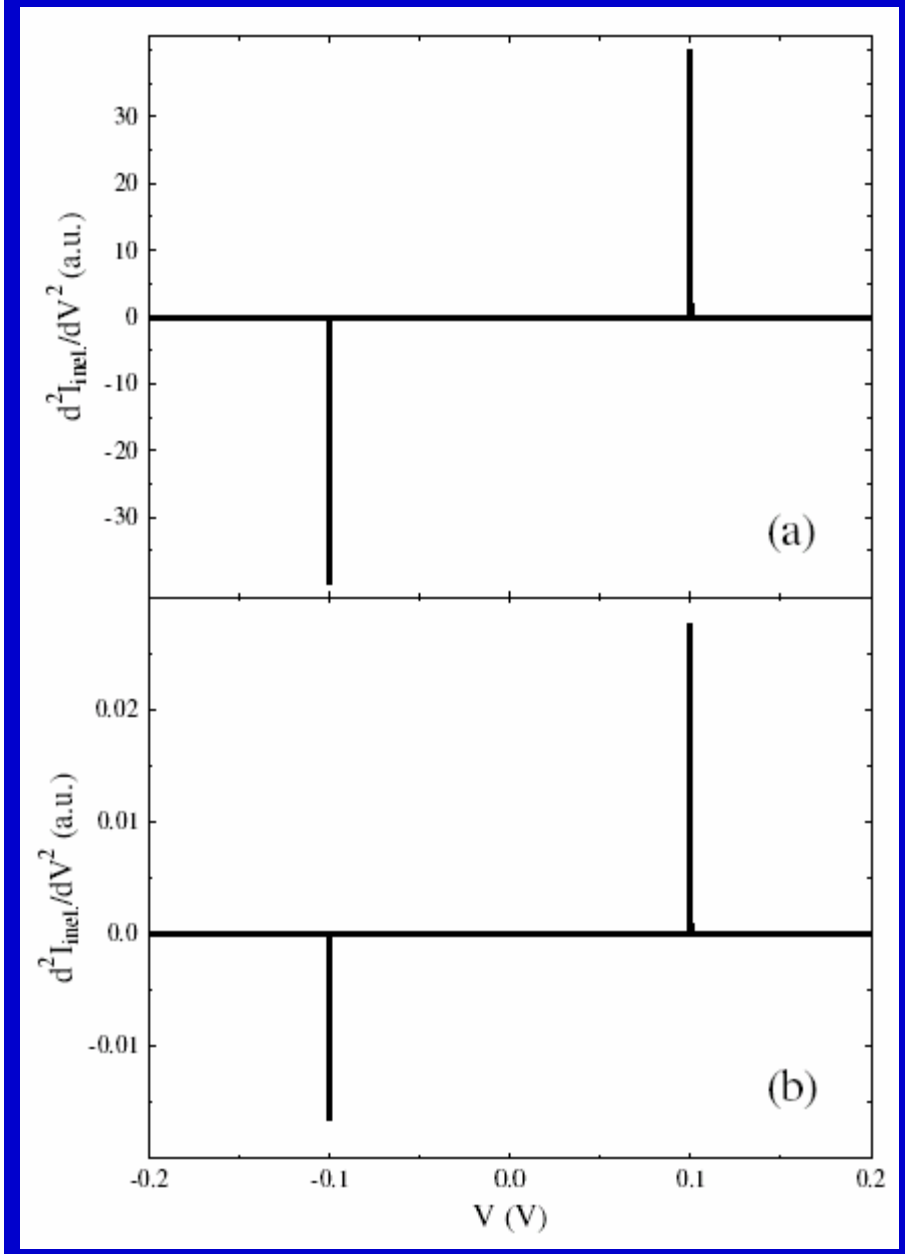
$d^2I_{inel.}/dV^2$ (a.u.)
30
20
10
0
-10
-20
-30
(a)
$d^2I_{inel.}/dV^2$ (a.u.)
0.02
0.01
0.0
-0.01
(b)
-0.2
-0.1
0.0
0.1
0.2
V (V)

Barrier dynamics effects on electron transmission through molecular wires

- Relevant timescales
- Inelastic contributions to the tunneling current
- Dephasing and activation
- Heating of current carrying molecular wires
- HEAT CONDUCTION and rectification
- INELASTIC TUNNELING SPECTROSCOPY
- MULTISTABILITY AND HYSTERESIS
- LIGHT

Elastic transmission vs. maximum heat generation:

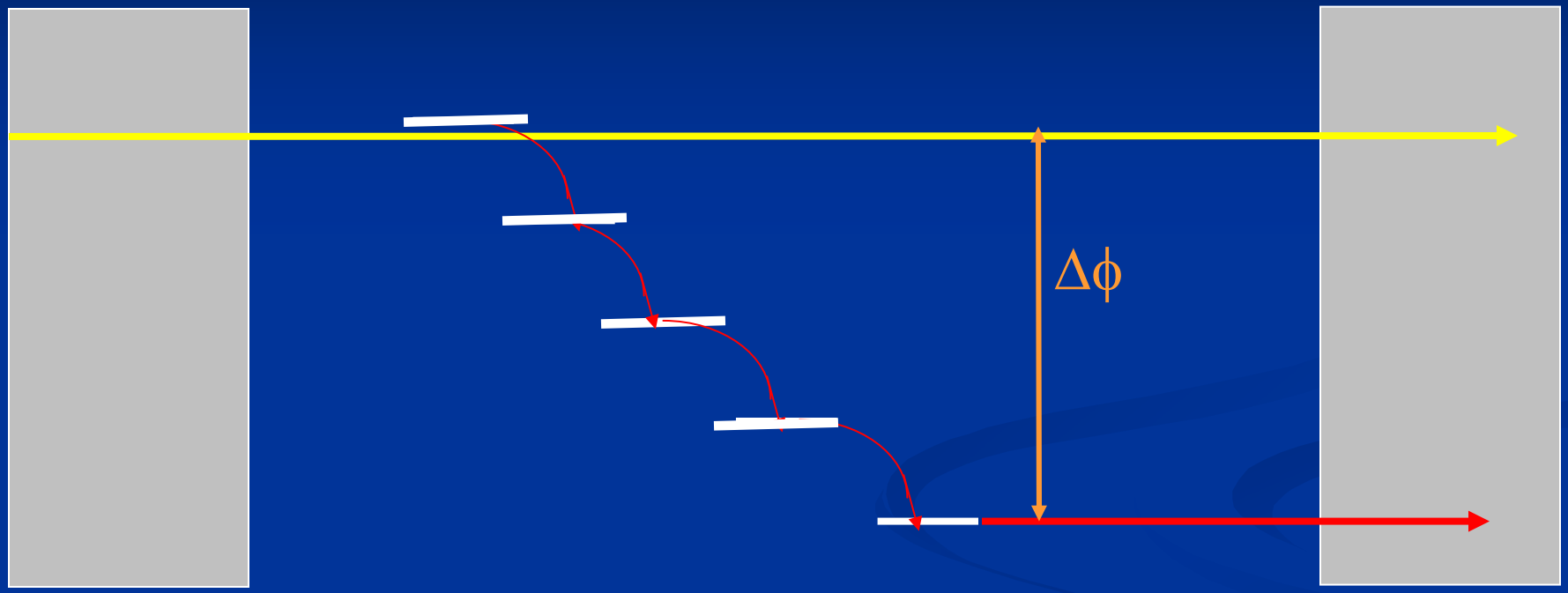

Heating

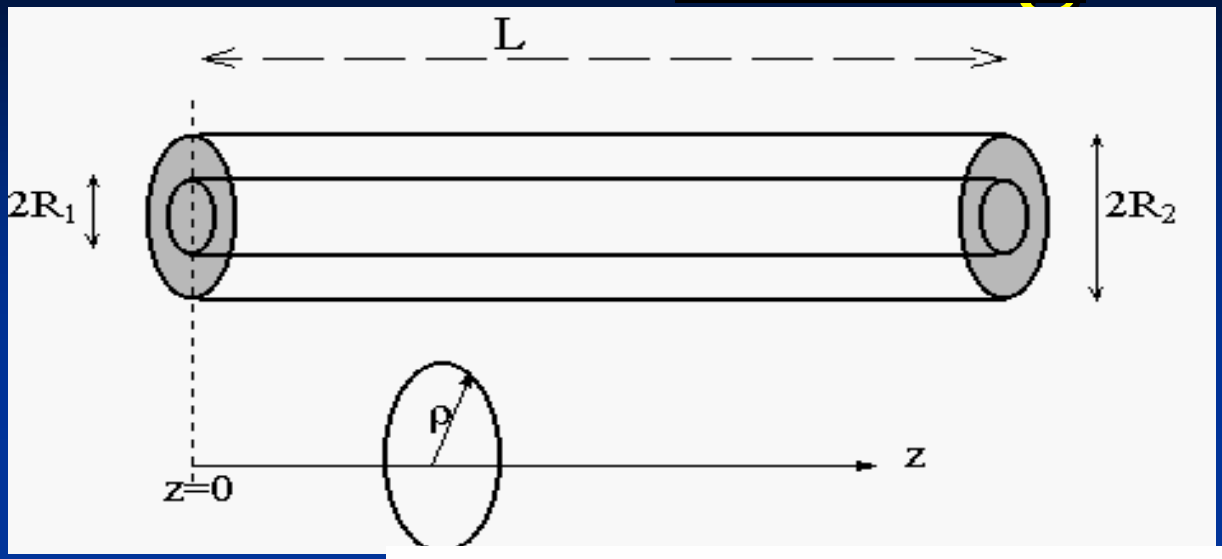

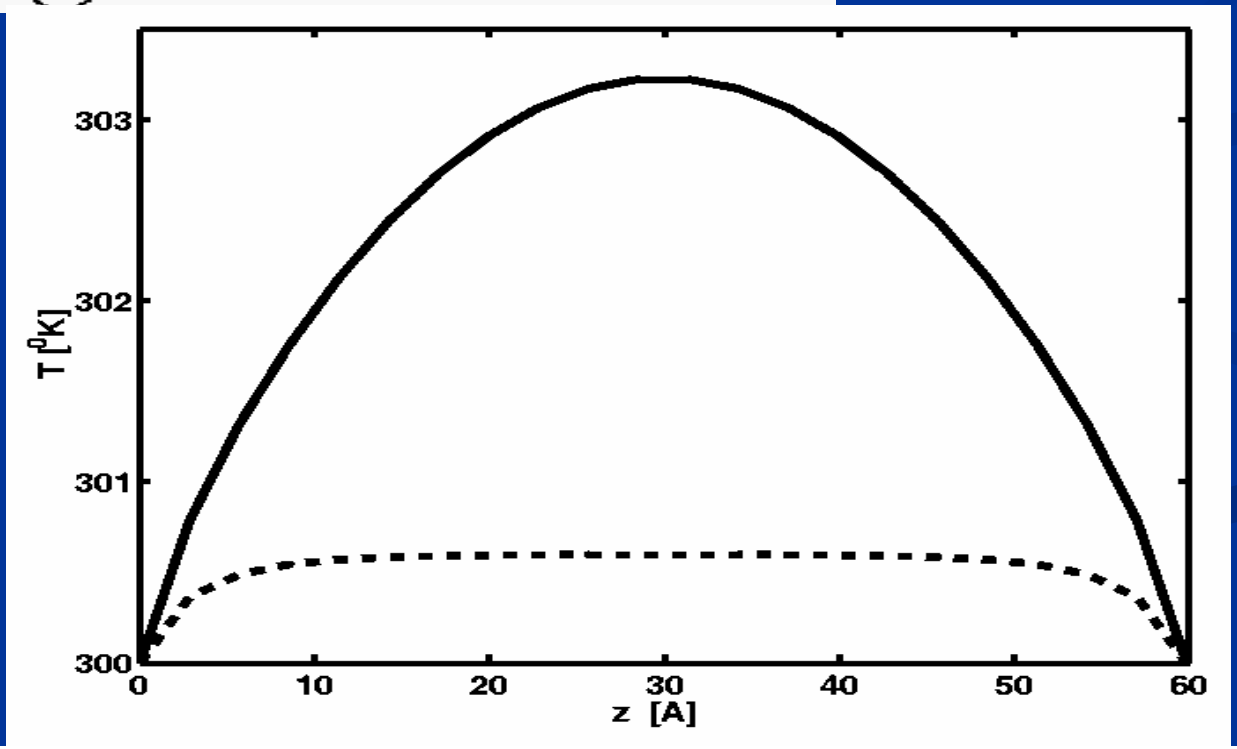

Thermal conduction by molecules

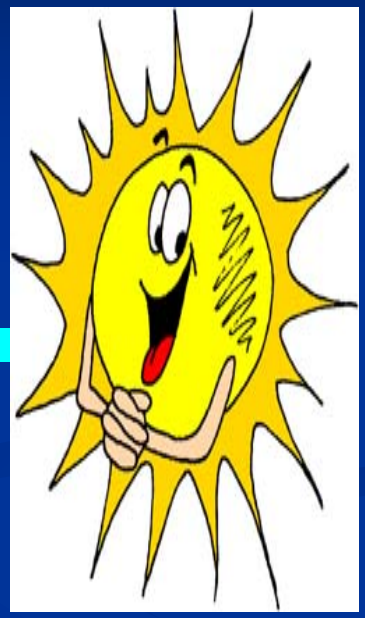

With Dvira Segal and Peter Hanggi

Model:

$$H = H_{mol} + H_B + H_{\text{int}}$$

Phonon mechanism. Only end atoms 1 and N of the molecule to couple to the thermal solids. The latter are taken as baths of independent harmonic modes

The molecule: A collection of normal modes:

$$H_{Mol} = \sum_k \left\{ \frac{1}{2}\omega_k y_k^2 + \frac{p_k^2}{2} \right\}$$

The solids and their coupling to the molecule:

$$H_{\text{int}} = \sum_l \left\{ \frac{1}{2} m_l \omega_l^2 \left(\bar{x}_l - \frac{g_{1,l}\bar{x}_1}{m_l \omega_l^2} \right)^2 + \frac{\bar{p}_l^2}{2m_l} \right\}$$

$$+ \sum_r \left\{ \frac{1}{2} m_r \omega_r^2 \left(\bar{x}_r - \frac{g_{N,r}\bar{x}_N}{m_r \omega_r^2} \right)^2 + \frac{\bar{p}_r^2}{2m_r} \right\}$$

The quantum heat flux

$$I_h = \int \mathcal{T}(\omega)\left[n_L(\omega) - n_R(\omega)\right]\omega d\omega$$

Transmission coefficient at frequency ω

Bose Einstein populations for left and right baths.

$$T(\omega) = \frac{1}{8\pi}\sum_{k,k'} \frac{\Gamma^{(R)}_{k,k'}(\omega)\Gamma^{(L)}_{k,k'}(\omega)}{\sqrt{\omega_k \omega_{k'}}} \left\langle \bar{A}_k(\omega)\bar{A}^{\dagger}_{k'}(\omega)\right\rangle$$

$$\left(\omega_k{}^2 - \omega_0{}^2\right) A_k - i\omega_0 \sum_{k'} \gamma_{k,k'}(\omega_0) A_{k'} = V_{0,k} A_0$$

With Dvira Segal and Peter Hanggi

J. Chem. Phys. **119**, 6840-6855 (2003)

Anharmonicity effects

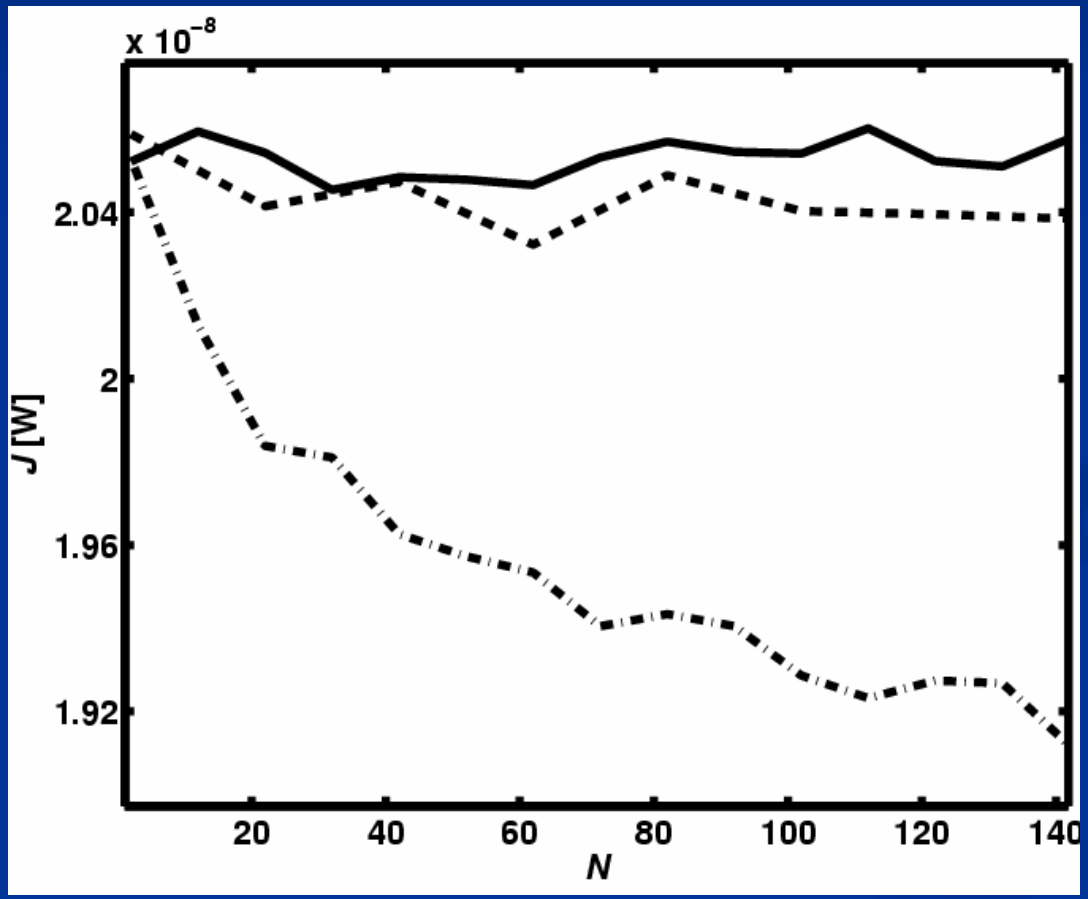

Heat current vs. chain length from classical simulations. Full line: harmonic chain; dashed line: anharmonic chain using the alkane force field parameters; dash-dotted line: anharmonic chain with unphysically large (x 30) anharmonicity

Heat conduction in alkanes of different chain length

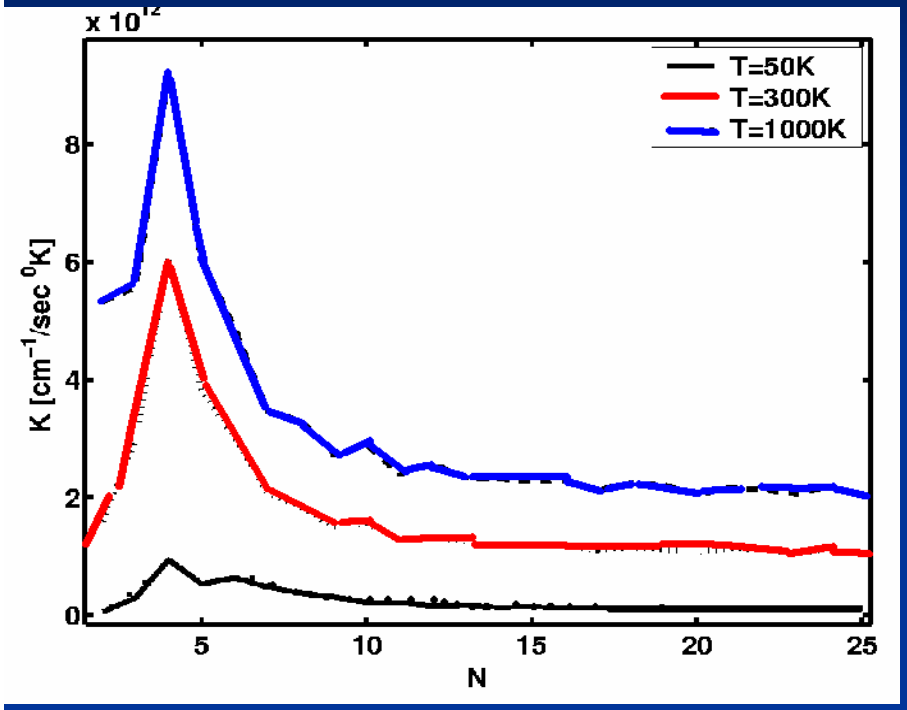

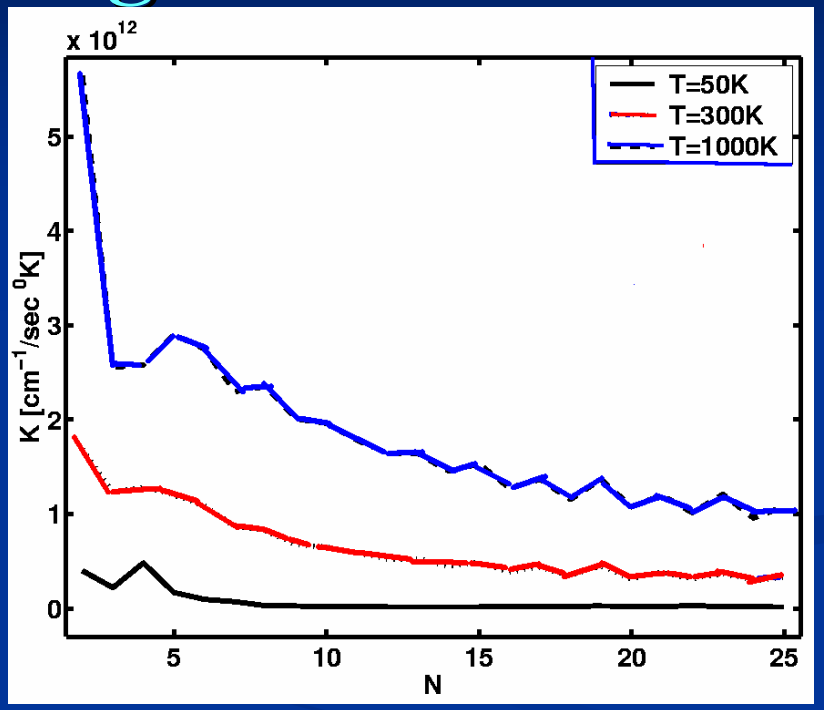

The thermal conductance vs. the chain length for Alkanes, ω_c=400 cm^{-1} , V_L=V_R=50 cm^{-2}. Black: T=50K; Red: T=300K; Blue: T=1000K

ω_c=400 cm^{-1} , V_L=V_R=200 cm^{-2}. Black: T=50K; Red: T=300K; Blue: T=1000K.

Density of normal modes in alkanes

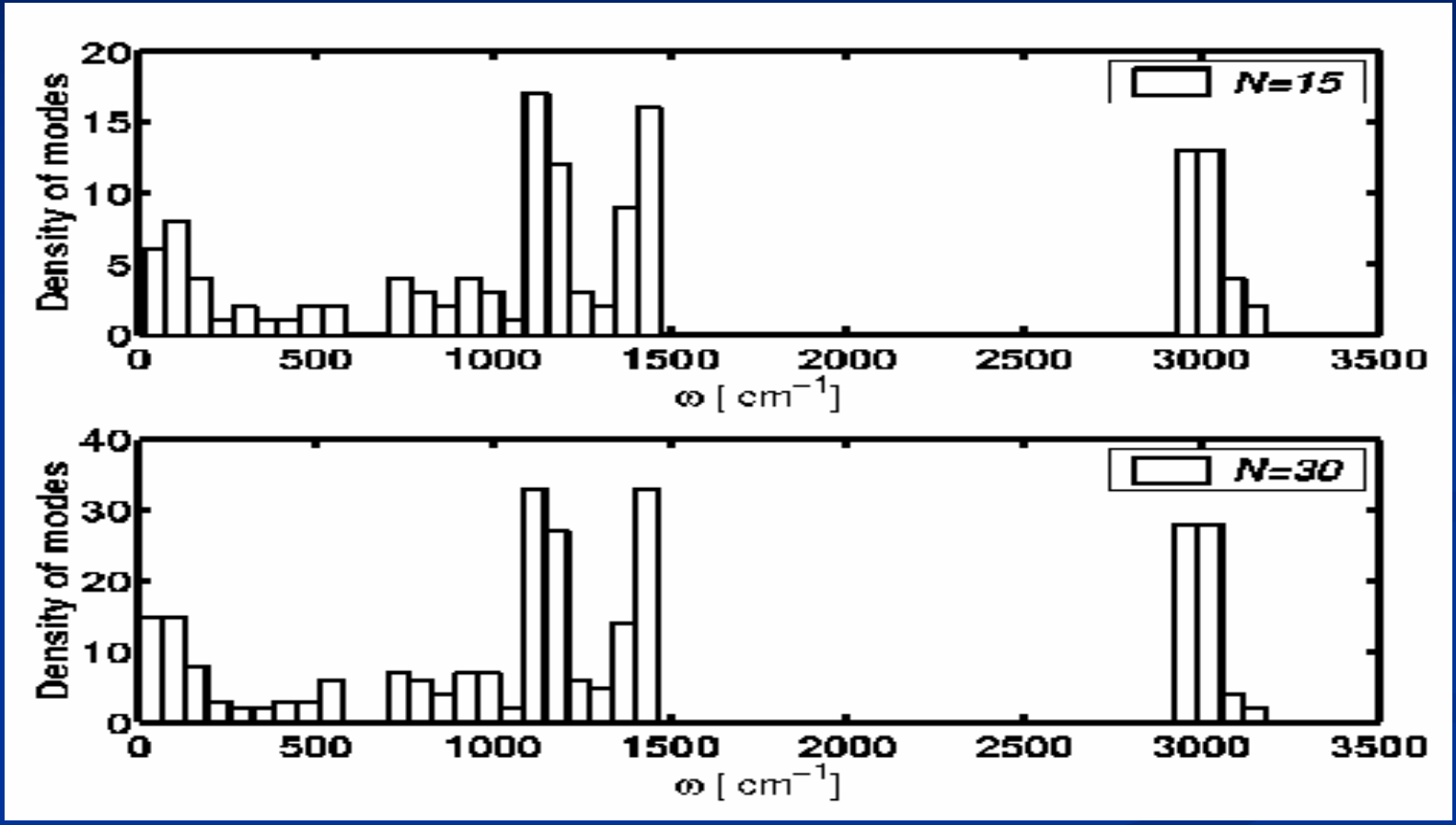

Low frequency group: 0-600cm^{-1};
Intermediate frequency group: 700-1500cm^{-1}
High frequency group: 2900-3200cm^{-1}

Heat conduction by the lower frequency groups

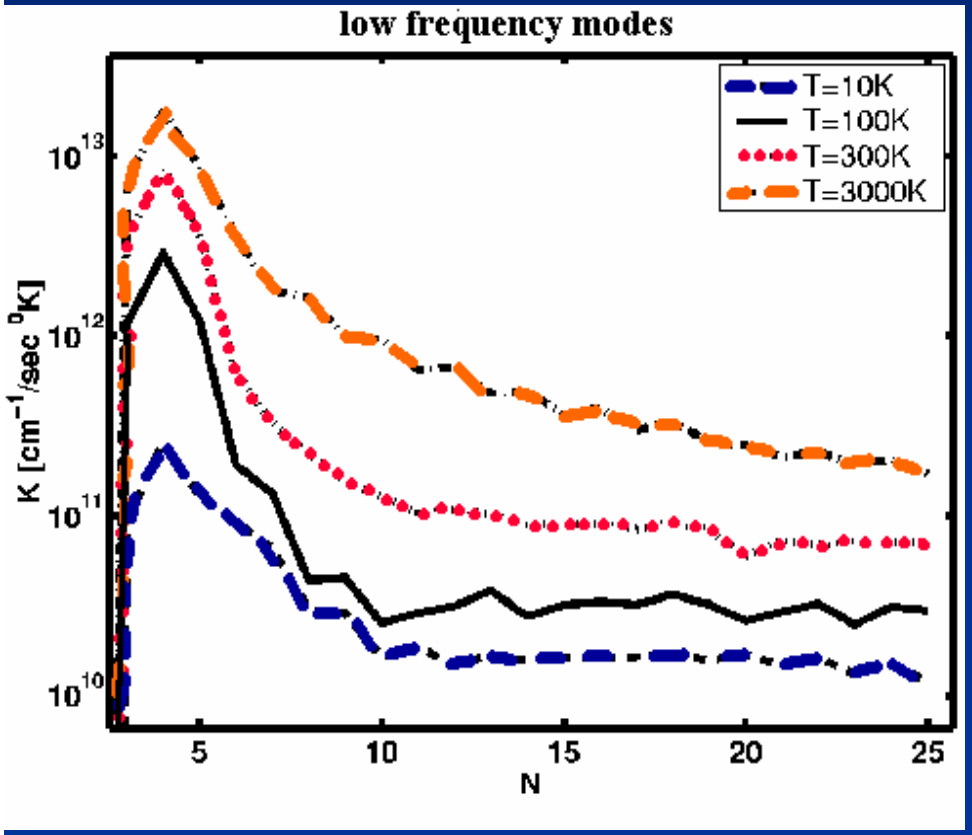

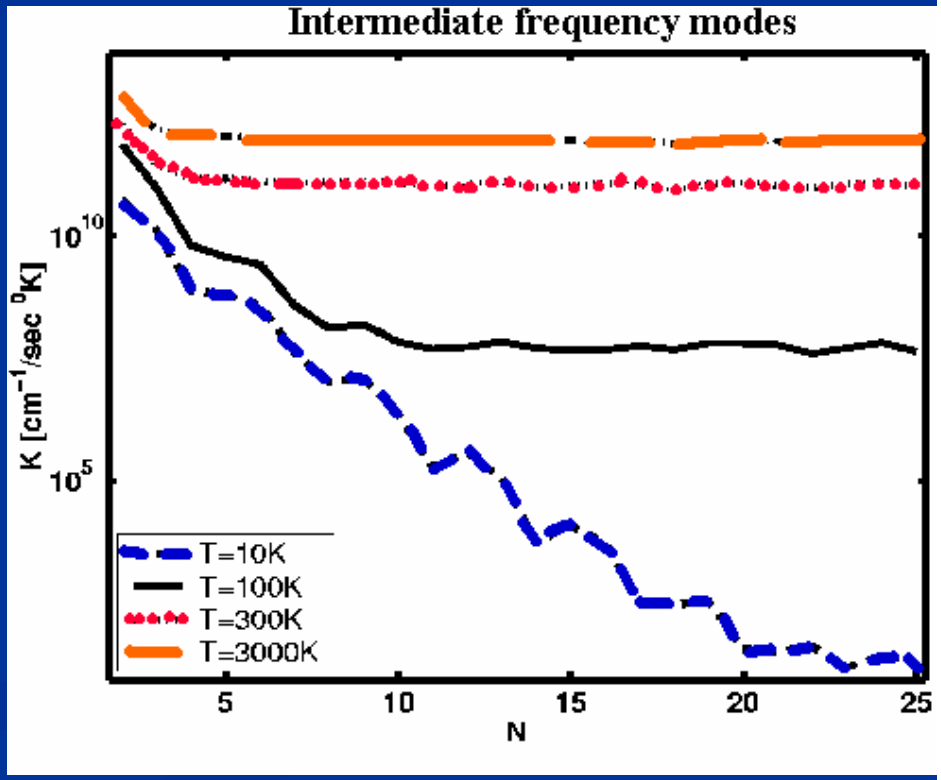

Thermal conduction vs. alkane chain length

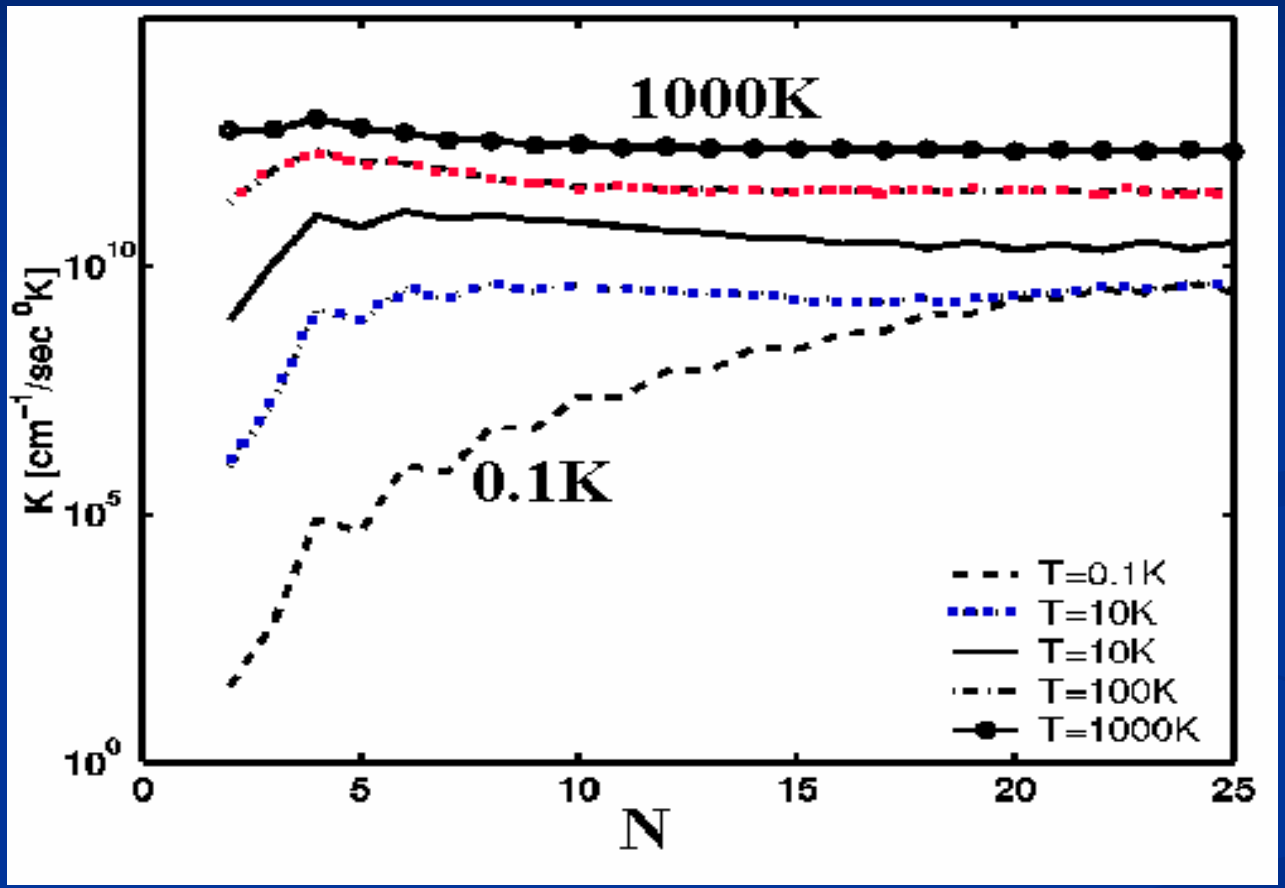

Dashed line: T=0.1K; Blue dotted line: T=1K; Full line: T=10K; Red- dotted line: T=100K; Line with circles: T=1000K. ω_c=400 cm^{-1} ,V_L=V_R=50 cm^{-2}.

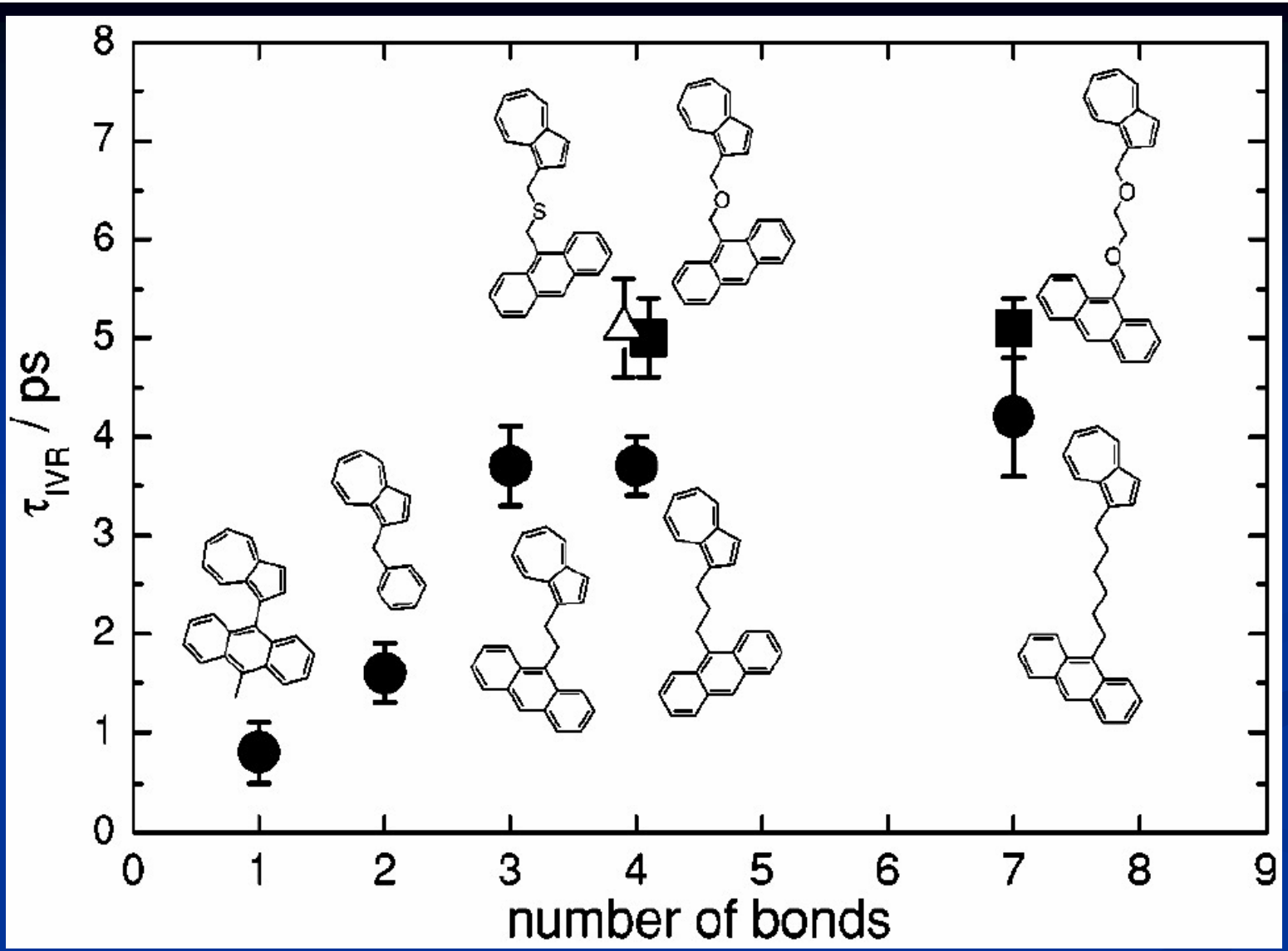

D.Schwarzer, P.Kutne, C.Schroeder and J.Troe, J. Chem. Phys., 2004
Intramolecular vibrational energy redistribution in bridged azulene-anthracene compounds:Ballistic energy transport through molecular chains

Barrier dynamics effects on electron transmission through molecular wires

- Relevant timescales
- Inelastic contributions to the tunneling current
- Dephasing and activation
- Heating of current carrying molecular wires
- HEAT CONDUCTION -- RECTIFICATION
- INELASTIC TUNNELING SPECTROSCOPY
- MULTISTABILITY AND HYSTERESIS
- LIGHT

Rectification of heat transport

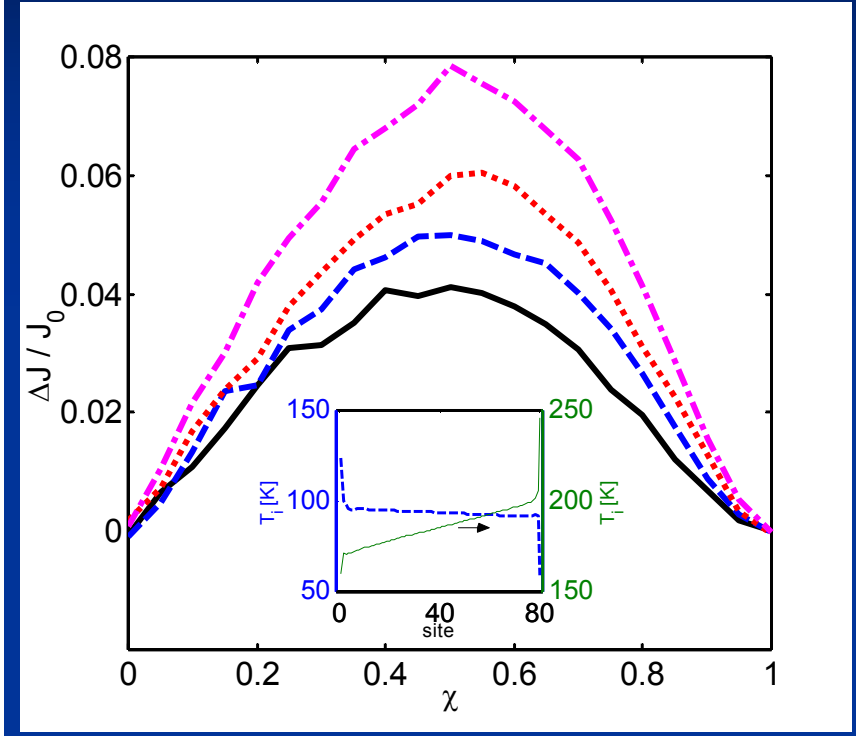

$$H = (2m)^{-1}\sum_{i=1}^{N} p_i^2 + \sum_{i=1}^{N-1} D\left(e^{-\alpha(x_{i+1}-x_i-x_{eq})}-1\right)^2 + D\left(e^{-\alpha(x_1-a)}-1\right)^2 + D\left(e^{-\alpha(b-x_N)}-1\right)^2$$

$$\ddot{x}_i = -\frac{1}{m}\frac{\partial H}{\partial x_i}; \quad i = 2,3,\ldots N-1$$

$$\ddot{x}_1 = -\frac{1}{m}\frac{\partial H}{\partial x_1} - \gamma_L \dot{x}_1 + F_L(t)$$

$$\ddot{x}_N = -\frac{1}{m}\frac{\partial H}{\partial x_N} - \gamma_R \dot{x}_N + F_R(t)$$

$$\gamma_L = \gamma(1-\chi)$$

The asymmetry in the thermal conduction plotted as a function of χ. parameters used: *D*=3.8/c^2 eV, *α*=1.88c Å-1, *xeq*=1.538 Å and *m*=*m*_carbon (c=1 is from standard carbon-carbon force field in alkanes). Here we artificially increase the system anharmonicity by taking c=6. Full, dashed, dotted and dashed-dotted lines correspond to *N*=10, *N*=20, *N*=40 and *N*=80, respectively, with γ=50 ps-1, *Th* = 300K and *Tc* = 0K. The inset presents the temperature profile for the *N*=80, χ=0.5 case with *TL*=*Tc*,; *TR*=*Th* (full), *TL*=*Th* ; *TR*=*Tc* (dashed).

Spin-boson heat rectifier

$$H = E_0 \,|0><0|\, + E_1 \,|1><1|\, + H_B + H_{MB}$$

$$H_B = H_L + H_R \,; \;\; H_K = \sum_{j \in K} \omega_j a_j^\dagger a_j \;\; ; \;\; K = L, R$$

$$H_{MB} = B \,|0><1|\, + B^\dagger \,|1><0|\, ; \;\; B = B_L + B_R$$

$$H_{MB} = \sum_{n=1}^{N-1} \sqrt{n} \left(B \,|n-1><n|\, + B^\dagger \,|n><n-1|\, \right)$$

$$B_K = B_K^\dagger = \sum\nolimits_{j \in K} \bar{\alpha}_j \left(a_j^\dagger + a_j \right) ; \;\; K = L, R$$

AN& D. Segal, Phys. Rev. Lett. 94, 034301 (2005)

Master equation

$$\dot{P}_n = -\left(nk_L + nk_R + (n+1)(k_L e^{-\beta_L \omega_0} + k_R e^{-\beta_R \omega_0}) X_n \right) P_n$$

$$+ (n+1)(k_L + k_R) X_n P_{n+1} + n(k_L e^{-\beta_L \omega_0} + k_R e^{-\beta_R \omega_0}) P_{n-1}$$

$X_n = \delta_{n,0}$ for the 2-level (n=0,1) system and X_n=1 for harmonic oscillator (n=0, …infinity)

$$k_K = \Gamma_K(\omega_0)(1 + n_K(\omega_0)); \quad K = L, R$$

$$n_K(\omega) = \left(e^{\hbar\omega/(k_B T_K)} - 1 \right)^{-1} \qquad \Gamma_K(\omega) = \frac{\pi}{2m\omega^2} \sum_{j \in K} \alpha_j^2 \delta(\omega - \omega_j)$$

harmonic oscillator:

$$J = \omega_0 \frac{\Gamma_L \Gamma_R}{\Gamma_R + \Gamma_L} (n_L - n_R)$$

two level system:

$$J = \omega_0 \frac{\Gamma_L \Gamma_R (n_L - n_R)}{\Gamma_L (1 + 2n_L) + \Gamma_R (1 + 2n_R)}$$

HEAT RECTIFICATION BY A 2-LEVEL BRIDGE

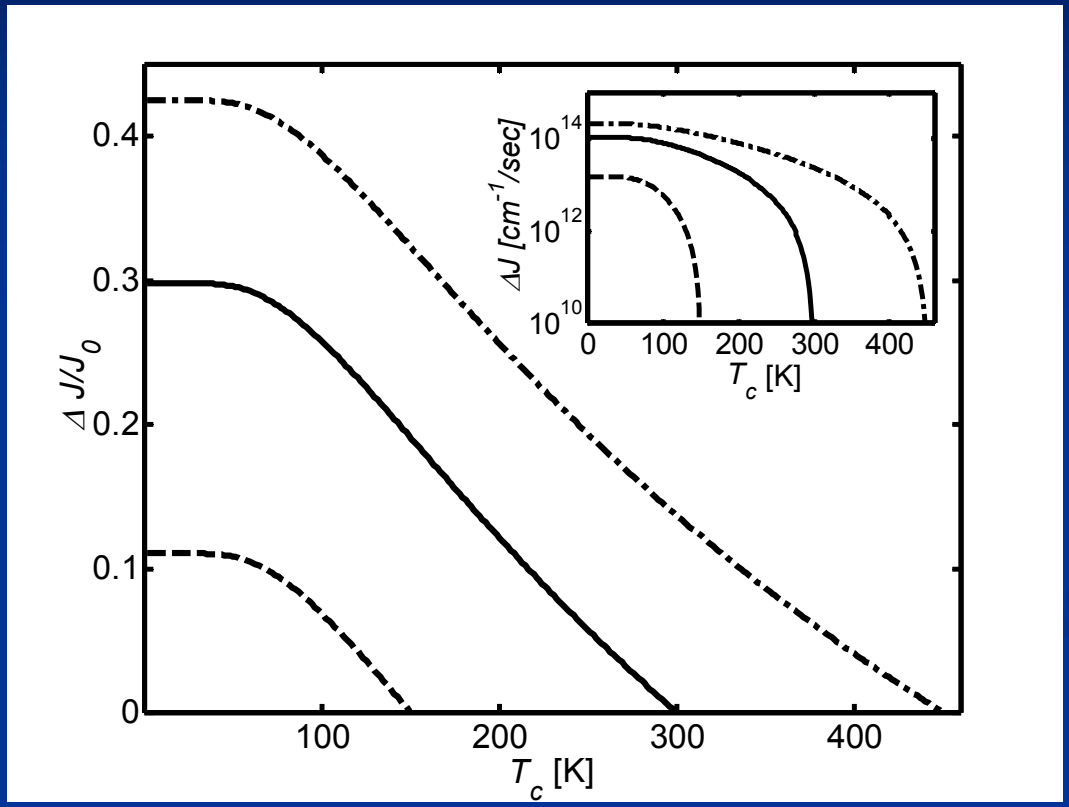

$$\Gamma_K = \Gamma(1 \pm \chi)$$

Heat rectification by a 2-level bridge in the linear coupling model The ratio $\Delta J/J0$ is plotted against T_c while the hot reservoir is kept at a fixed temperature: T_h=150 K (dashed), T_h=300 K (full) and T_h=450 K (dash-dotted), ω_0=200 cm^{-1}, χ=1/2. The inset shows ΔJ for the three cases.

HEAT RECTIFICATION BY A 2-LEVEL BRIDGE

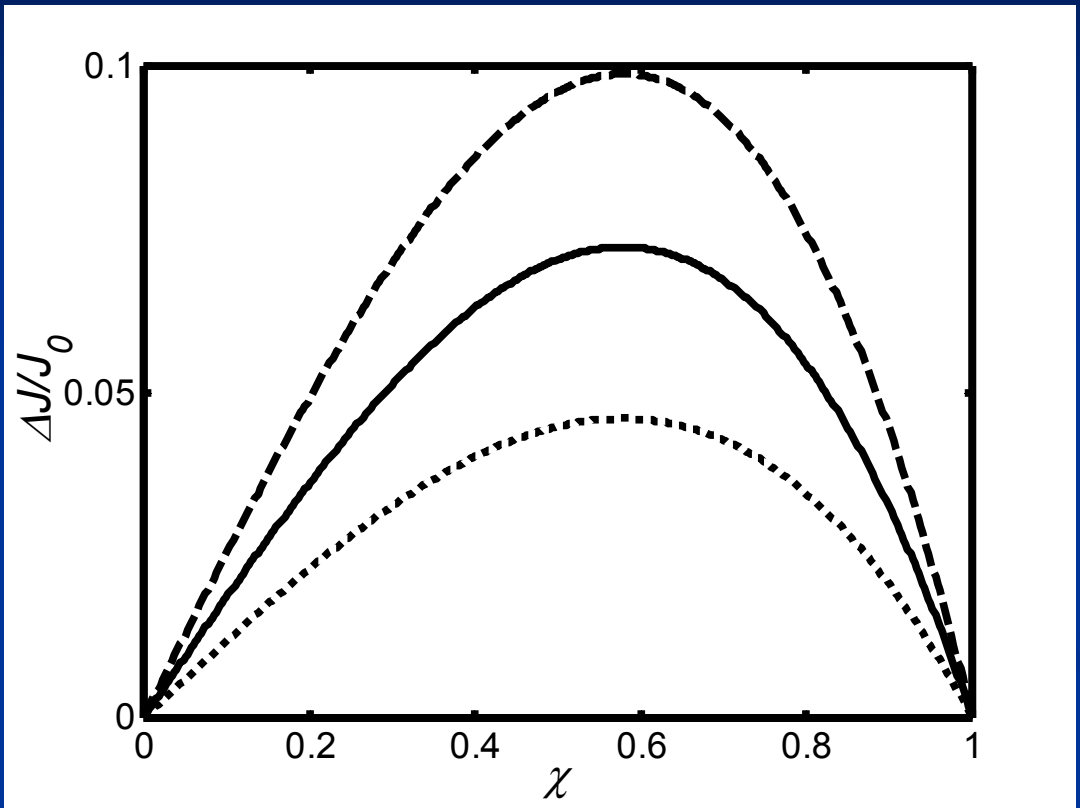

$$\Gamma_K = \Gamma(1 \pm \chi)$$

. The ratio $\Delta J/J_0$ vs. the asymmetry parameter χ for several two-level bridges characterized by different level spacing ω_0: Dashed line ω_0 =200 cm-1; full line ω_0=400 cm-1; dotted line ω_0 = 600 cm-1. The baths temperatures are *Th*=400 K, *Tc*=300 K.

Barrier dynamics effects on electron transmission through molecular wires

- Relevant timescales
- Inelastic contributions to the tunneling current
- Dephasing and activation
- Heating of current carrying molecular wires
- HEAT CONDUCTION -- RECTIFICATION
- INELASTIC TUNNELING SPECTROSCOPY
- MULTISTABILITY AND HYSTERESIS
- LIGHT

Negative differential resistance

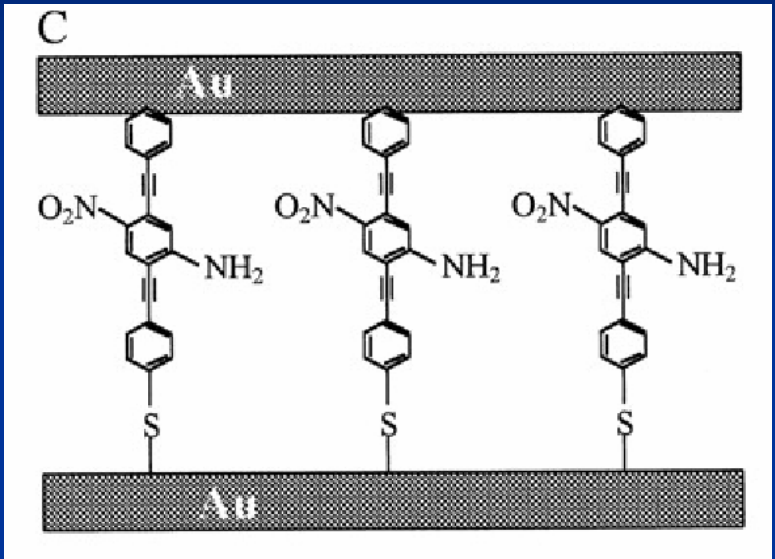

J. Chen, M. A. Reed, A. M. Rawlett, and J. M. Tour, *Science* 286: 1550-1552 (1999)

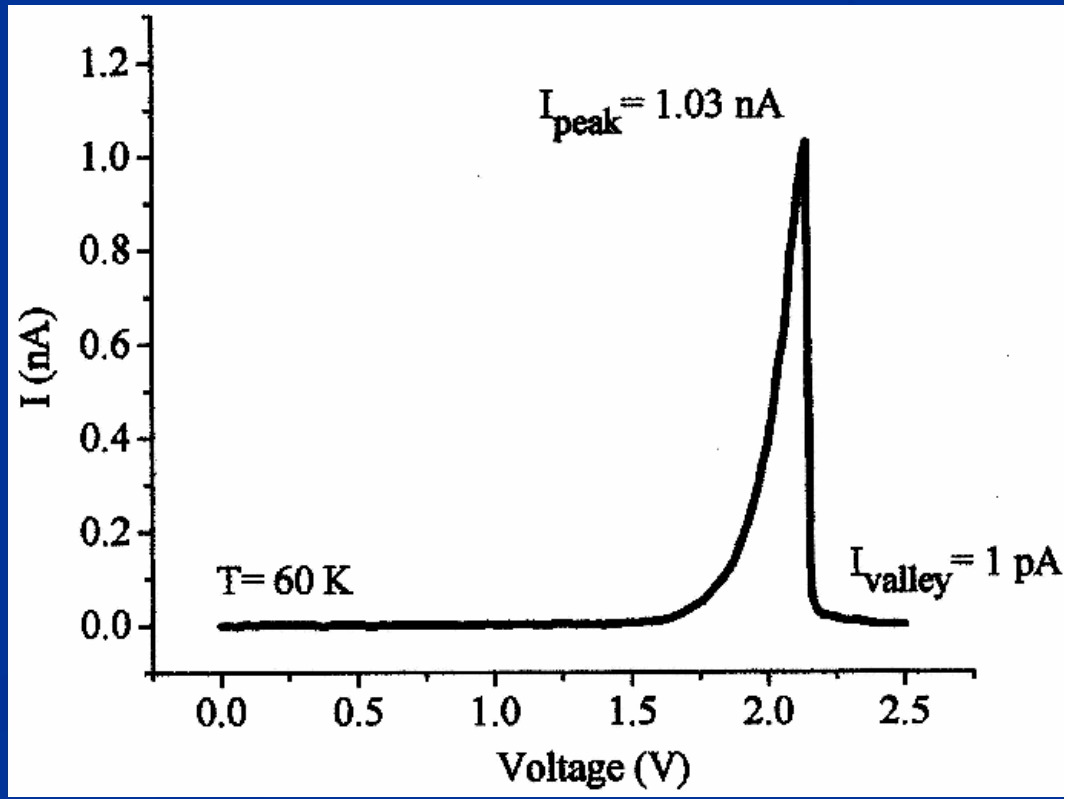

Negative differential resistance

A.M.Rawlett et al. Appl. Phys. Lett. **81** , 3043 (2002)

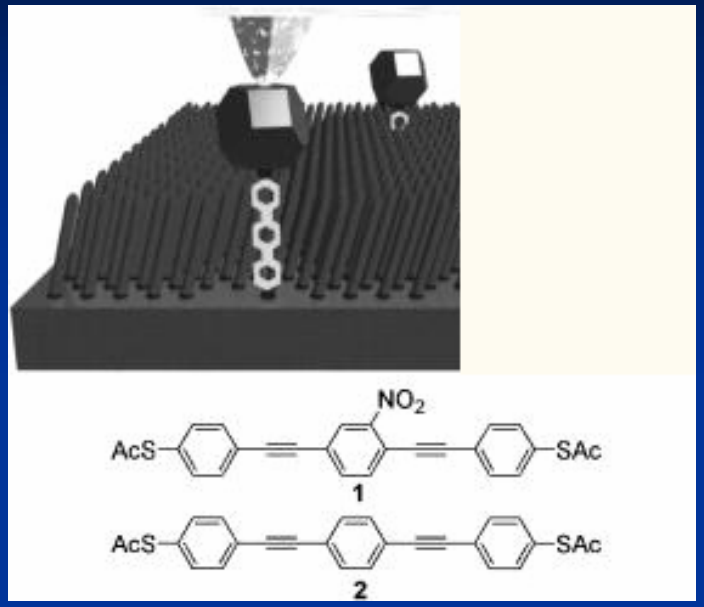

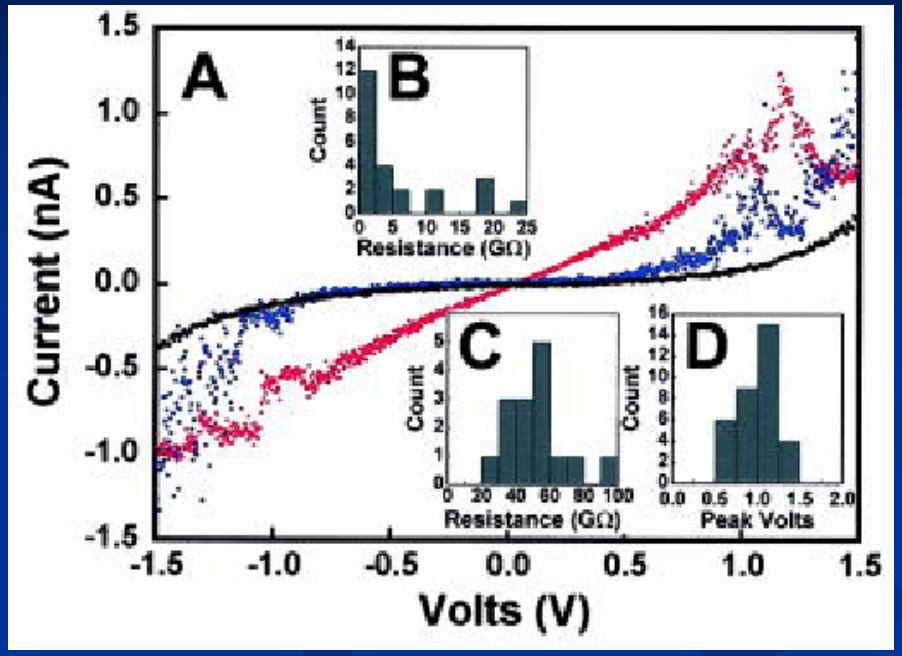

(Color) Representative current–voltage characteristics (a) for molecule 1 (red/ blue curves) and molecule 2 (black curve). Molecule 1 (red/ blue curves) exhibits both the negative differential resistance peak and a wide range of background ohmic currents. The distribution of resistances is shown by the histogram inset (b). In contrast, molecule 2 (black curve) shows no NDR-like features and resistances in the ohmic region are much more tightly clustered [51.6±18 G , *N* = 15, see histogram inset and resistances in the ohmic region are much more tightly clustered [51.6±18]Gohm

Hysteresis

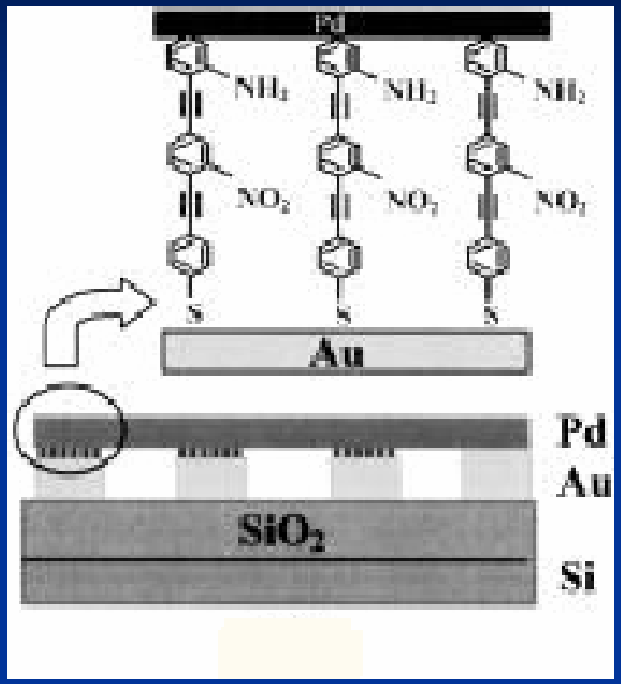

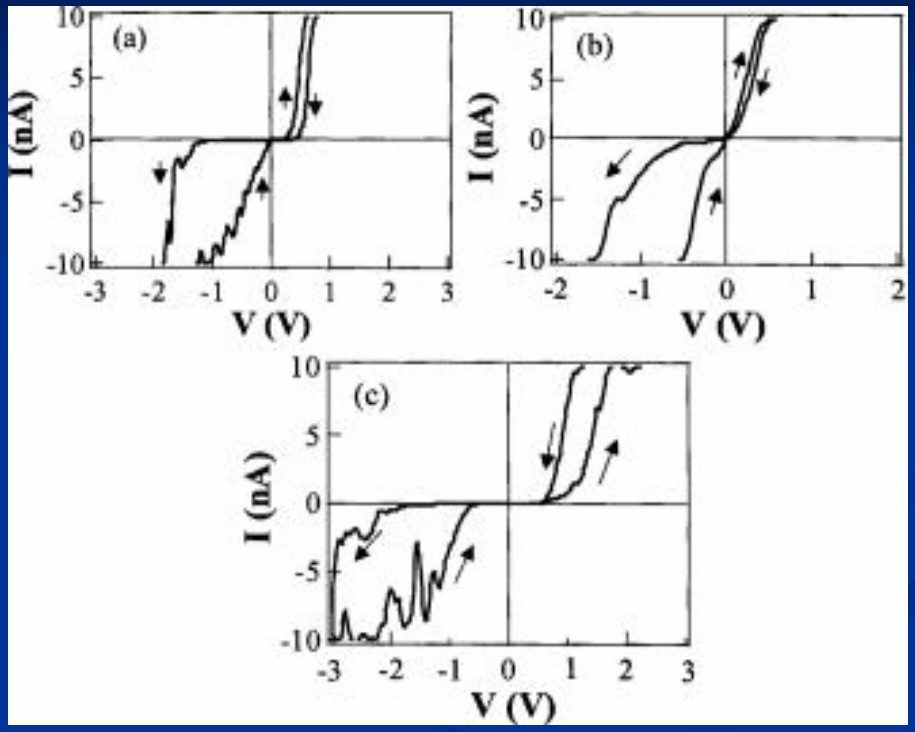

Typical *I–V* curves of molecular devices. (a), (b), and (c) correspond to molecules a, b, and c shown in Fig. 2, respectively

C.Li et al. Appl. Phys. Lett. 82 , 645 (2003)

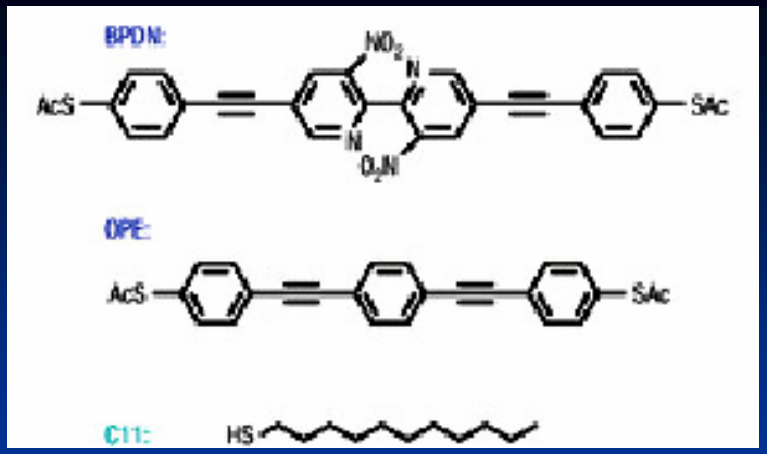

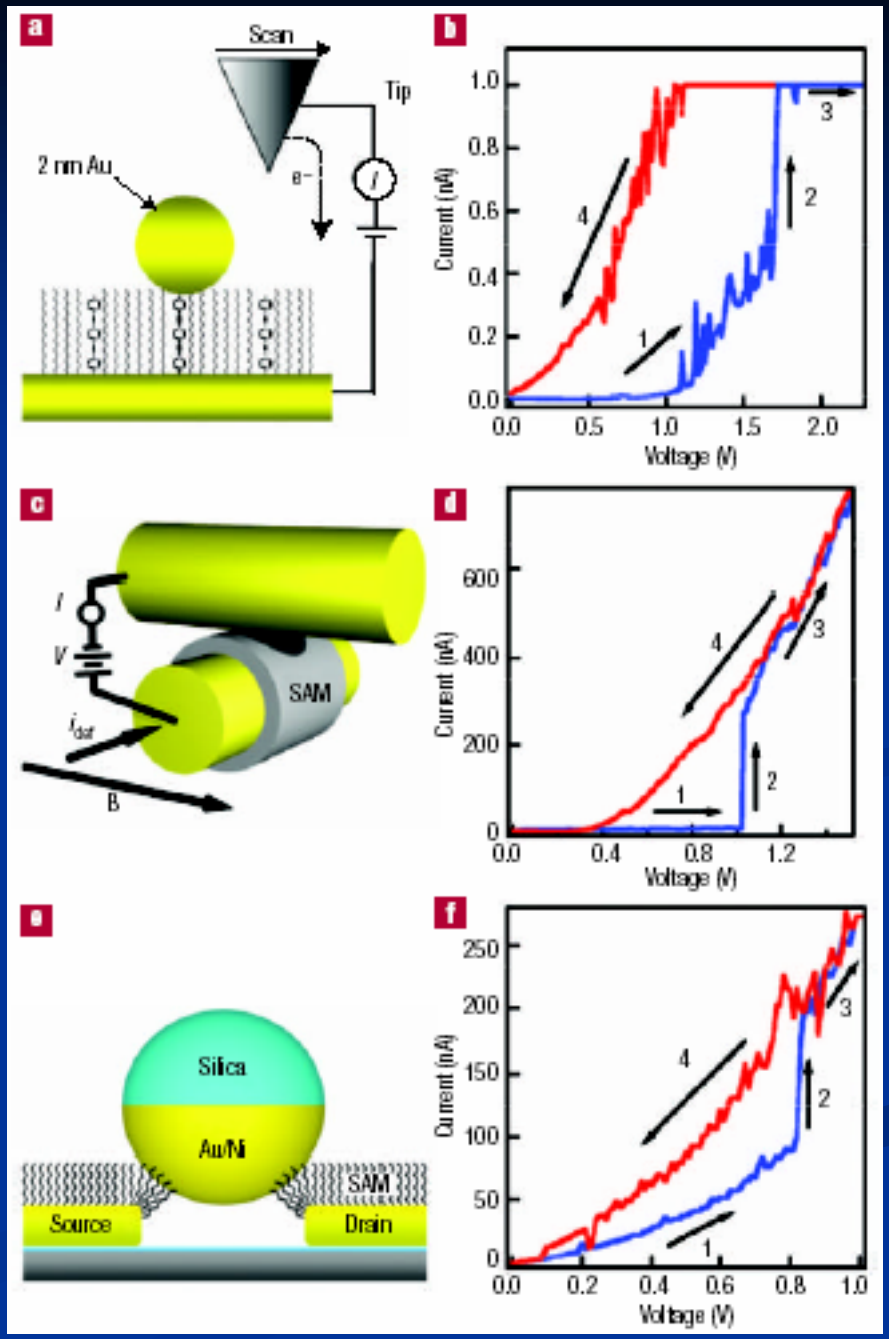

a, Diagram of STM *I*/*V* experiment. The tip is positioned over the gold nanoparticle to measure the properties of an individual BPDN molecule inserted into the C11 alkane matrix. b, *I*/*V* measurement of an isolated BPDN molecule from the Type II STM experiment.

Blum et al, Nature Materials, 2005

Strong coupling – localization and switching behavior

$$\hat{H} = \varepsilon_0 \hat{c}_0^\dagger \hat{c}_0 + \omega_0 \hat{a}^\dagger \hat{a} + \sum_{k \in L,R} \varepsilon_k \hat{c}_k^\dagger \hat{c}_k$$

$$+ \sum_{k \in L,R} \left(V_k \hat{c}_k^\dagger \hat{c}_0 + h.c \right) + M \hat{c}_0^\dagger \hat{c}_0 \left(\hat{a}^\dagger + \hat{a} \right)$$

+ Thermal relaxation of the phonon

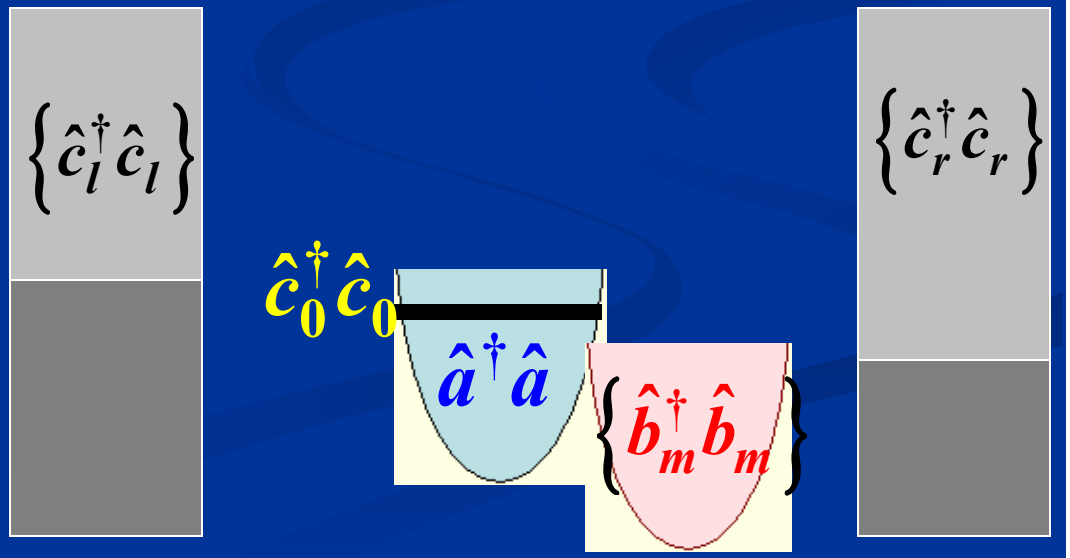

BORN OPPENHEIMER APPROXIMATION

$c_0^\dagger c_0$

$$\hat{H}_{ph} = \omega_0 \hat{a}^\dagger \hat{a} + Mn_0\left(\hat{a}^\dagger + \hat{a}\right) + \sum_\eta \left\{ \omega_\eta \hat{b}_\eta^\dagger \hat{b}_\eta + U_\eta \left(\hat{a}^\dagger + \hat{a}\right)\left(\hat{b}_\eta^\dagger + \hat{b}_\eta\right) \right\}$$

Coupling to thermal bath

At equilibrium or in steady state:

$$\left\langle \hat{a} + \hat{a}^\dagger \right\rangle = \frac{2\omega_0}{{\omega_0}^2 + \left(\gamma/2\right)^2} Mn_0$$

The electronic Hamiltonian

$$\hat{H}_{el} = \tilde{\varepsilon}_0(n_0)\hat{c}_0^\dagger \hat{c}_0 + \sum_{k\in L,R} \varepsilon_k \hat{c}_k^\dagger \hat{c}_k + \sum_{k\in L,R} \left(V_k \hat{c}_k^\dagger \hat{c}_0 + h.c \right)$$

$$\tilde{\varepsilon}_0(n_0) = \varepsilon_0 - 2\varepsilon_{reorg} n_0$$

$$\varepsilon_{reorg} = M^2 \frac{\omega_0}{\omega_0^{\,2} + (\gamma/2)^2}$$

$$\varepsilon_0 + M\left(\hat{a}^\dagger + \hat{a}\right)$$

Self consisten equation for electronic population

$$n_0 = \int_{-\infty}^{\infty} \frac{dE}{2\pi} \frac{f_L(E)\Gamma_L + f_R(E)\Gamma_R}{\left[E - \tilde{\varepsilon}_0(n_0)\right]^2 + (\Gamma/2)^2}$$

$$\Gamma = \Gamma_L + \Gamma_R$$

$$\Gamma_K = 2\pi \sum_{k \in K} |V_k|^2 \, \delta(E - \varepsilon_k); \quad K = L, R$$

$$f_K(E) = \left[e^{(E-\mu_K)/k_B T} + 1 \right]^{-1}$$

T=0

$$n_0 = \frac{\Gamma_L}{\pi\Gamma}\arctan\left(\frac{\mu_L - \tilde{\varepsilon}_0(n_0)}{\Gamma/2}\right) + \frac{\Gamma_R}{\pi\Gamma}\arctan\left(\frac{\mu_R - \tilde{\varepsilon}_0(n_0)}{\Gamma/2}\right) + \frac{1}{2}$$

$$\mu_L = E_F + \frac{\Gamma_R}{\Gamma}V \qquad \mu_R = E_F - \frac{\Gamma_L}{\Gamma}V$$

$$n_0 = \frac{\Gamma_L}{\pi\Gamma}\arctan\left(x + \frac{2\Gamma_R V}{\Gamma^2}\right) + \frac{\Gamma_R}{\pi\Gamma}\arctan\left(x - \frac{2\Gamma_L V}{\Gamma^2}\right) + \frac{1}{2}$$

$$n_0 = \frac{\Gamma}{4\varepsilon_{reorg}}x + \frac{\varepsilon_0 - E_F}{2\varepsilon_{reorg}}$$

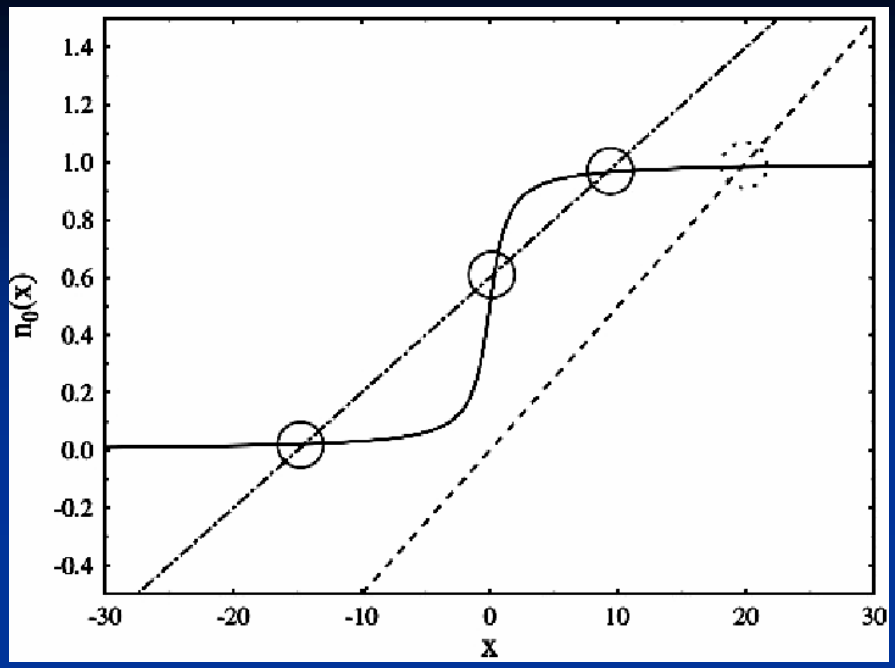
1.4
1.2
1.0
0.8
0.6
0.4
0.2
0.0
-0.2
-0.4
$n_0(x)$
-30
-20
-10
0
10
20
30
x

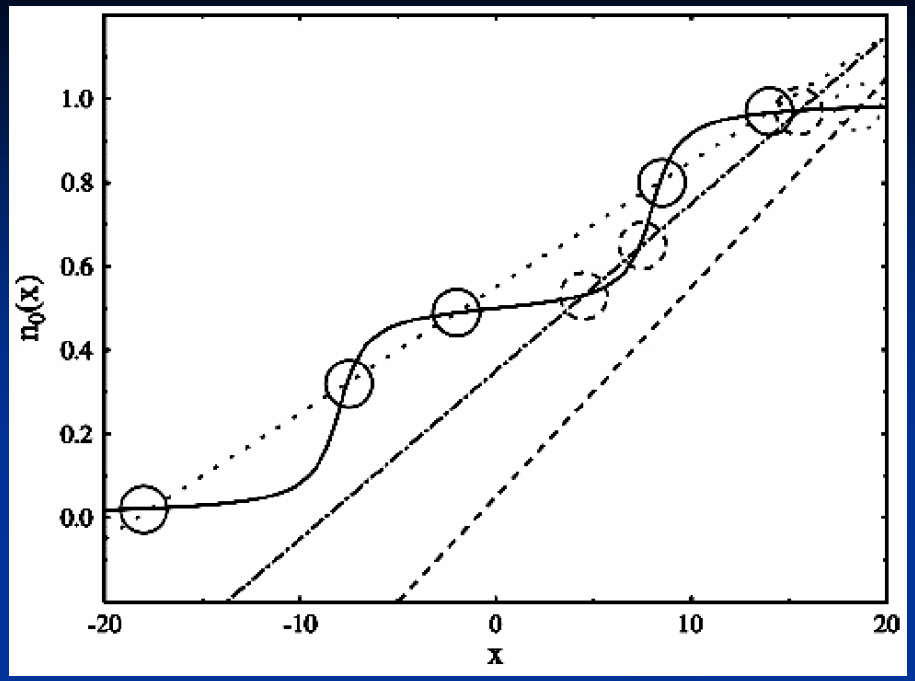
1.0
0.8
0.6
0.4
0.2
0.0
$n_0(x)$
-20
-10
0
10
20
x

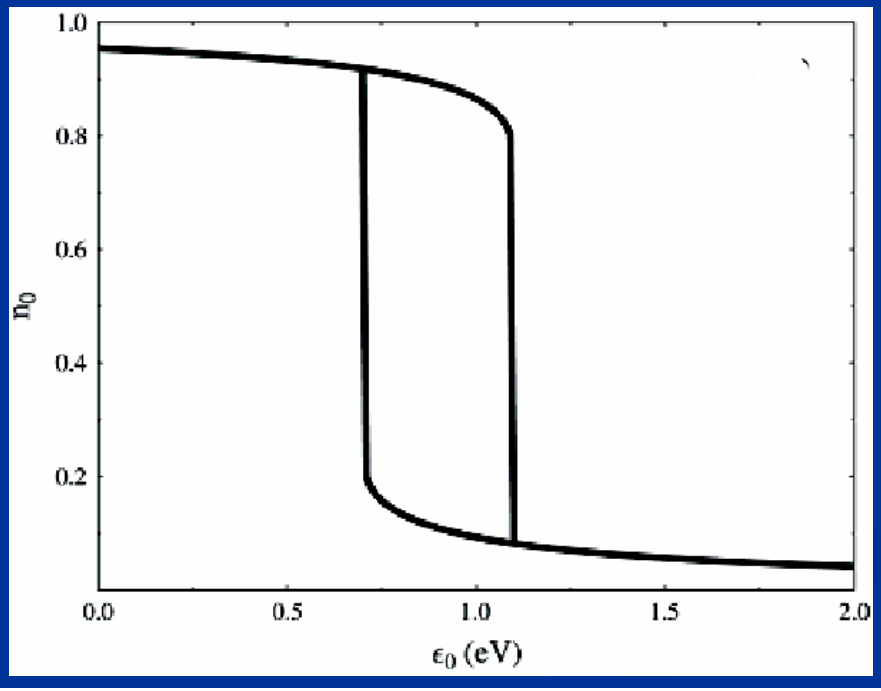
1.0
0.8
0.6
0.4
0.2
n_0
0.0
0.5
1.0
1.5
2.0
ϵ_0 (eV)

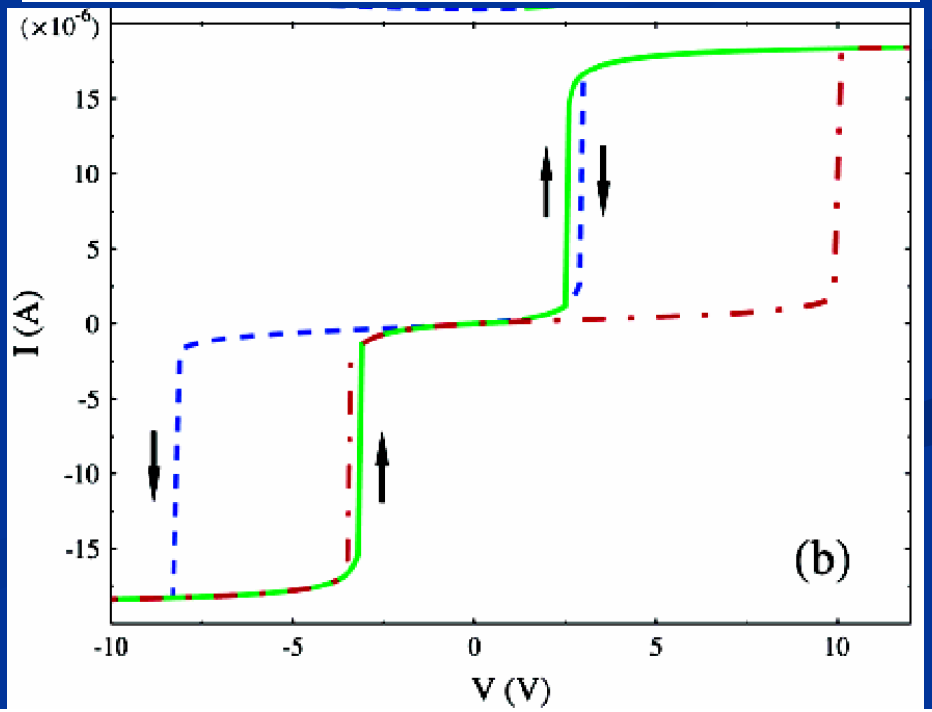
($\times 10^{-6}$)
15
10
5
0
-5
-10
-15
I (A)
-10
-5
0
5
10
V (V)
(b)

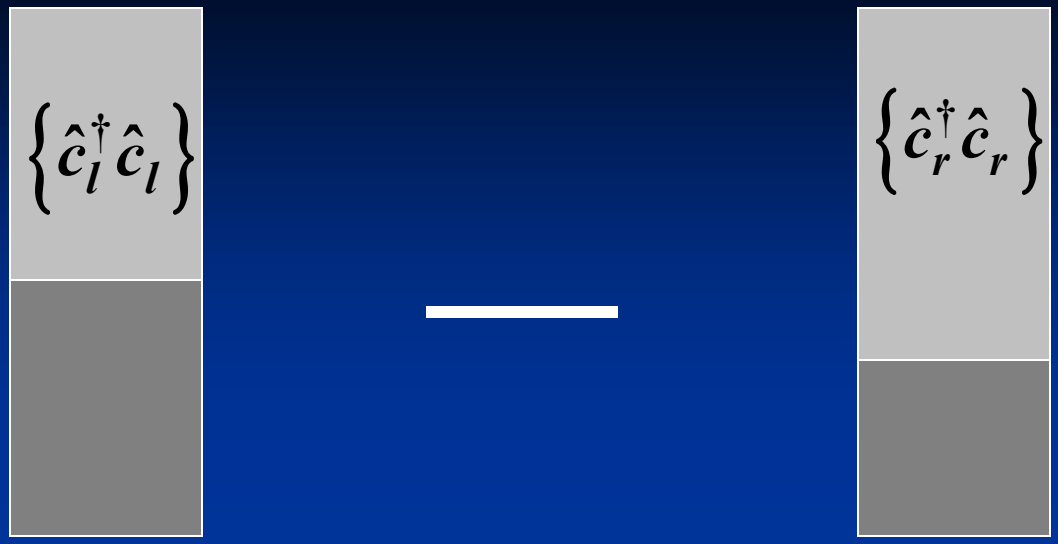

- Obvious feedback mechanism on the mean field level
- Is mean field good enough?
- Timescale considerations critical

NDR

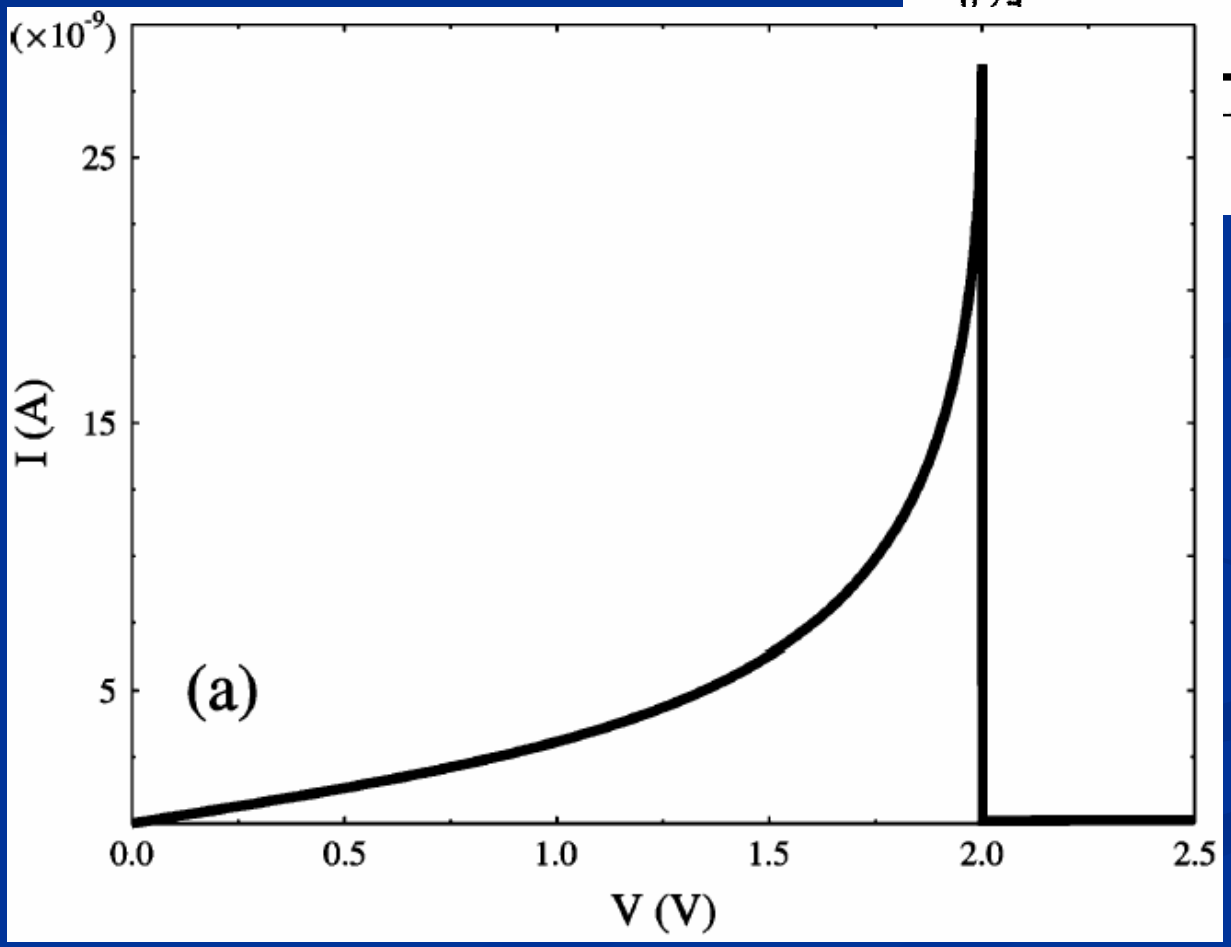
(×10^-9)
25
15
5
I (A)
(a)
0.0
0.5
1.0
1.5
2.0
2.5
V (V)

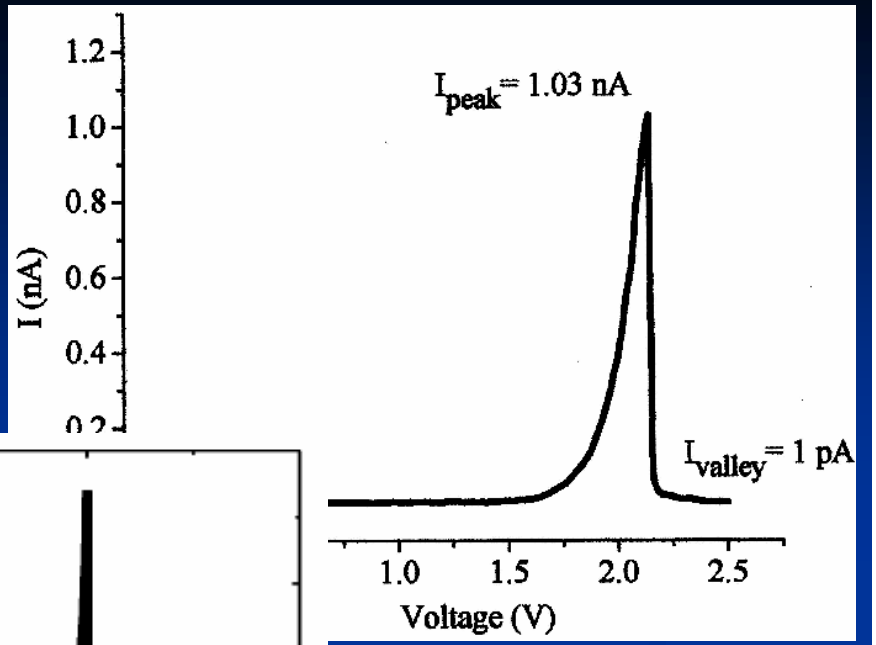
1.2
1.0
0.8
0.6
0.4
I (nA)
I_peak = 1.03 nA
I_valley = 1 pA
1.0
1.5
2.0
2.5
Voltage (V)

Summary: Barrier dynamics effects on electron transmission through molecular wires

- Relevant timescales
- Inelastic contributions to the tunneling current
- Dephasing and activation
- Heating of current carrying molecular wires
- HEAT CONDUCTION -- RECTIFICATION
- INELASTIC TUNNELING SPECTROSCOPY
- MULTISTABILITY AND HYSTERESIS
- LIGHT

Current induced light emission and light induced current in molecular tunneling junctions

M. Galperin &AN , cond- mat/ 0503114, 4 Mar 2005-03-23

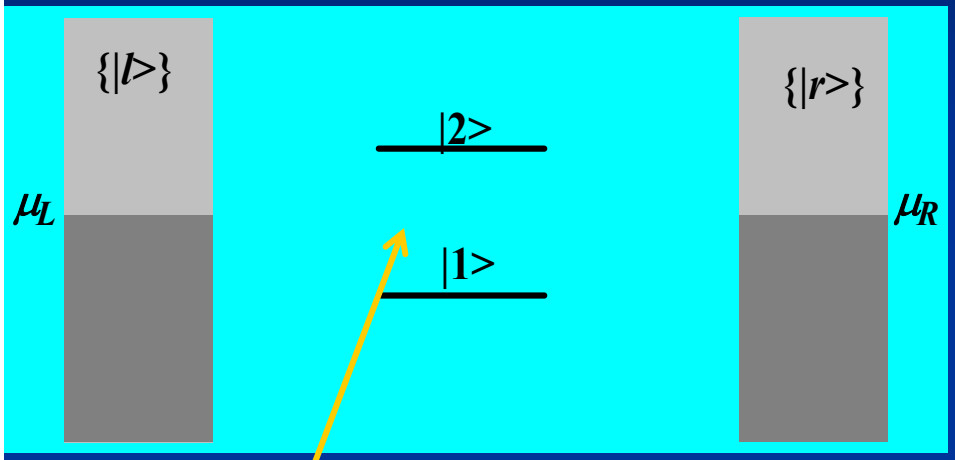

light

$$\hat{H}_0 = \sum_{m=1,2} \varepsilon_m \hat{c}_m^\dagger \hat{c}_m + \sum_{k\in\{L,R\}} \varepsilon_k \hat{c}_k^\dagger \hat{c}_k + \hbar \sum_\alpha \omega_\alpha \hat{a}_\alpha^\dagger \hat{a}_\alpha$$

$$\hat{V}_M = \sum_{K=L,R} \sum_{m=1,2;k\in K} \left(V_{k,m}^{(MK)} \hat{c}_k^\dagger \hat{c}_m + h.c. \right)$$

$$\hat{V}_N = \sum_{K=L,R} \sum_{k\neq k'\in K} \left(V_{k,k'}^{(NK)} \hat{c}_k^\dagger \hat{c}_{k'} \hat{c}_2^\dagger \hat{c}_1 + h.c. \right)$$

$$\hat{V}_R = \left(V_0^{(P)} \hat{a}_0 \hat{c}_2^\dagger \hat{c}_1 + h.c \right) + \sum_{\alpha\neq 0} \left(V_\alpha^{(P)} \hat{a}_\alpha \hat{c}_2^\dagger \hat{c}_1 + h.c \right)$$

Characteristics:

- Near resonance processes
- Weak incident radiation field
- Optimal for molecular stability
- Rotating wave approximation

Currents

$$I_B = \int_{-\infty}^{\infty} \frac{dE}{2\pi\hbar} \mathrm{Tr}\left[\Sigma_B^{<}(E) G^{>}(E) - \Sigma_B^{>}(E) G^{<}(E)\right]$$

Processes B:

Landauer:

$$I_{sd} = \frac{1}{\hbar} \int_{-\infty}^{+\infty} \frac{dE}{2\pi} \sum_{m=1,2} \Gamma_{ML,m}\, G^r_{mm}(E)\, \Gamma_{MR,m}\, G^a_{mm}(E) \times \left[f_L(E) - f_R(E)\right]$$

I_{abs}	Absorbed flux (coupling to one populated mode)
I_{em}	Emitted flux (coupling to a continuum of unpopulated modes)
I_N	Non radiative flux (creation of e-h pairs)

The source-drain process

$$\Sigma_{MK}(\tau_1,\tau_2)=\begin{bmatrix}\Sigma_{MK,11}(\tau_1,\tau_2) & \Sigma_{MK,12}(\tau_1,\tau_2)\\ \Sigma_{MK,21}(\tau_1,\tau_2) & \Sigma_{MK,22}(\tau_1,\tau_2)\end{bmatrix}$$

$$\Sigma_{MK,mm'}(\tau_1,\tau_2)=\sum_{k\in K}V_{mk}^{(MK)}g_k(\tau_1,\tau_2)V_{km'}^{(MK)}\ \cdots$$

(On Keldysh contour)

The radiative processes

$$\Sigma_P(\tau_1,\tau_2)=i\sum_\alpha\left|V_\alpha^{(P)}\right|^2\begin{bmatrix}F_\alpha(\tau_2,\tau_1)G_{22}(\tau_1,\tau_2) & 0\\ 0 & F_\alpha(\tau_1,\tau_2)G_{11}(\tau_1,\tau_2)\end{bmatrix}$$

$$\Sigma_P^<(E)=\sum_\alpha\left|V_\alpha^{(P)}\right|^2\begin{bmatrix}(1+N_\alpha)G_{22}^<(E+\omega_\alpha) & 0\\ 0 & N_\alpha G_{11}^<(E-\omega_\alpha)\end{bmatrix}$$

$$\Sigma_P^>(E)=\sum_\alpha\left|V_\alpha^{(P)}\right|^2\begin{bmatrix}N_\alpha G_{22}^>(E+\omega_\alpha) & 0\\ 0 & (1+N_\alpha)G_{11}^>(E-\omega_\alpha)\end{bmatrix}$$

The set α depends on the observable (absorption, emission, integrated or frequency resolved)

Non radiative process (e-h formation)

$$\Sigma_{NK}(\tau_1,\tau_2)=\sum_{k\neq k'\in K}\left|V_{kk'}^{(NK)}\right|^2 g_k(\tau_2,\tau_1)g_{k'}(\tau_1,\tau_2)\begin{bmatrix}G_{22}(\tau_1,\tau_2) & 0\\ 0 & G_{11}(\tau_1,\tau_2)\end{bmatrix}$$

$$\Sigma_{NK}^{<}(E)=\int\frac{d\omega}{2\pi}B_{NK}\left(\omega,\mu_K\right)\begin{bmatrix}G_{22}^{<}(E+\omega) & 0\\ 0 & G_{11}^{<}(E+\omega)\end{bmatrix}$$

$$\Sigma_{NK}^{>}(E)=\int\frac{d\omega}{2\pi}B_{NK}\left(\omega,\mu_K\right)\begin{bmatrix}G_{22}^{>}(E-\omega) & 0\\ 0 & G_{11}^{>}(E-\omega)\end{bmatrix}$$

$$B_{NK}\left(\omega,\mu_K\right)=\int\frac{dE}{2\pi}C_{NK}\left(E,\omega\right)f_K\left(E\right)\left[1-f_K\left(E+\omega\right)\right]$$

$$C_{NK}\left(E,\omega\right)=\left(2\pi\right)^2\sum_{k\neq k'\in K}\left|V_{kk'}^{(NK)}\right|^2\delta\left(E-\varepsilon_k\right)\delta\left(E+\omega-\varepsilon_{k'}\right)$$

NOTE: Self energies and therefore Green functions depend on the populations of molecular levels, which need to be calculated self consistently

ABSORPTION LINESHAPE

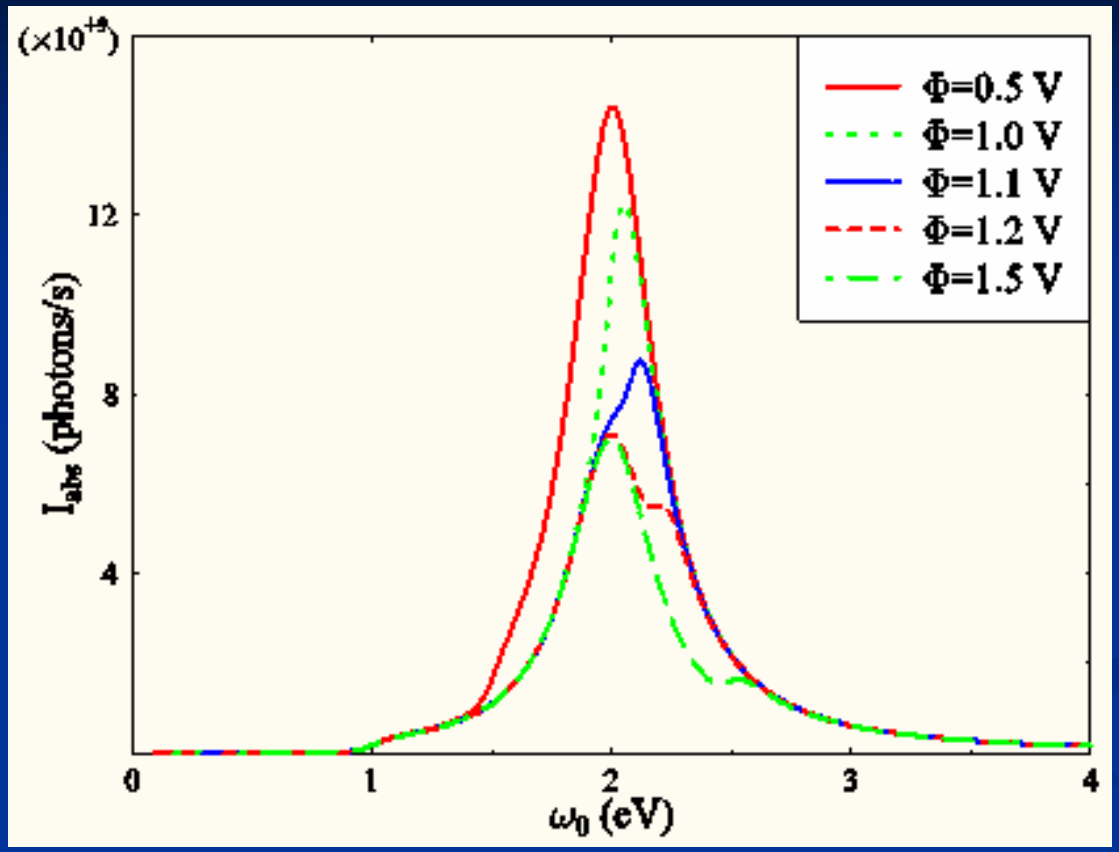

$$\varepsilon_{21} = 2\,eV$$

$$\gamma_P = 10^{-6}\,eV$$

$$B_{NL} = B_{NR} = 0.1\,eV$$

$$T = 300\,K$$

$$\Gamma_{ML,1} = \Gamma_{MR,1} = 0.01\,eV$$

$$\Gamma_{ML,2} = \Gamma_{MR,2} = 0.2\,eV$$

Fig.2 The absorption current (photons/s). The molecular electronic levels are assumed pinned to the right electrode, i.e. the bias shifts upward the electronic states of the left electrode.

CHARGE TRANSFER TRANSITIONS

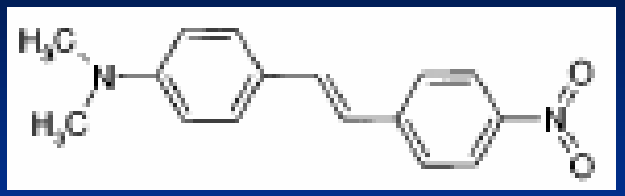

μ_g=7 D μ_e=31+/-1.5 D

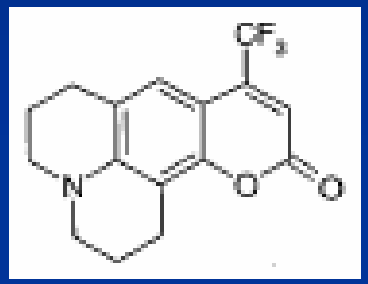

μ_g=5.5 D μ_e=15.5+/-1.5 D

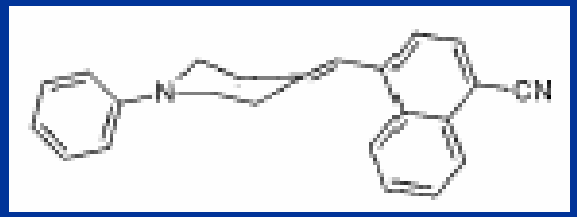

μ_g=7 D μ_e=30+/-1.5 D

S. N. Smirnov & C. L. Braun, REV. SCI. INST. 69, 2875 (1998)

Here we will make the reasonable assumption that a charge-transfer transition within the bridge is expressed in changing the relative coupling strengths of the molecular HOMO and LUMO to their metallic contacts. We thus investigate models in which $\Gamma_2 \neq \Gamma_1; \Gamma_{ML,2} \neq \Gamma_{MR,2}$

Light induced current

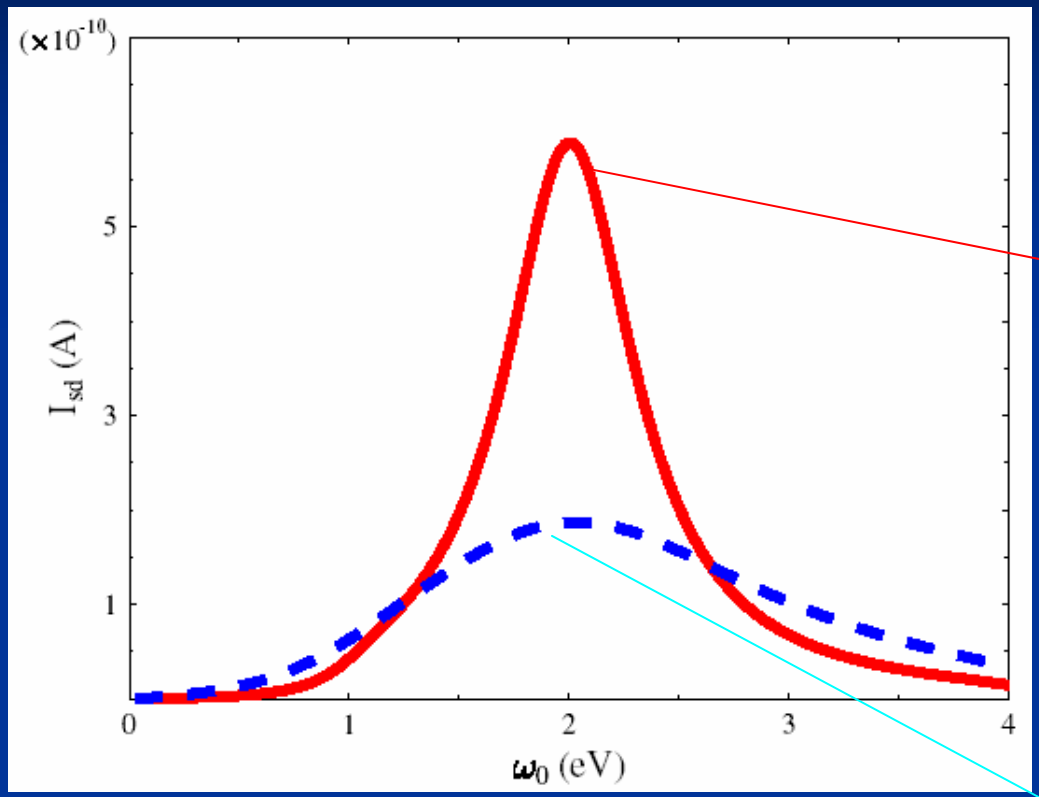

E_{21}=2eV

$\Gamma_{M,1}$=0.2eV

$\Gamma_{M,2}$=0.3eV, 0.02eV

Γ_N=0.1eV

Incident light =10^8 W/cm^2

Same parameters with
Γ_M 3 times larger

LIGHT INDUCED CURRENT: APPROXIMATE ANALYTICAL RESULTS

$$I_{sd} = \int \frac{dE}{2\pi\hbar} \sum_{m=1,2} \Gamma_{ML,m} G^r_{mm}(E) \Gamma_{MR,m} G^a_{mm}(E) \left[f_L(E) - f_R(E) \right]$$

$$+ \left| V_0^{(P)} \right|^2 \int \frac{dE}{2\pi\hbar} \frac{1}{\left(E - \varepsilon_2\right)^2 + \left(\Gamma_2/2\right)^2} \frac{1}{\left(E - \omega_0 - \varepsilon_1\right)^2 + \left(\Gamma_1/2\right)^2}$$

$$\times \left\{ \Gamma_{ML,1} \Gamma_{MR,2} f_L(E - \omega_0) \left[1 - f_R(E) \right] - \Gamma_{ML,2} \Gamma_{MR,1} f_R(E - \omega_0) \left[1 - f_L(E) \right] \right\}$$

NO BIAS:

$$I_{sd} = \left| V_0^{(P)} \right|^2 \int \frac{dE}{2\pi\hbar} \frac{1}{\left(E - \varepsilon_2\right)^2 + \left(\Gamma_2/2\right)^2} \frac{1}{\left(E - \omega_0 - \varepsilon_1\right)^2 + \left(\Gamma_1/2\right)^2}$$

$$\times f(E - \omega_0) \left[1 - f(E) \right] \left\{ \Gamma_{ML,1} \Gamma_{MR,2} - \Gamma_{ML,2} \Gamma_{MR,1} \right\}$$

$$\xrightarrow{f(E-\omega_0)\left[1-f(E)\right]=1} \frac{\left| V_0^{(P)} \right|^2}{\hbar} \frac{\Gamma}{\left(\varepsilon_2 - \omega_0 - \varepsilon_1\right)^2 + \left(\Gamma/2\right)^2} \frac{\Gamma_{ML,1} \Gamma_{MR,2} - \Gamma_{ML,2} \Gamma_{MR,1}}{\Gamma_1 \Gamma_2}$$

Current induced light

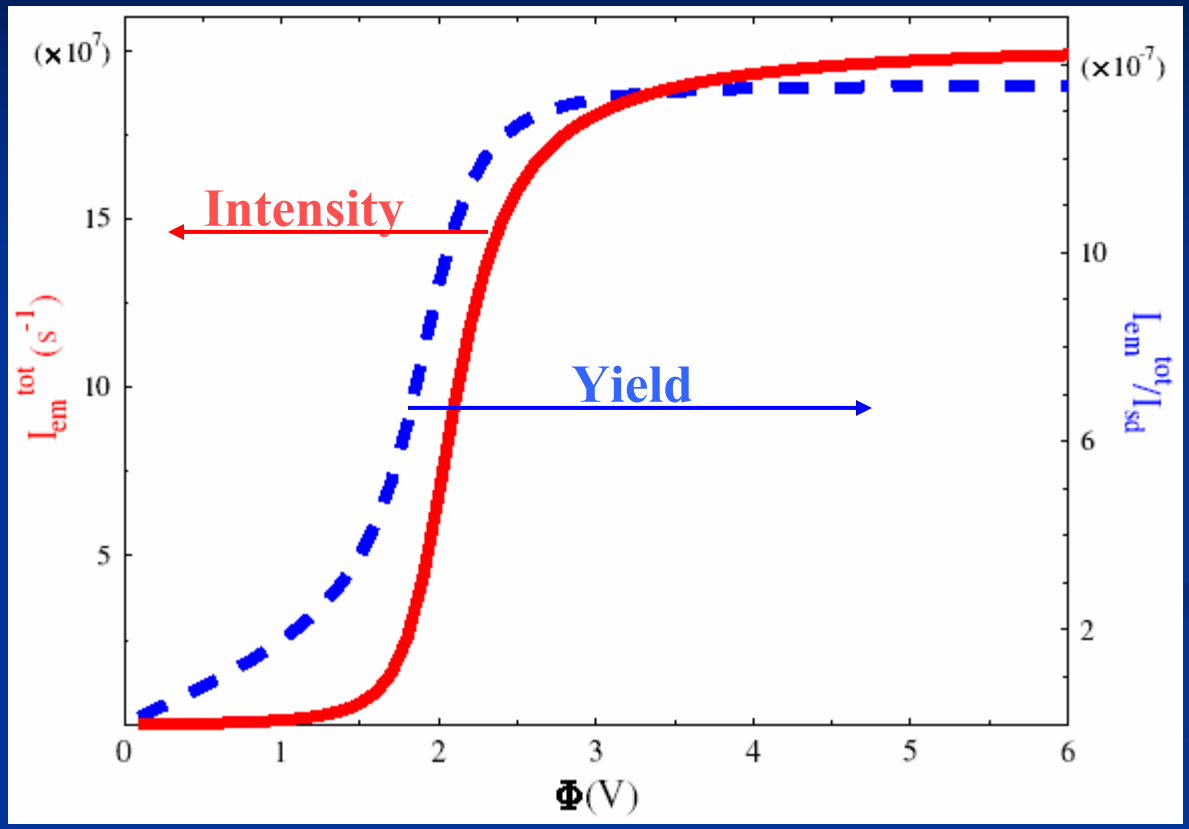

E_{21}=2eV

$\Gamma_{M,1}=\Gamma_{M,2}$=0.1eV

Γ_N=0.1eV

Observations: Flaxer et al, Science 262 , 2012 (1993),

Qiu et al, Science 299 , 542 (2003).

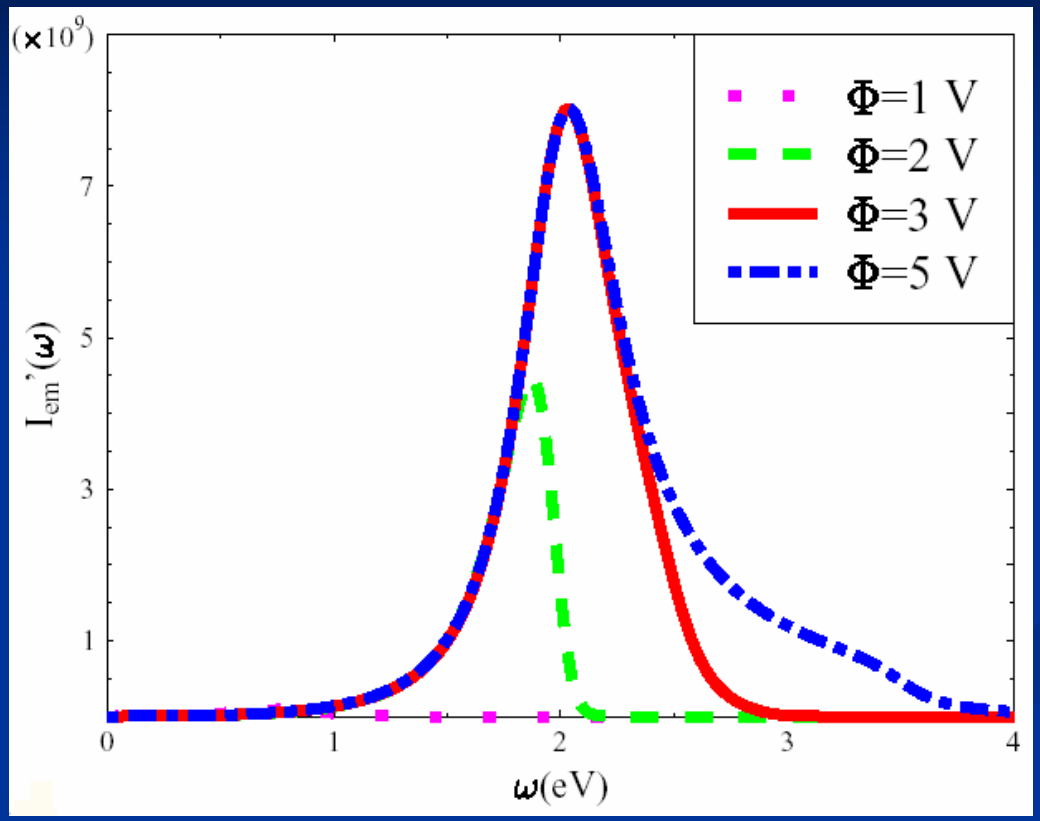

Frequency resolved emission computed for the model of Fig. 1 using the same parameters as in previous slide, for different bias potentials.

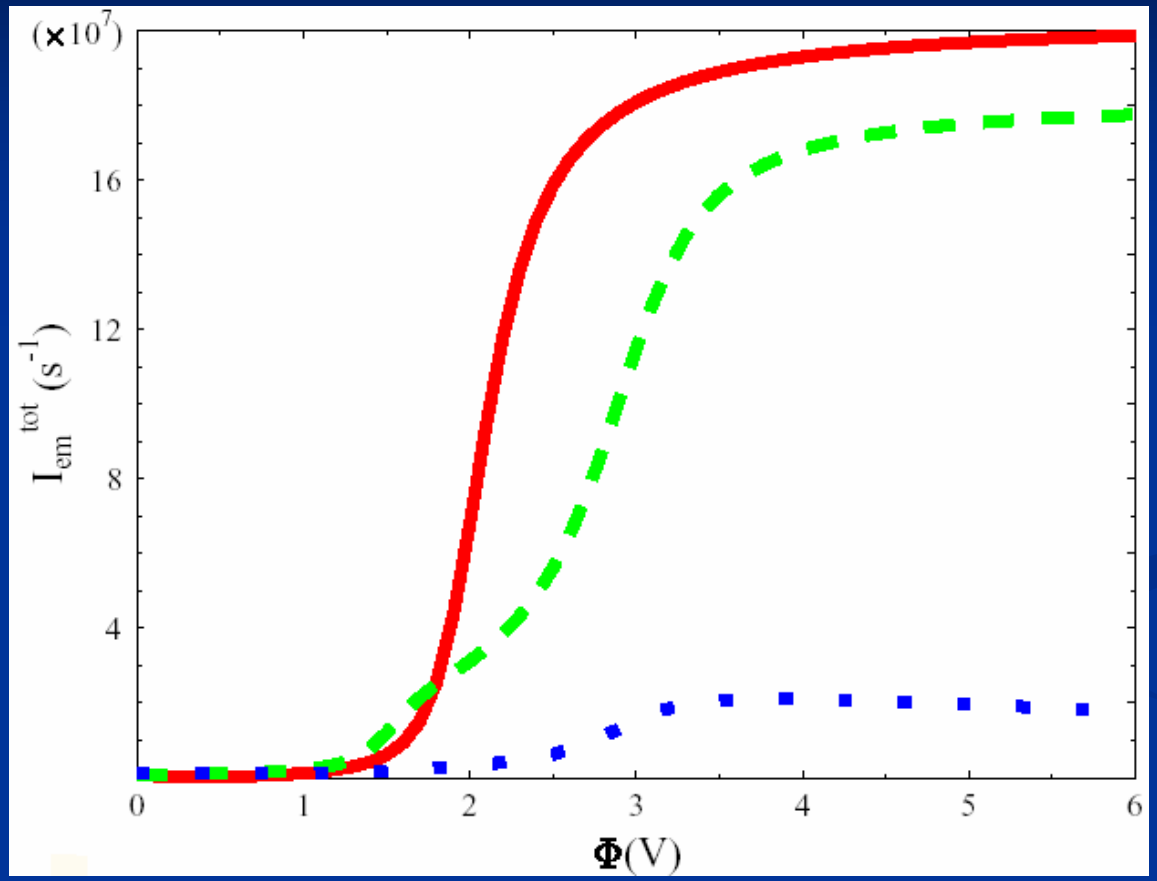

Photon emission from junctions characterized by different voltage division factors (see text). Full line (red) η=0.5; dashed line (green) η=0.66; dotted line (blue) η=0.99

Summary: Barrier dynamics effects on electron transmission through molecular wires

- Relevant timescales
- Inelastic contributions to the tunneling current
- Dephasing and activation
- Heating of current carrying molecular wires
- HEAT CONDUCTION -- RECTIFICATION
- INELASTIC TUNNELING SPECTROSCOPY
- MULTISTABILITY AND HYSTERESIS
- LIGHT